INFORMATION TO USERS

The most advanced technology has been used to photograph and reproduce this manuscript from the microfilm master. UMI films the text directly from the original or copy submitted. Thus, some thesis and dissertation copies are in typewriter face, while others may be from any type of computer printer.

The quality of this reproduction is dependent upon the quality of the copy submitted. Broken or indistinct print, colored or poor quality illustrations and photographs, print bleedthrough, substandard margins, and improper alignment can adversely affect reproduction.

In the unlikely event that the author did not send UMI a complete manuscript and there are missing pages, these will be noted. Also, if unauthorized copyright material had to be removed, a note will indicate the deletion.

Oversize materials (e.g., maps, drawings, charts) are reproduced by sectioning the original, beginning at the upper left-hand corner and continuing from left to right in equal sections with small overlaps. Each original is also photographed in one exposure and is included in reduced form at the back of the book.

Photographs included in the original manuscript have been reproduced xerographically in this copy. Higher quality 6" x 9" black and white photographic prints are available for any photographs or illustrations appearing in this copy for an additional charge. Contact UMI directly to order.

U·M·I

University Microfilms International
A Bell & Howell Information Company
300 North Zeeb Road Ann Arbor MI 48106-1346 USA
313 761 4700 800 521 0600

Order Number 9119618

Mass transfer and interactions in microemulsions

Chan, Yeung Yu, Ph.D.

City University of New York, 1991

U·M·I
300 N. Zeeb Rd.
Ann Arbor, MI 48106

MASS TRANSFER AND INTERACTIONS IN MICROEMULSIONS

BY

YEUNG YU CHAN

A Dissertation Submitted to the Graduate Faculty in Engineering in Partial Fulfillment of the Requirements for the Degree of Doctor of Philosophy

THE CITY UNIVERSITY OF NEW YORK
1991

This manuscript has been read and accepted for the Graduate Faculty in Engineering in satisfaction of the dissertation requirement for the Degree of Doctor of Philosophy.

October 1, 1990

Professor Kevin McKeigue
Chair of Examining Committee

1/29/91
October 1, 1990

Dean Gerard Lowen
Executive Officer

Professor Charles Maldarelli

Professor Carol Steiner

Professor Gabriel Tardos

Doctor W. Brian Bedwell
Supervisory Committee

The City University of New York

ABSTRACT

MASS TRANSFER AND INTERACTIONS IN MICROEMULSIONS

by

Yeung Yu Chan

Advisor: Professor Kevin McKeigue

Interactions between the dispersed-phase droplets strongly influence the physical, thermodynamic, and transport properties of microemulsions. In water-in-oil microemulsions, these interactions have been incorrectly attributed to van der Waals forces acting between droplet's water cores. A novel mechanism is proposed for interdroplet interactions in water-in-oil microemulsions.

This theory is based on the premise that the random arrangement of the small number of ions within the water core of a microemulsion results in the droplet possessing a relatively large dipole moment. A series of Monte Carlo simulations were performed to determine the magnitude of this dipole moment and its polarizability for several water-in-oil microemulsion systems. The number of ions, the droplet size, and the surfactant's dissociation constant were varied in the

simulations. A new theory for the interdroplet potential function is formulated which explicitly accounts for dipole - dipole and dipole - induced dipole attractions between droplets. A perturbation approach with a hard-sphere reference system is used to generate thermodynamic properties from the interdroplet potential function. The Hamaker constants and osmotic pressures predicted by this theory are found to be in good agreement with data in the literature. Specifically, the theory correctly predicts the decrease in attractions between droplets with increasing salt concentration.

An approach based on Smoluchowski's theory of colloid stability is used to generate an interdroplet mass transfer rate from the potential function. Finally, as an example to illustrate the utility of this approach, the particle size distribution of a microemulsion polymerization process is calculated. The results clearly suggest that the control of product size and product size distribution depends to a large degree on the ratio of interdroplet mass transfer rate to the rate of polymerization.

ACKNOWLEDGEMENTS

I would like to express my deepest gratitude to my advisor, Dr. Kevin McKeigue, for his support and guidance throughout this project. It was the many hours of stimulating discussions with him that contributed most to my knowledge and interest in the fields covered by this dissertation. I am also grateful to members of my examination committee, Drs. Charles Maldarelli, Carol Steiner, and Gabriel Tardos, for their helpful review and advice on the content of this thesis. I owe a special debt of gratitude to Dr. Brian Bedwell for serving on my examination committee and for his pioneering research that was the foundation of this work. Finally, special thanks to my family, especially my wife Peggy, for their constant encouragement and support throughout my graduate studies.

TABLE OF CONTENTS

LIST OF TABLES

LIST OF FIGURES

CHAPTER 1

INTRODUCTION AND BACKGROUND

In recent years, several novel microemulsion based technologies have been proposed. Because of its commercial potential, the use of microemulsions to synthesize microparticles in situ has received a great deal of attention. During the development of these processes, however, it was discovered that the rapid exchange of mass between droplets prevents the formation of products with the desired particle size distribution.

This dissertation is a study of interdroplet mass transfer in water-in-oil microemulsions, and in particular, its application to the design and development of novel microemulsion based processes.

The specific objectives of this research are to :

1). understand the underlying physicochemical phenomena governing the exchange of mass between water-in-oil microemulsion droplets;

2). formulate a mathematical description of the interdroplet mass transfer process;

3). assess the implication of mass transfer process on technologically important applications such as microparticle productions, that is, to establish the

extent to which product size and polydispersity can be controlled.

This dissertation is divided into six chapters. The following sections in Chapter 1 detail a literature review on the subjects which are relevant to the studies of mass transfer and interactions in microemulsions. Chapter 2 to Chapter 5 is a collection of papers that contain the results from this investigation and which are currently being submitted for publications. The formulation of an interdroplet potential function according to the physics of the problem for a W/O microemulsion system containing a non-ionic surfactant is presented in Chapter 2. Chapter 3 gives the interdroplet potential function for a microemulsion system containing an anionic surfactant. Quantitative parameters calculated from the new potential functions and their comparison with data in the literature are detailed in Chapter 4. A mass transfer theory that utilizes the new potential function, along with the results of a microemulsion polymerization process, in which it is demonstrated that the product size distribution can be controlled by varying the rate of interdroplet mass transfer, are presented in Chapter 5. Chapter 6 gives a summary of the important conclusions drawn from this dissertation and outlines the recommendations for future work.

1.1. Microemulsions : Structures and Properties

It is a well known phenomenon that oil and water do not mix. When one applies energy (mechanical and/or heat) and surface active agents (surfactants) to a water-oil mixture, a suspension of oil droplets dispersed in water (O/W) or water droplets in oil (W/O) is formed. Such a suspension is created by the decrease of interfacial energy and is called an emulsion[1]. In general, the droplets so formed are rather large and greatly polydisperse. Their sizes range from 100 nm to 10 μm in diameter[2]. Emulsions are also thermodynamically unstable. Attractive forces between neighboring droplets cause them to coalesce back into two liquid phases separated by a single interface.

Hoar and Schulman[3] discovered that by choosing an "appropriate" surfactant mixture, it is possible to spontaneously form a nonviscous, thermodynamically stable, and optically isotropic transparent dispersion. This special type of emulsion is commonly known as a "microemulsion".

Microemulsions consist of at least three components, water, oil, and surfactant. The surfactant is adsorbed at the oil-water interface. To obtain a thermodynamically stable system, often a fourth component - a cosurfactant - is needed. In many cases, the cosurfactant is a four to six carbon alcohol. Eicke[4] has shown that aside from alcohols, a wide

variety of substances can act as cosurfactants in microemulsion systems as well. The cosurfactant is distributed at the interface along with the surfactant.

The dispersed particles in microemulsions are much smaller than those in emulsions. The typical droplet size is usually less than 100 A[4]. In addition, the thermodynamic stability gives rise to some special properties that are of interest in practical applications. For example, its spontaneous formations when the various components are brought together at a suitable temperature range; its stability under shear; and its infinite stability at constant chemical composition and temperature[5]. Hence microemulsions have been the subject of extensive research over the past two decades. The results of these investigations suggest that depending on the system and the relative concentrations of each component, microemulsions can display a wide variety of microstructures and behaviors. Morphology ranging from dispersions of monodisperse spherical droplet-like aggregates or swollen micelles[6] to polydisperse bicontinuous structures[7-9] have been reported. The physics of such structural transitions is still unknown, yet there have been speculations that both the interactions between droplets and the relative fluidity of the interface are the dominant factors in determining the microstructure of microemulsions[7,10].

The present work addresses water-in-oil (W/O) type

microemulsions. Over a fairly wide concentration range, this type of microemulsion can effectively be described as a stable collection of monodisperse "water" microdroplets in an oil continuous phase. Each droplet consists of a 10 - 500 A diameter "bulk" water drop surrounded by a 20 - 30 A thick surface phase (interphase) consisting of surfactant, and in some cases cosurfactants as well. The potential application of water-in-oil microemulsions in a wide range of novel technologies of industrial importance provides the motivation for this investigation.

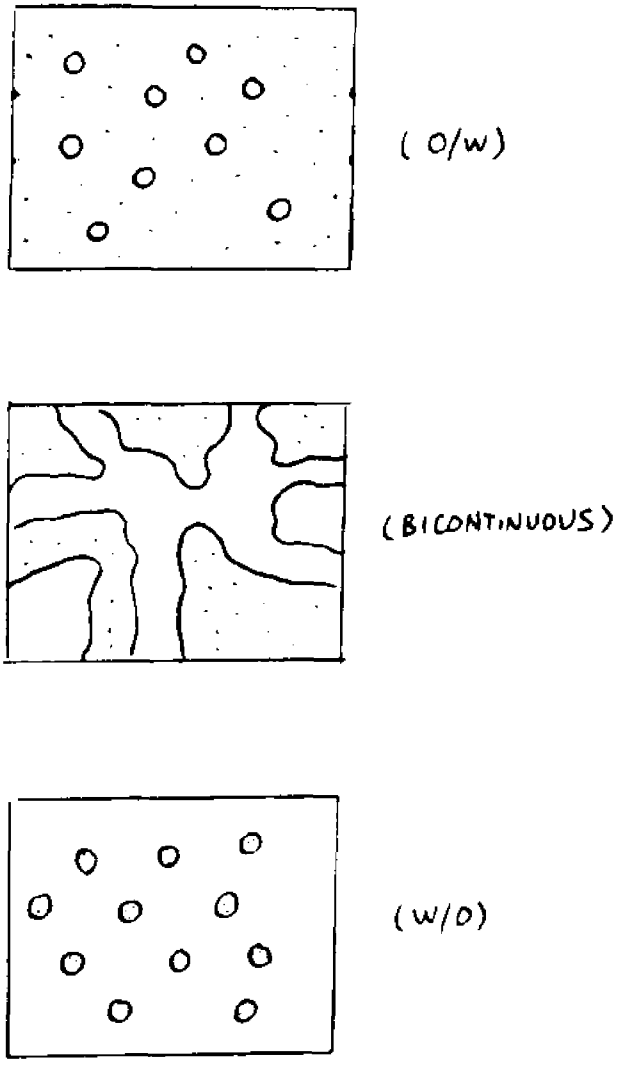

FIG. 1-1 **Schematic description of various microemulsion structures**

1.2. Applications of Microemulsions

Currently, microemulsions are used commercially in waxes and polishes, cutting oils, cleaning fluids, automotive antifreezes, and a variety of pharmaceutical, agricultural, and food products. They have also received a lot of attention for use as chemical flooding agents for enhanced oil recovery[12,13]. Other applications of commercial interest that are being developed included phase transfer catalysts[14], high-stability ink for use in jet printing[15], fire-extinguishing components[16], and improved engine fuels[17].

Due to their small uniform droplet size and their solubilization properties, some innovative and technologically important applications for microemulsions have been proposed recently. Among them are the use of microemulsions as a reaction media[18-23], production of fine colloidal particles[24-38], formulations in controlled and time-released drug delivery techniques[39-42], and as active carriers in liquid membrane separations process[43-49].

The main objective of the current work is to acquire the knowledge and expertise to design and develop these novel processes, in particular, the production of extremely small (1 - 100 nm) colloidal particles. Here microemulsions are essentially acting as microscopic batch reactors. The possible products of such reactions include but not limited to

polymer latex spheres for paints and coatings, metallic crystallites for use in catalysis or optical and magnetic recording media, ceramic precursors for high performance materials, and colloidal semiconductor particles of cadmium sulfide for photochemical and catalytic reactions. In general, the particles produced from microemulsions based reactions possess unique properties that cannot be obtained via other means. For example, the modification in the structure of the electron bands in cadmium sulfide due to the very small size of the particle allow one to obtain reactions that are impossible with bulk material. The success of these novel processes, however, depends on a thorough understanding of the interdroplet mass transfer rates. To illustrate this point, let us consider the production of polymer latex spheres. In such process, a water soluble monomer can be solubilized at the core of water in oil (W/O) microemulsion droplet. By using gamma-rays or ultra-violet light, polymerization is initiated and the resulting polymer should contain no more than the initial number of monomers present in each droplet. Similarly, chloroplatinic acid can be solubilized in a microemulsion droplet, then reduced by hydrogen gas or hydrazine to produce small (possibly down to 10 A) monodisperse platinum particles[28]. To achieve a reaction environment that offers better control of particle size and particle size distribution, the mass transfer between droplets, or between the droplet and the continuum during the course of the reaction has to be negligible.

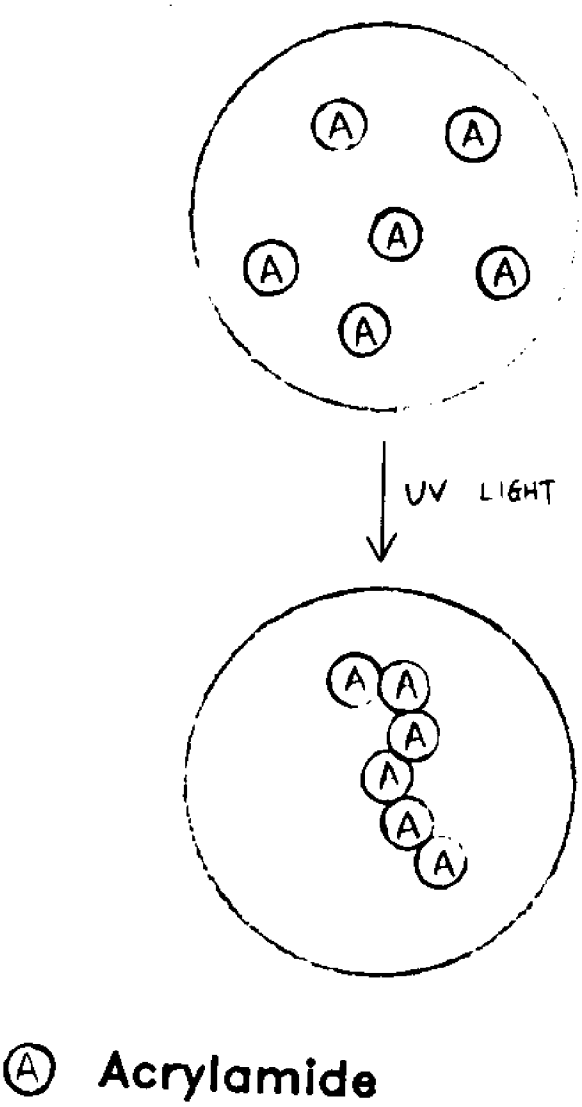

FIG. 1-2 Polymerization inside a microemulsion droplet

Unfortunately, in the actual attempts[24-38] to produce such colloidal particles, the exchange of mass between droplets was found to be significant. As a result, researchers have not been able to obtain the monodisperse particles that they have expected. In a study by Tang, et. al.[24], the latex particles produced by the polymerization of styrene in microemulsions had a bimodal product distribution, with final particles size an order of magnitude larger than the initial microemulsions. In another study of microemulsion based polymerization, Candau, et. al.[25] and Beckman et. al.[31] showed that the addition of acrylamide monomer to a water-in-oil microemulsion of AOT/oil/water could not solve the polydispersity problem. It did change the characteristic size of the product droplets however. Here, the products are some 5 to 20 times larger than the initial droplets. These studies also found that the addition of acrylamide shifted the phase boundary of the microemulsion region and increased the attraction between droplets significantly. One possible explanation for this behavior is that acrylamide somehow acted as a cosurfactant and altered the characteristics of the interface, consequently enhancing the interdroplet mass transfer.

In short, even though polymers[27] and platinum[28] particles with some interesting properties have been produced, the main objective of achieving a narrow product size distribution was unsuccessful because of the rapid interdroplet mass transfer.

Instead of acting as a system of small batch reactors, it appears that the microemulsion was acting more in the capacity of a dispersing agent that increased the number of nucleation sites.

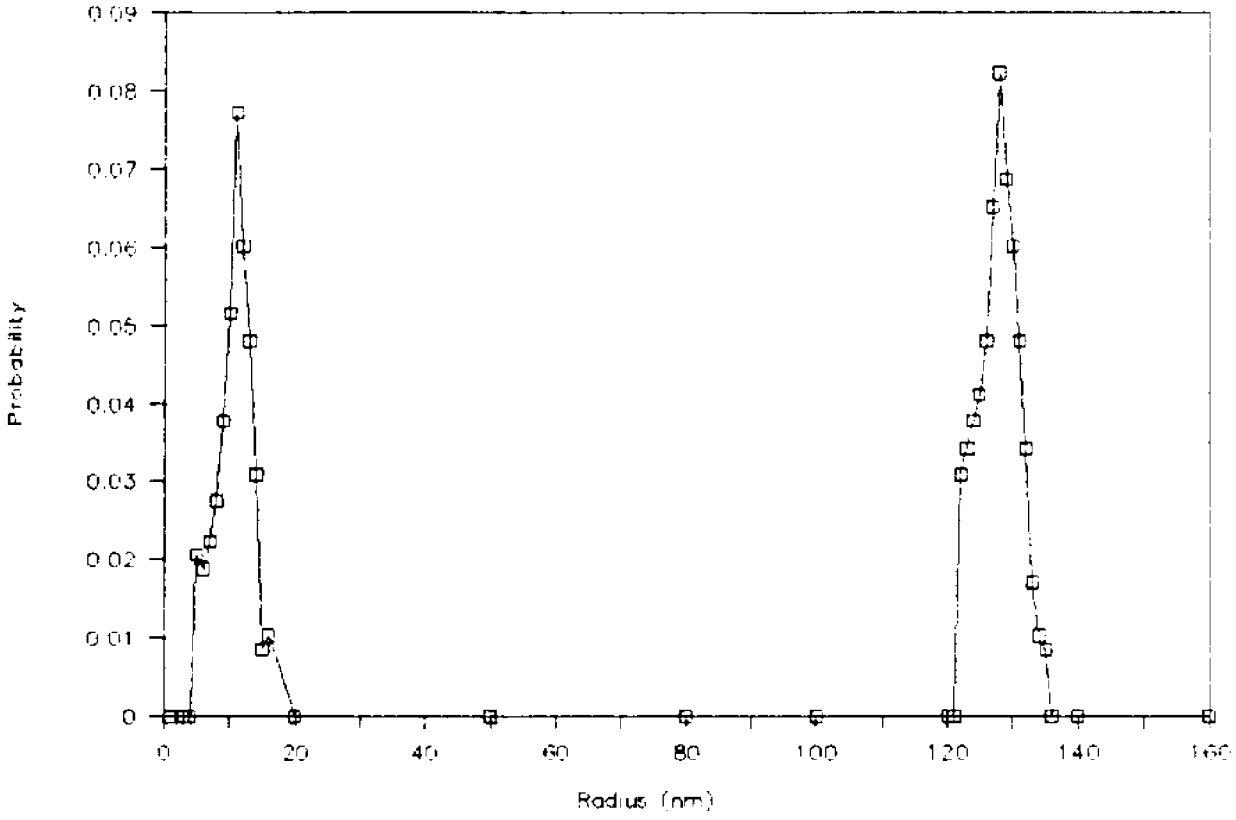

FIG. 1-3 Product distribution of a photo-induced microemulsion polymerization process

1.3. Mass Transfer and Interdroplet Interactions

From a series of fluorescent probe experiments[50] and esterification reaction rate measurements[51], Eicke and Robinson respectively concluded that the exchange of mass between microemulsion droplets was a very fast phenomenon, in the order of microsecond or less. This conclusion has been verified by other studies[52-55] investigating the same phenomenon. The consensus among the researchers is that the exchange of mass occurs through interparticle collision and transient merging of the colliding droplets.

In the case of microparticle production, this instantaneous mass transfer rate must be significantly slowed to achieve the desired products. In general, successful commercialization of the aforementioned novel processes depends critically on the ability to control the interdroplet mass transfer rates. Unfortunately, no one has yet recognized the importance of this aspect of microemulsions research. The present work is to our knowledge the first attempt to address the engineering process and product development of novel microemulsions applications, in particular the possibility of controlling the interdroplet mass transfer rates through various parameters.

At this point, it is logical to ask the question " Can interdroplet mass transfer in microemulsions really be

controlled? " The answer to this question seems to be yes. In a study on water-in-oil (W/O) microemulsions, Bedwell[56] reported that the addition of electrolyte to an AOT/oil/water microemulsion system resulted in a decrease of both the polydispersity and the attraction between droplets. The rheology of such system also resembled that of a suspension of hard spheres. This result has been verified by Hou[57] using the same system. Other microemulsions with similar behavior have also been reported[58].

Based on this result and fundamental principles of colloid stability theory, specifically Smoluchowski's equation[2], it is conceivable to control the rate of mass transfer between microemulsion droplets by reducing their attractions. To achieve this objective, we must, however, understand the nature of interdroplet interaction in microemulsions and to determine parameters that could modify the interaction potential. The topic of interaction forces between the particles in water-in-oil (W/O) microemulsions has in fact been studied extensively using light scattering[56-66], neutron scattering[67-69], fluorescent probe[70], sedimentation[68], viscosity[68], and water solubilities[71] experiments.

At first glance, van der Waals force between water molecules in different microemulsion droplets appears to be a reasonable candidate to explain the attraction observed. To establish if this indeed is true, Calje et. al.[60] calculated

the Hamaker constant, a parameter that characterize the total energy of interaction. The theoretical value they obtained, however, is two orders of magnitude smaller than the experimental results. This implies that van der Waals forces are too small to account for the interdroplet attractions. Consequently, we have to explore other alternatives in explaining the attractions between droplets.

From a series of fluorescent quenching experiments on microemulsions, Atik and Thomas[70] observed a significant differences in the quenching reaction kinetics when two different alcohols were used as cosurfactants. The exchange of quencher between droplets was much faster when pentanol was used instead of hexanol. Similar results was obtained by Lang et. al.[52] and Cazabat et. al.[62]. They found the droplet interactions to be strongly attractive in the microemulsions containing butanol as cosurfactant, and much less attractive in those containing pentanol or hexanol.

Some qualitative theories of microemulsion formation were put forward to offer explanation for this phenomenon. These theories suggest that the flexibility of the droplet interface might be highly dependent on the cosurfactant. Thus, by strengthening the surfactant interface, hexanol might have provided limited kinetic stability to the droplets, lowering the rate of coalescence and redispersion in the system. None of the existing theories, however, is able to explain the

peculiar behavior observed in electrolyte moderated interactions, specifically, the reason for the decrease in attractive potential when the concentration of electrolytes in the core of the droplet is increased. Hence, we have to look at still other possibilities in explaining the attractive force between microemulsion droplets.

As discussed earlier, various researchers[56-57] have experimentally demonstrated the existence of electrolyte moderated interactions in microemulsions. They speculated that the origin of such interactions could be either fluctuating dipole moments or interfacial structural changes, though no detailed mechanism for either was put forward. DeRozieres et. al.[72] made the first concerted attempt to create a theory based on these hypotheses. In their model, the interdroplet interactions is proposed to be the result of induced dipole-induced dipole attractions. They suggested the mobility of counterions led to the existence of such induced dipole moments. Despite the failure of this model in explaining the electrolyte-moderated interaction phenomena, the possibility of a dipole interactions in W/O microemulsions do seem plausible. From basic principles of statistical mechanics, it is conceivable that when the number of ions in the water core is small, a sizable dipole moment may arise from the non-symmetrical arrangement of these ions. The existence of such dipole moment could lead to dipole -dipole and dipole - induced dipole attractions between microemulsion

droplets.

1.4. Interdroplet Potential in Microemulsions

Ever since the pioneering work of Calje et. al.[60], statistical mechanics theories for simple fluids have consistently been applied to studies of interparticle interactions in microemulsions[56-57,60-62,73-74]. In these studies, interacting colloidal dispersions have been treated as macroscopic analogues of simple atomic and molecular fluids. Basically, the interaction behavior of the particles is effectively described by a hard sphere potential, extended by a small supplementary attractive force as a perturbation. Unfortunately, the interdroplet potentials are usually obtained by fitting a suitable functional form such as square well potential[57,60] or Yukawa potential[73-74] to the equilibrium osmotic compressibility and viscosity data. Few attempts have been made to create an interdroplet potential based on realistic physical considerations. Consequently, although there has been an abundance of excellent experimental data, no one has yet been able to convert the results into a sufficiently accurate and verifiable picture of microemulsion interactions.

The present investigation will make an attempt to develop a more realistic interdroplet potential based solely on the underlying physics. Such information is essential to the mass

transfer model that will be developed in the latter part of this study.

For an assembly of charges located in a certain limited region, the dipole moment, p, can be defined as[75]

$$p = \sum_{\hat{}} q_i d_i \qquad \ldots (1)$$

where d_i is the displacement of charge i from the reference point.

To verify the existence of dipole moment in a microemulsion droplet, the spatial distribution of ions in the water core therefore first has to be determined. Although the problem can be formulated exactly, like most many-body problems, it can not be solved analytically. The most convenient way to find an approximate solution to the problem is by the Metropolis Monte Carlo method[76-78]. Another parameter that can be conveniently obtained from this simulation is polarizability α .

With this information, perturbation theory[79-80] can be applied to analyze the present problem by treating the microemulsion as a macroscopic analogue of a simple fluids. In this approach, the pair potential of mean force U(r) is separated into two parts, a reference hard sphere and a perturbation part:

$$U(r) = U_{hs}(r) + U_a(r) \quad \ldots (2)$$

where the potential of mean force for the hard sphere is

$$U_{hs}(r) = \infty \qquad r < \sigma_{HS}$$
$$= 0 \qquad r > \sigma_{HS} \quad \ldots (3)$$

Since the interactions between droplets is the result of dipole - dipole and dipole - induced dipole attractions, the perturbation part of potential of mean force can therefore be expressed as

$$U_a(r) = \frac{p^2}{(4\pi\varepsilon_0\varepsilon)^2 r^6}\left(\frac{p^2}{3kT} + 2\alpha\right) \quad \ldots (4)$$

To assess the accuracy of this interdroplet potential function, the osmotic compressibility and Hamaker constant will be generated and compared with existing values in the literature.

1.5. AOT/water/oil Microemulsions

In this investigation, sodium bis(2-ethylhexyl) sulfosuccinate (AOT) water-in-oil microemulsions will be used as the model system. There are several advantages for using AOT in this study. Because of its structure, AOT can form a thermodynamically stable microemulsions without the addition of short chain alcohols as cosurfactants. The main objective

of this study is to determine the effect of electrolytes on interdroplet interactions. The presence of any alcohol partitioning between the interface and the continuum, however, is likely to complicate the analysis of results. Thus, the absence of alcohols makes AOT an ideal system for studying interdroplet interactions. In addition, the dilute AOT/water/oil system consists of monodisperse spherical droplets with hard spheres behavior. Previous investigations[56,57] suggested that the attraction between particles in this system could be reduced by the addition of electrolytes, making this system promising for use in microparticle production. Finally, the AOT water in oil microemulsion is one of the most thoroughly studied systems in the colloid literature. It has been investigated extensively using laser light scattering[56-57], NMR[73-74,81-82], small-angle neutron scattering (SANS)[83-87], small angle X-ray scattering[88-90], phase diagram determinations[91], dielectric response measurements[92-94], fluorescence probes[22,52,95], ultrasonics[96], and electrical conductivity measurements[97-98]. Results obtained from our investigation can readily be compared to this wealth of data to check for the validity of the model.

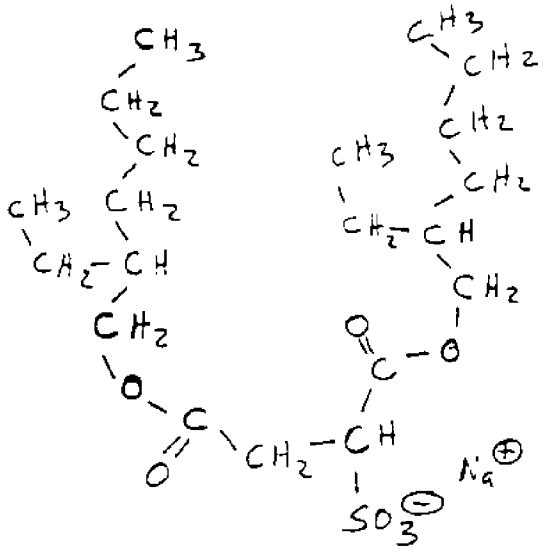

FIG. 1-4 Structure of Aerosol-OT (AOT)

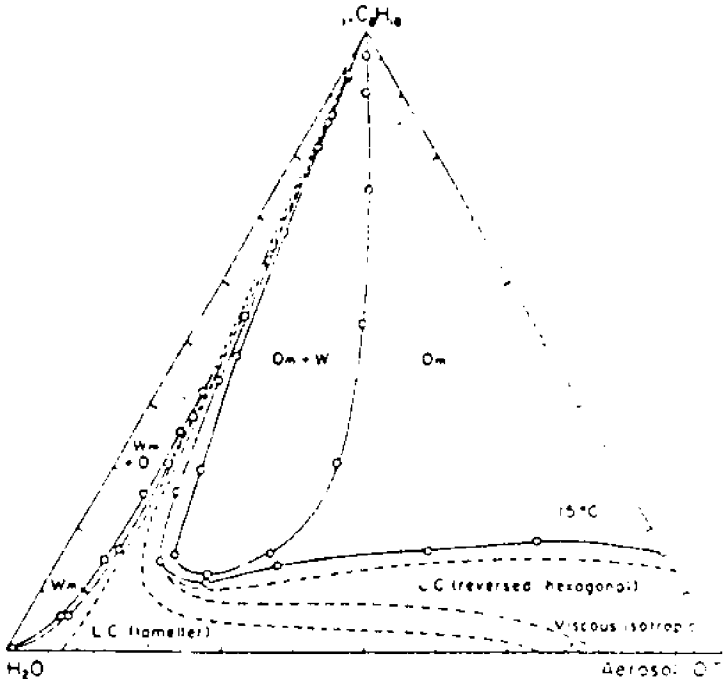

FIG. 1-5 Ternary phase diagram of AOT, water, and oil

BIBLIOGRAPHY

1. Heimenz, P.C., "Principles of Colloid and Surface Chemistry," Marcel Dekker, New York, 1986.

2. Shaw, D.J., "Introduction to Colloid and Surface Chemistry," Butterworths, London, 1980.

3. Hoar, T.P., and Schulman, J.H., Nature, 152, 102 (1943).

4. Eicke, H.F., J. Colloid Interface Sci., 68, 440 (1979).

5. Cebula, D.J., Myers, D.Y., and Ottewill, R.H., Colloid & Polymer Science, 260, 96 (1982).

6. Prince, L.M., "Microemulsions : Theory and Practice," Academic Press, New York, 1977.

7. Mitchell, D.J., and Ninham, B.W., J. Phys. Chem., 87, 2996 (1983).

8. deGennes, P.G., and Taupin, C., J. Phys. Chem., 86, 2294 (1982).

9. Talmon, Y., and Prager, S., J. Chem. Phys., 69, 2984 (1978).

10. Scriven, L.E., Nature, 263, 2984 (1976).

11. Winsor, P.A., Trans. Faraday Soc., 44, 376 (1948).

12. Widom, B., J. Chem. Phys., 81, 1030 (1984).

13. Shah, D.O., ed., "Surface Phenomena in Enhanced Oil Recovery," Plenum, New York, 1982.

14. Taber, J.J., Pure & Appl. Chem., 52, 1323 (1980).

15. Fendler, J.H., and Fendler, E.J., "Catalysis in Micellar and Macromolecular Systems," Academic Press, New York, 1975.

16. LePesant, J.P., and Tantot, G., (Hotchkins-Brandt Sogeme H.B.S.), Eur. Patent Appl. EP 36,790 (1981).

17. Robbins, M.L., and Brownawell, D.W., (Esso Res. and Eng. Co.), U.S. Patent 3,641,181 (1972).

18. Mackay, R.A., Adv. Colloid Interface Sci., 15, 131 (1981).

19. Jones, C.E., and Mackay, R.A., J. Phys. Chem., 82, 63

(1978).

20. Jones, C.E., and Mackay, R.A., J. Phys. Chem., 83, 803 (1979).

21. Kiwi, J., and Graetzel, M., J. Phys. Chem., 84, 1503 (1980).

22. Atik, S.S., and Thomas, J.K., J. Am. Chem. Soc., 103, 3543 (1981).

23. Atik, S.S., and Thomas, J.K., J. Am. Chem. Soc., 103, 4367 (1981).

24. Tang, H.I., Johnson, P.L., and Gulari, E., in "Measurement of Suspended Particles by Quasi-Elastic Light Scattering," B.E. Dahneke, ed., Wiley, New York, 1983.

25. Candau, F., Leong, Y.S., Pouget, G., and Candau, S., J. Colloid Interface Sci., 101, 167 (1984).

26. Lianos, P., J. Phys. Chem., 86, 1935 (1982).

27. Leong, Y.S., and Candau, F., J. Phys. Chem., 86, 2269 (1982).

28. Boutonnet, M., Kizling, J., Stenius, P., and Marie, G., Colloids and Surfaces, 5, 209 (1982).

29. Candau, F., Zekhnini, Z., and Durand, J.-P., J. Colloid Interface Sci., 114, 398 (1986).

30. Schauber, C., and Riess, G., Polym. Mater. Sci. Eng., 57, 945 (1987).

31. Beckman, E.J., and Smith, R.D., J. Phys. Chem., 94, 345 (1990).

32. Petit, C., and Pileni, M.P., J. Phys. Chem., 92, 2282 (1988).

33. Lianos, P., and Thomas, J.K., Chem. Phys. Lett., 125, 299 (1986).

34. Lianos, P., and Thomas, J.K., J. Colloid Interface Sci., 117, 505 (1987).

35. Dannhauser, T., O'Neal, M., Johansson, K., Whitten, D., and McLennon, G., J. Phys. Chem., 90, 6074 (1986).

36. Steigewald, M.L., Alirisatos, A.P., Gibson, J.M., Harris, T.D., Korten, R., Muller, A.J., Thoyer, A.M., Duncan, T.M., Douglas, D.C., and Brus, L.E., J. Am. Chem. Soc.,

110, 3046 (1988).

37. Petit, C., Lixon, P., and Pileni, M.P., J. Phys. Chem., 94, 1598 (1990).

38. Petit, C., Brochette, P., and Pileni, M.P., J. Phys. Chem., 90, 6517 (1986).

39. Tanquary, A.C., and Lacey, R.E., eds., "Controlled Release of Biologically Active Agents," Plenum, New York, 1974.

40. Ziegenmeyer, J., and Fuehrer, C., Acta Pharm. Technol., 26, 273 (1980).

41. Fubini, B., Gasco, M.R., and Gallarate, M., Int. J. Pharm., 42, 19 (1988).

42. Halbert, G.W., Stuart, J.F.B., and Florence, A.T., Int. J. Pharm., 21, 219 (1984).

43. Tondre, C., and Xenakis, A., Colloid & Polymer Sci., 260, 232 (1982).

44. Tondre, C., and Xenakis, A., Faraday Discuss. Chem. Soc., 77, 115 (1984).

45. Xenakis, A., and Tondre, C., J. Phys. Chem., 87, 4737 (1983).

46. Xenakis, A., and Tondre, C., J. Colloid Interface Sci., 117, 442 (1987).

47. Kim, H.S., and Tondre, C., Sep. Sci. Technol., 24, 485 (1989).

48. Tondre, C., and Derouiche, A., J. Phys. Chem., 94, 1624 (1990).

49. Derouiche, A., and Tondre, C., J. Chem. Soc., Faraday Trans. I, 85, 3301 (1989).

50. Eicke, H.F., Shepard, J.C., and Steinman, A.J., J. Colloid Interface Sci., 56, 168 (1975).

51. Robinson, B., in "Surfactants in Solution," K.L. Mittal, ed., Plenum, New York, 1984.

52. Lang, J., Jada, A., and Malliaris, A., J. Phys. Chem., 92, 1946 (1988).

53. Fletcher, P.D.I., Howe, A.M., and Robinson, B.H., J. Chem. Soc. Faraday Trans. I, 83, 185 (1987).

54. Howe, A.M., McDonald, J.A., and Robinson, B.H., J. Chem. Soc. Faraday Trans. I, 83, 1007 (1987).

55. Jada, A., Lang, J., Zana, R., Makhloufi, R., Hirsch, E., and Candau, S.J., J. Phys. Chem., 94, 387 (1990).

56. Bedwell, B., and Gulari, E., J. Colloid Interface Sci., 102, 88 (1984).

57. Hou, M.J., Kim, M., and Shah, D.O., J. Colloid Interface Sci., 123, 398 (1988).

58. Cazabat, A.M., Chatenay, D., Langevin, D., and Pouchelon, A., J. Physique Lett., 41, 441 (1980).

59. Agterof, W.G.M., van Zomeren, J.A.J., and Vrij, A., Chem. Phys. Lett., 43, 363 (1976).

60. Calje, A.A., Agterof, W.G.M., and Vrij, A., in "Micellization, Solubilization and Microemulsions," K.L. Mittal, ed., Plenum, New York, 1977.

61. Cazabat, A.M., Langevin, D., and Pouchelon, A., J. Colloid Interface Sci., 73, 1 (1980).

62. Cazabat, A.M., and Langevin, D., J. Chem. Phys., 74, 3148 (1981).

63. Gulari, E., Bedwell, B., and Alkhafaji, S., J. Colloid Interface Sci., 77, 202 (1980).

64. Hou, M.J., and Shah, D.O., Langmuir, 3, 1086 (1987).

65. Leung, R., and Shah, D.O., J. Colloid Interface Sci., 120, 320 (1987).

66. Leung, R., and Shah, D.O., J. Colloid Interface Sci., 120, 330 (1987).

67. Cebula, D.J., Ottewill, R.H., Ralston, G., and Pusey, P.N., J. Chem. Soc. Faraday Trans. I, 77, 2585 (1981).

68. Dvolaitzky, M., Guyot, M., Lagues, M., Lepesant, J.P., Ober, R., Sauterey, C., and Taupin, C., J. Chem. Phys., 69, 3279 (1978).

69. Ober, R., and Taupin, C., J. Phys. Chem., 84, 2418 (1980).

70. Atik, S., and Thomas, J.K., J. Phys. Chem., 85, 3921 (1981).

71. Jada, A., Lang, J., and Zana, R., J. Phys. Chem., 94, 381

(1990).

72. de Rozieres, J., Middleton, M.A., and Schechter, R.S., J. Colloid Interface Sci., 124, 407 (1988).

73. Hayter, J.B., and Penfold, J., Mol. Phys., 42, 109 (1981).

74. Hayter, J.B., and Penfold, J., J. Chem. Soc. Faraday Trans. I, 77, 1851 (1981).

75. Feynman, R.P., Leighton, R.B., and Sands, M., "The Feynman Lectures on Physics," Addison-Wesley, Reading, Mass., 1964.

76. Metropolis, N., Rosenbluth, A.W., Rosenbluth, M.N., Teller, A.H., and Teller, E., J. Chem. Phys., 21, 1087 (1953).

77. Binder, K., ed., "Applications of the Monte Carlo Method," Springer-Verlag, New York, 1983.

78. Heermann, D.W., "Computer Simulation Methods in Theoretical Physics," Springer-Verlag, New York, 1986.

79. Barker, J.A., and Henderson, D., J. Chem. Phys., 47, 2856 (1967).

80. Barker, J.A., and Henderson, D., J. Chem. Phys., 47, 4714 (1967).

81. Martin, C.A., and Magid, L.J., J. Phys. Chem., 85, 3938 (1981).

82. Wong, M., Thomas, J.K., and Nowak, T., J. Am. Chem. Soc., 99, 4730 (1977).

83. Kotlarchyk, M., Chen, S.H., and Huang, J.S., J. Phys. Chem., 86, 3273 (1982).

84. Kotlarchyk, M., Chen, S.H., Huang, J.S., and Kim, M.W., Phys. Rev. A, 29, 2054 (1984).

85. Kotlarchyk, M., Huang, J.S., and Chen, S.H., J. Phys. Chem., 89, 4382 (1985).

86. Robinson, B.H., Toprakcioglu, C., Dore, J.C., and Chieux, P., J. Chem. Soc. Faraday Trans. I, 80, 13 (1984).

87. Toprakcioglu, C., Dore, J.C., Robinson, B.H., and Howe, A., J. Chem. Soc. Faraday Trans. I, 80, 413 (1984).

88. Cabos, C., and Marignan, J., J. Phys. Lett., 46, L-267

(1985).

89. Pileni, M.P., Zemb, T., and Petit, C., Chem. Phys. Lett., 118, 414 (1985).

90. Assih, T., Larche, F., and Delord, P., J. Colloid Interface Sci., 89, 35 (1982).

91. Kuneida, H., and Shinoda, K., J. Colloid Interface Sci., 33, 215 (1970).

92. Peyrelasse, J., and Boned, C., J. Phys. Chem., 89, 370 (1985).

93. Henze, R., and Schreiber, U., Colloid & Polymer Sci., 263, 164 (1985).

94. Gestblom, B., and Sjoblom, J., Langmuir, 4, 360 (1988).

95. Ganz, A.M., and Boeger, B.E., J. Colloid Interface Sci., 109, 504 (1986).

96. D'Arrigo, A., Paparelli, A., D'Aprano, A., Donato, I.D., Goffredi, M., and Turco Liveri, V., J. Phys. Chem., 93, 8367 (1989).

97. Eicke, H.F., Borkovec, M., and Das-Gupta, B., J. Phys. Chem., 93, 314 (1989).

98. Hall, D.G., J. Phys. Chem., 94, 429 (1990).

CHAPTER 2

Simulations of Water-in-Oil Microemulsions I: Monte Carlo Calculations of Dipole Moment Distributions and Polarizabilities.

ABSTRACT

Monte Carlo simulations are performed on a model water-in-oil microemulsion system. The model microemulsions considered here is composed of water, oil, a non-ionic surfactant, and NaCl. From the spatial distribution of ions within the droplets' aqueous cores, the dipole moment distributions are determined for droplets containing from one to thirty NaCl ion pairs. Perturbation of the system with a small external dipole allows the magnitude of the induced dipole moment and the zero-frequency polarizability to be determined. Beyond a critical point, possibly because of electrostatic stabilization, the value of the induced dipole is found to decrease with increasing ionic concentration. In the interdroplet potential proposed, dipole-induced dipole interactions are shown to be dominant over both dipole-dipole interactions and the droplets' molecular van der Waals interactions. Thus, the overall attractions between droplets are found to at first increase with increasing ionic strength and then decrease with the further addition of salt, a result in agreement with experimental findings.

I. INTRODUCTION

Depending on the system and the relative concentrations of oil and water, microemulsions can display a wide variety of microstructures and behaviors[1]. These microstructures range from dispersions of monodisperse spherical droplets[1] to polydisperse bicontinuous structures[2-3]. The present work addresses the so called water-in-oil microemulsion system. Over a fairly wide concentration range, this system can effectively be described as a stable collection of monodisperse "water" microdroplets in an oil continuous phase.

Because of their potential application in a wide range of technologies, especially in enhanced oil recovery[4], such W/O systems have received considerable attention. In particular, interdroplet interactions has been the subject of a number of investigations[5-18]. The motivation for these studies is to gain a sufficiently accurate understanding of various phenomena ranging from the thermodynamic and transport properties to local ordering and structures in microemulsions. All these effects are influenced strongly by interdroplet interactions.

In most of the above studies[5-15], interacting colloidal dispersions have been treated as macroscopic analogies of simple atomic and molecular fluids, allowing statistical

mechanics of simple fluids to be applied to the microemulsion dispersions. Typically, the interaction behavior of the particles is described by a hard sphere potential[19], perturbed by a small supplementary attractive force[20-21]. In these investigations, the interdroplet potential are generally obtained by fitting a suitable functional form such as square well potential[6-7,9,12-13] or Yukawa potential[10-11] to the equilibrium osmotic compressibility and viscosity data. Few attempts[16-18] have been made to create an interdroplet potential based on theoretical considerations alone. Consequently, despite an abundance of excellent experimental data, no one has yet been able to generate an accurate and verifiable model of interparticle interactions in microemulsions.

deRozieres and coworkers[16] made the first concerted attempt to establish such theoretical potential function. In their model, the mobile surfactant counterions are located in the aqueous core of a water-in-oil microemulsion droplet. Placing the droplet in an applied electric field, the counterions in the aqueous core moved in response to the imposed field and as a consequence polarization of the droplet occurred. Thus, they conclude the interaction between droplets is essentially due to an induced dipole - induced dipole attraction. Nevertheless, because of symmetry considerations, their use of a continuum approach to describe the distribution of counterions in water core is quite

questionable. Moreover, the complex permittivity data obtained could not be readily translated into interdroplet potential or any other equilibrium or transport properties such as osmotic compressibility or diffusion coefficient. Using a different approach, Eicke et. al.[17] and Hall[18] proposed that the migration of fluctuating charged droplets is responsible for the interactions. Again, the relationship between the conductivity and the interactions is not well established. However, the biggest drawback of these models is their inability to account for the peculiar behavior of electrolyte moderated interactions[8-9] observed in W/O microemulsions, viz., the attraction between droplets decrease with increasing electrolyte concentration.

From basic principles of statistical mechanics, it is expected that when the number of ions in the water core is small, a sizable dipole moment should arise from the non-symmetrical arrangement of those ions. The existence of such a dipole moment could lead to dipole-dipole and dipole-induced dipole attractive forces between microemulsion droplets. To calculate the magnitude of the interaction energy $U_a(r)$ based on these dipole attractive forces, the Keesom equation[22] (dipole-dipole) and the Debye equation[22] (dipole-induced dipole) can be employed. Prior to applying these equations, however, two parameters, dipole moment p and polarizability α, first have to be determined.

The work presented here has two objectives. The first is to determine the magnitude of what we will call the "configurational dipole moment" as a function of droplet size and ion concentration. The second objective is to determine the polarizability of the droplet by monitoring the change in the dipole moment when the droplet is subject to an applied electric field. To meet these objectives, equilibrium ionic distributions in the water core of W/O microemulsion droplets are generated by the Metropolis Monte Carlo method[23-25], a widely used stochastic technique that allows accurate calculations of equilibrium properties. We begin, in section II, by introducing the model system and giving a brief review on the simulation procedures. Section III contains the results and the discussions. The spatial distribution is described in terms of a configurational dipole moment. The existence of an induced dipole moment and the corresponding polarizability is also analyzed. Construction of an interdroplet potential function based on the various dipole interactions complete this section. The final section summarizes the conclusions drawn from the results.

II. MODEL AND COMPUTER SIMULATIONS

The model system (fig.1) used in this work consists of a spherical aqueous core comprising equal number of sodium and chloride ions. The surrounding surfactant interface and the nonpolar (oil) region are treated as a continuum. While the

model system bears a close resemblance to a W/O microemulsion droplet, it does assume the interfacial surfactant region has no effect on the long-range interdroplet interactions and thus considers it to be part of the surrounding nonpolar continuum.

Inside the water core, interactions among the ions are evaluated explicitly according to the restrictive primitive model[26]. That is, all ions are assumed to be hard spheres of equal diameter, σ_{HS} , and the solvent, water in this case, is represented as a continuous medium of uniform dielectric constant ϵ_{H_2O} . In addition, the potentials are assumed to be purely coulombic and pairwise additive. Thus, the interionic potential of mean force (PMF), $U_{ij}(r)$, between ions i and j having respective charges of q_i and q_j can be expressed as

$$U_{ij}(r) = \infty \quad \text{for} \quad r < \sigma_{HS} \qquad \ldots (1)$$

$$= \frac{q_i q_j}{4 \pi \epsilon_0 \epsilon_{H_2O} r} \quad \text{for} \quad r > \sigma_{HS}$$

and the total potential energy of the system is therefore

$$U_N = \sum_{i>j}^{n} \frac{q_i q_j}{4 \pi \epsilon_0 \epsilon_{H_2O} | r_i - r_j |} \qquad \ldots (2)$$

While interionic PMF based on the more realistic RISM[27-28] solution model have better qualitative agreement with experimental data, their quantitative accuracy have been questioned[29] and different studies led to different results. It is also suggested that results from Coulomb's law are correct to within a few percent of these molecular approach[29], a fact confirmed by our preliminary calculations. Thus, for computational simplicity, the restricted primitive model is chosen in this study.

In this work, the simulations were performed in an NVT ensemble (number of particles, volume and temperature constant). The water core of the microemulsion droplet was modeled by a spherical simulation cell bounded by hard, structureless walls. Spherical radii of 25 A and 15 A were considered. One to thirty ion pairs were present in the cell. Each ion was modeled as a hard sphere of radius 1.50 A with the appropriate charge located at the center of the ionic sphere. Due to the small size of the system and the small number of ions involved, it was not necessary to impose the customary periodic boundary condition. Instead, a non-standard boundary condition[25] was applied where the entry and exit of ions from the water core is prohibited. This procedure allows the equilibrium properties to be obtained by averaging over the entire system rather than just a small fraction of the system as is usually the case.

The Metropolis Monte Carlo method is an importance sampling technique that utilizes the theory of the Markov chain. The calculation is initiated by placing a certain number of ions in a random configuration in the aqueous core. Interacting through the pair potential given in eqn.(1), the particles move through the phase space by a random walk with certain restrictions placed on the movements. As a consequence, a very large number of configurations representative of equilibrium are generated. The sequence of states possesses the following characteristics: First, it has a lack of memory. That is, the conditional probability can be represented as

$$P (\underline{X}_n \ \underline{X}_{n-1}, \cdots \underline{X}_0) = P (\underline{X}_n \ \underline{X}_{n-1}) \qquad \cdots (3)$$

The transition probabilities from one state $\underline{X}$ of the system to a state $\underline{X}'$ are restricted by

$$\sum_{\underline{X}'} W (\underline{X} , \underline{X}') = 1 \qquad \cdots (4)$$

Finally, the configurations or states, S, generated have probability densities given by

$$\varphi(S) = \frac{\exp [-\beta U(S)]}{\int \exp [-\beta U(S)] dS} \qquad \cdots (5)$$

where $\beta = 1/kT$ and $U(S)$ = potential at state S.

The properties reported in this paper are obtained by averaging four runs, each with one million configurations. During each of those runs, the first one-half million configurations are discarded to reduce the initial configuration effect. To demonstrate that the initial configuration effect has indeed been eliminated, the average dipole moment for 1 pair and 4 pairs of ions are plotted against the number of configurations in figures 2 and 3 respectively. It is apparent that the initial fluctuations quickly die down after several hundred thousand configurations and the average dipole moment approach an equilibrium value. In figure 4, results of all 4 runs for 1 pair of ions are plotted. Despite the vast discrepancies observed during the first several hundred thousand configurations, the average dipole moments from all 4 runs rapidly converge to an equilibrium value. From these plots, we can confidently conclude that our choice of number of configurations is reasonable and the initial effect could be eliminated by discarding the first one-half million configurations.

III. RESULTS AND DISCUSSIONS

A. Ionic Distribution

The most direct result from our present Monte Carlo simulation is the ionic distribution. i.e. the probability of finding the ions at a certain distance apart. Figure 5 is a

plot of such distribution for 1 pair of ions. Besides the simulation data, results from an approximate analytical calculation that combine Boltzmann's distribution law with Coulomb's expression is also plotted in the same figure. The results from both methods are quite similar, especially when the separation distance is small. The Monte Carlo method, however, yields a larger probability at medium separation distance, from about 5 A to 17 A, and a lower probability at large distance than did the approximate analytical method. This discrepancy is not unexpected however. For oppositely charged ions, the smaller the separation distance, the larger is its probability as this is energetically more favorable. The greatest probability should correspond to a state where the two ions are apart by a length of hard sphere diameter, the lowest potential energy available. In a restricted volume such as a microemulsion droplet, entropic effects should also be taken into consideration. This effect, however, is completely ignored in the approximate method as the Boltzmann distribution is assumed for distances up to infinity.

The medium separation distances are the entropically more favorable states as more configurations are associated with them than with either extreme distances. Thus, in this region, the probabilities should be larger than those calculated by the approximate method. In the case of large ionic separation, both energetic and entropic effects are unfavorable. Consequently, their actual values should be

lower than that calculated by approximate method. The Monte Carlo method correctly accounts for the entropic as well as the energetic effects, and therefore it is far superior to the approximate analytical technique.

B. Dipole Moment

For an assembly of charges located in a certain limited region, the dipole moment, p, can be defined as[24]

$$p = \sum_i q_i d_i \qquad \ldots (6)$$

where d_i is the displacement of charge i from the reference point. In the present system, the center of the water core is conveniently chosen as this point. Figure 6 is a comparison of the effective dipole length distribution for 1, 2, 4, and 8 pair of ions respectively. When there is more than 1 pair of ions in the aqueous core, the effective dipole length approaches a gaussian distribution. This is to be expected as the entropic effect should increase rapidly with the number of ion pairs present. Increasing the number of ions shifts the distribution curve to the larger dipole length region and increases the average dipole moment of the system.

Utilizing eqn.(6), the dipole moment distribution is readily available by multiplying the ionic distribution with charge q_i. The average dipole moment could then be evaluated

by finding the mean of the dipole distribution.

Figure 7 shows the average configurational dipole moment plotted against the number of ion pairs in the core. The average dipole moment increases with increasing ionic concentration. The rate of the increase, however, is not linear. The dipole moment increases sharply at low ion concentrations but is nearly constant when a large number of ions are present. This result can be explained by basic principles of statistical mechanics. Consider the analogy of two different type of gas molecules in a box. When there are a large number of molecules present, the probability that the two types would be separated at opposite ends of the box at the same instant is vanishingly small. Rather, the most probable state would correspond to a uniform mixing of the two type of molecules. The same probability law holds in the liquid state as well. In addition, the electrostatic attraction between oppositely charged ions and the repulsion between ions of the same charge is rather formidable. Obviously when the number of ions is large, the formation of a large dipole moment is unlikely as it correspond to a state where ions of the same sign being held close to each other while opposite sign ions are all far apart. Thus, increasing the ions at high ionic concentration should not dramatically increase the dipole moment.

The magnitude of dipole generated seems to have a linear

relationship with the size of the water core. In fact, by defining a dimensionless, reduced dipole moment, pr

$$p_r = p / (q * r) \qquad \ldots (7)$$

where r is radius of droplet and q is $1.602 * 10^{-19}$ Coulomb, the data in figure 7 can recalculated and plotted as shown in figure 8. The reduced dipole moments from the different size droplets are nearly identical. This suggests that the magnitude of dipole moment is directly proportional to the size of the droplet. Otherwise, the dependence of the configurational dipole moment on the ionic concentration is about the same for both size droplets.

B. Polarizability and induced dipole moment

In addition to dipole-dipole interactions, the electric field from a dipole can result in a polarizing force on ions in nearby droplets. The result would be a dipole-induced dipole type attraction. From electromagnetic theory, the polarizability α of a particle is defined according to the strength of the induced dipole moment p_{ind} acquired in an applied field E:

$$\alpha = p_{ind} / E \qquad \ldots (8)$$

To determine the behavior of the induced dipole moment

and thus the polarizability of a W/O microemulsion droplet, an additional set of Monte Carlo calculations were performed. The procedures used for this computation are similar to those used in the previous computations except for the addition of a term to the interaction potential. The external field used in the new Monte Carlo calculations should be large enough to allow for accurate measurement of the induced dipole, yet at the same time should cause only a small perturbation within the droplet. To account for the polarizing force acting on the individual ions by the external electric field, the total potential energy of the system have been modified. Instead of equation 2, the potential

$$U_N = \sum_{i>j} \frac{q_i q_j}{4\pi\varepsilon_0\varepsilon_{eff}|r_i - r_j|} + \sum_i \frac{p_{ext} \cdot q_i}{4\pi\varepsilon\varepsilon_{eff} l_i^2} \quad \ldots (9)$$

was used, where ε_{eff} is the effective dielectric constant of the interacting medium, p_{ext} is the external dipole moment, and l_i is the distance of external dipole from ion i. As discussed in the previous section, the first term of this potential is due to the interionic interactions based on the pairwise additive Coulomb approach. In the presence of an applied electric field, the pair electrostatic interaction energy between ions and this external field is give by the second term of equation 9. The effective dielectric constant, ε_{eff}, of the interacting medium is expressed as

$$\varepsilon_{eff} = (\varepsilon_{H2O}^{1/3} X_{H2O} + \varepsilon_{oil}^{1/3} X_{oil})^3 \ldots (9a)$$

where X_{H2O} is the volume fraction of water and X_{oil} is the volume fraction of oil.

The result generated from these calculations is the superposition of the induced dipole moment upon the configurational dipole moment. The induced dipole moment is then obtained by subtracting the configurational dipole moment from this value. Using equation 8, the zero frequency polarizability can be calculated from this induce dipole moment. The polarizability is plotted as a function of number of ions in figure 9.

An interesting characteristic of the polarizability is apparent in figure 9. In contrast to the configurational dipole moment, increasing the number of ions (increasing ionic concentration) only increases the induced dipole moment up to a certain point. Beyond that, additional ions will decrease the magnitude of induced dipole generated in a W/O microemulsion droplet. While this result may be counter-intuitive, it is reasonable given the physical situation. The presence of an external field will polarize the ions, causing oppositely charged ions to move apart from each other and creating an induced dipole moment, explaining the initial increase in induced dipole moment. However, increasing the ionic concentration will pack the ions closer to each other. A critical stage will eventually be reached where the ionic separation distance is close enough for the short range

coulombic attraction to dominate over any external polarizing force. Essentially, local ordering is created within the aqueous core because of this electrostatic stabilization. Hence, beyond this critical point, adding to the number of ions will actually increase the level of electrostatic stabilization and further decrease the magnitude of induced dipole moment generated.

C. Interdroplet Potential

As discussed in previous sections, the Monte Carlo results suggest the existence of a dipole moment and polarizability in a W/O microemulsion droplet resulting from the asymmetric arrangement of ions within the aqueous core. In this section, an interdroplet potential function based on these concepts will be formulated.

Treating the interacting colloidal dispersions as macroscopic analogues of simple atomic and molecular fluids, perturbation theory[19-21] is applied to the present problem. In this approach, the interaction forces are treated as a perturbation to the hard sphere potential. In short, the interacting energy U(r) is separated into two parts, a reference part, $U_{hs}(r)$, and a perturbation part, $U_a(r)$.

$$U(r) = U_{hs}(r) + U_a(r) \qquad \ldots (10)$$

The hard sphere potential of mean force $U_{hs}(r)$ is given by

$$U_{hs}(r) = \infty \quad \text{for} \quad r < \sigma_{HS}$$
$$= 0 \quad \text{for} \quad r > \sigma_{HS} \qquad \ldots (11)$$

For two droplets with identical dipole moment p_1, the dipole interaction energy is given by[22]

$$U_1(r) = \frac{p_1^2 p_1^2}{3(4\pi\varepsilon_0\varepsilon_{oil})^2 kT r^6} \qquad \ldots (12)$$

where k=boltzmann constant, T= temperature,

ε_{oil} = dielectric constant of the nonpolar medium

For two droplets with dipole moment p_1 and polarizability α, the dipole-induced dipole interaction is given by[22] :

$$U_2(r) = \frac{2 p_1^2 \alpha}{(4\pi\varepsilon_0\varepsilon_{oil})^2 r^6} \qquad \ldots (13)$$

In the present work, the perturbation part is assumed to be caused by the dipole-dipole and dipole-induced dipole interactions only. Hence, $U_a(r)$ in equation 10 is :

$$U_a(r) = \frac{p_1^2}{(4\pi\varepsilon_0\varepsilon_{oil})^2 r^6}\left(\frac{p_1^2}{3kT} + 2\alpha\right) \qquad \ldots (14)$$

Figure 10 is a plot of this perturbation potential for 1 pair of ions against distance while figure 11 plots the same

potential against number of ions at a separation distance of 100 A. These two plots clearly show that the dipole-induced dipole attraction is about an order of magnitude larger than the dipole-dipole attraction force. Since the dipole-induced dipole attraction term is directly proportional to the polarizability, the electrostatic stabilization characteristic is therefore also observed in the total perturbation potential, i.e., decreasing attraction with increasing number of ions beyond a critical point. The behavior is even more apparent when the perturbation potential is plotted against distance for various number of ions in figure 12. Again, it is clearly demonstrated that attractive potential will decrease beyond a critical ionic concentrations. This is in qualitative agreement with experimental data obtained by Bedwell[8] and Hou[9], and may explain the origin of the electrolyte moderated interactions they have observed.

IV. CONCLUSIONS

We have performed Monte Carlo simulations on a W/O microemulsion system. Analysis of the results suggest that the non-symmetrical arrangement of ions in the aqueous core of such reversed micelle can give rise to a dipole moment. This dipole moment can in turn induce an additional dipole in the neighboring particles.

While the dipole moment generally increases with

increasing ionic concentration within the aqueous core, the same cannot be said about the induced dipole moment. Beyond a critical ionic concentration, possibly because of electrostatic stabilization, increasing the number of ions decreases the induced dipole moment and consequently the polarizability.

Finally, an interdroplet potential function based on the dipole attractive force is proposed. It is found that the dipole-induced dipole attraction is much more significant than the corresponding dipole-dipole interactions. Consequently, the electrostatic stabilization phenomenon at higher ionic concentration is observed. The current result is qualitatively in agreement with the experimental data.

BIBLIOGRAPHY

1. Prince, L.M., "Microemulsions : Theory and Practice," Academic Press, New York, 1977.

2. Scriven, L.E., Nature, 263, 2984 (1976).

3. Talmon, Y., and Prager, S., J. Chem. Phys., 69, 2984 (1978).

4. Shah, D.O., ed., "Surface Phenomena in Enhanced Oil Recovery," Plenum, New York, 1982.

5. Cazabat, A.M., and Langevin, D., J. Chem. Phys., 74, 3178 (1981).

6. Agterof, W.G.M., van Zomeren, J.A.J., and Vrij, A., Chem. Phys. Lett., 43, 363 (1976).

7. Calje, A.A., Agterof, W.G.M., and Vrij, A., in "Micellization, Solubilization and Microemulsions," K.L. Mittal, ed., Plenum, New York, 1977.

8. Bedwell, B., and Gulari, E., J. Colloid Interface Sci., 102, 88 (1984).

9. Hou, M.J., Kim, M., and Shah, D.O., J. Colloid Interface Sci., 123, 398 (1988).

10. Hayter, J.B., and Penfold, J., Mol. Phys., 42, 109 (1981).

11. Hayter, J.B., and Penfold, J., J. Chem. Soc. Faraday Trans. I, 77, 1851 (1981).

12. Leung, R., and Shah, D.O., J. Colloid Interface Sci., 120, 320 (1987).

13. Leung, R., and Shah, D.O., J. Colloid Interface Sci., 120, 330 (1987).

14. Jada, A., Lang, J., and Zana, R., J. Phys. Chem., 94, 381 (1990).

15. Waaler, D., Strand, K.A., Stromme, G., and Sikkeland, T., J. Chem. Phys., 91, 3360 (1989).

16. de Rozieres, J., Middleton, M.A., and Schechter, R.S., J. Colloid Interface Sci., 124, 407 (1988).

17. Eicke, H.F., Borkovec, M., and Das-Gupta, B., J. Phys. Chem., 93, 314 (1989).

18. Hall, D.G., J. Phys. Chem., 94, 429 (1990).

19. Barker, J.A., and Henderson, D., Mol. Phys., 21, 187 (1971).

20. Barker, J.A., and Henderson, D., J. Chem. Phys., 47, 2856 (1967).

21. Barker, J.A., and Henderson, D., J. Chem. Phys., 47, 4714 (1967).

22. Israelachvili, J.N., "Intermolecular and Surface Forces," Academic Press, London, 1985.

23. Metropolis, N., Rosenbluth, A.W., Rosenbluth, M.N., Teller, A.H., and Teller, E., J. Chem. Phys., 21, 1087 (1953).

24. Binder, K., ed., "Applications of the Monte Carlo Method," Springer-Verlag, New York, 1983.

25. Heermann, D.W., "Computer Simulation Methods in Theoretical Physics," Springer-Verlag, New York, 1986.

26. McQuarrie, D.A., "Statistical Mechanics," Harper & Row, New York, 1976.

27. Pettitt, B.M., and Rossky, P.J., J. Chem. Phys., 84, 5836 (1986).

28. Kusalick, P.G., and Patey, G.N., J. Chem. Phys., 88, 7715 (1988).

29. Rashin, A.A., J. Phys. Chem., 93, 4664 (1989).

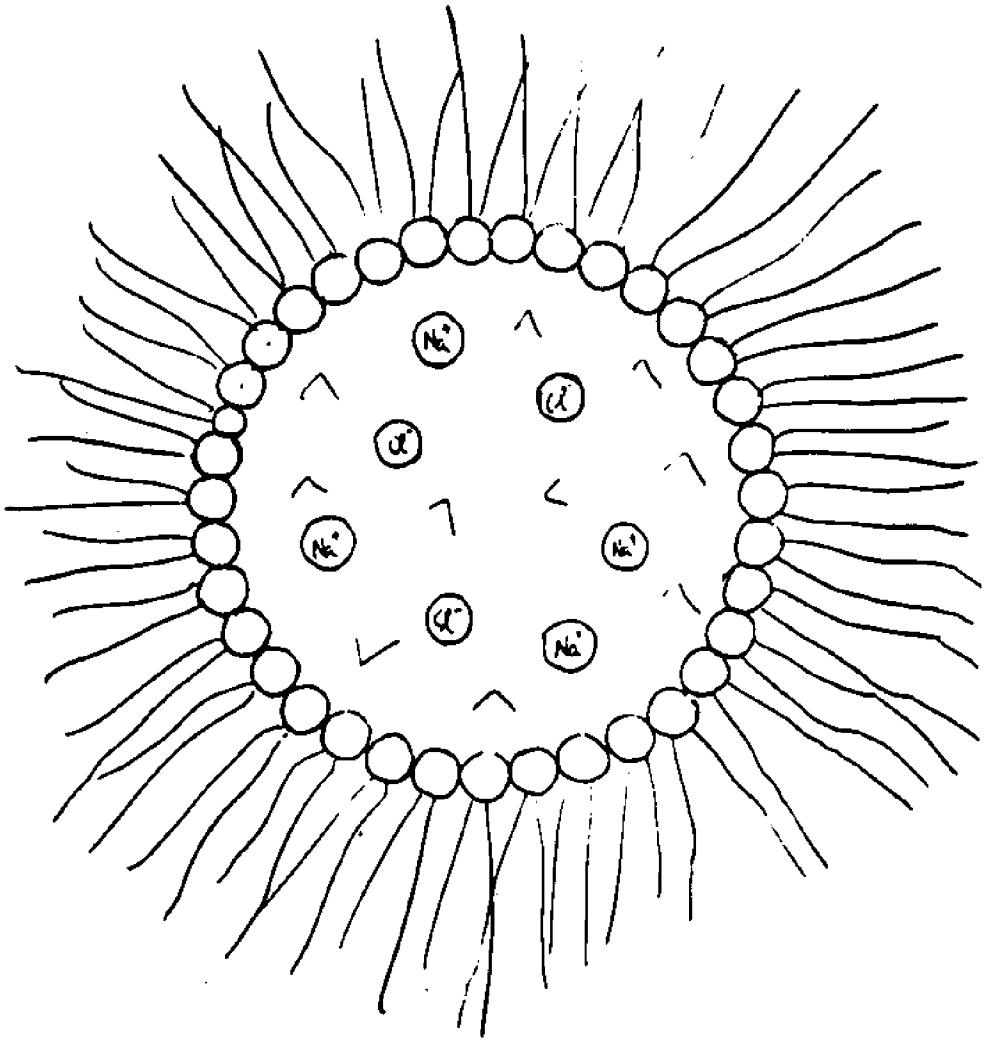

FIG. 2-1 Schematic description of a W/O microemulsion droplet

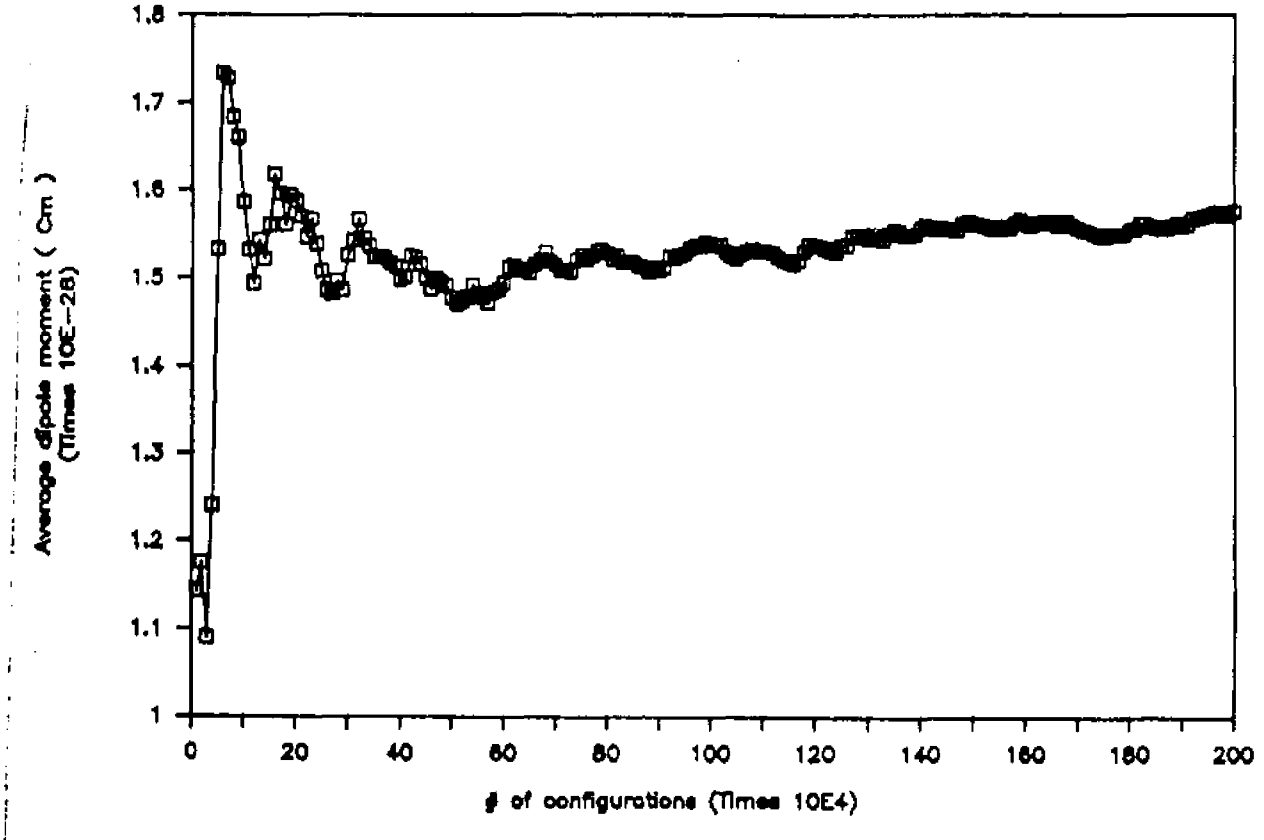

FIG. 2-2 Average dipole moment vs. number of configurations for 1 pair of ions

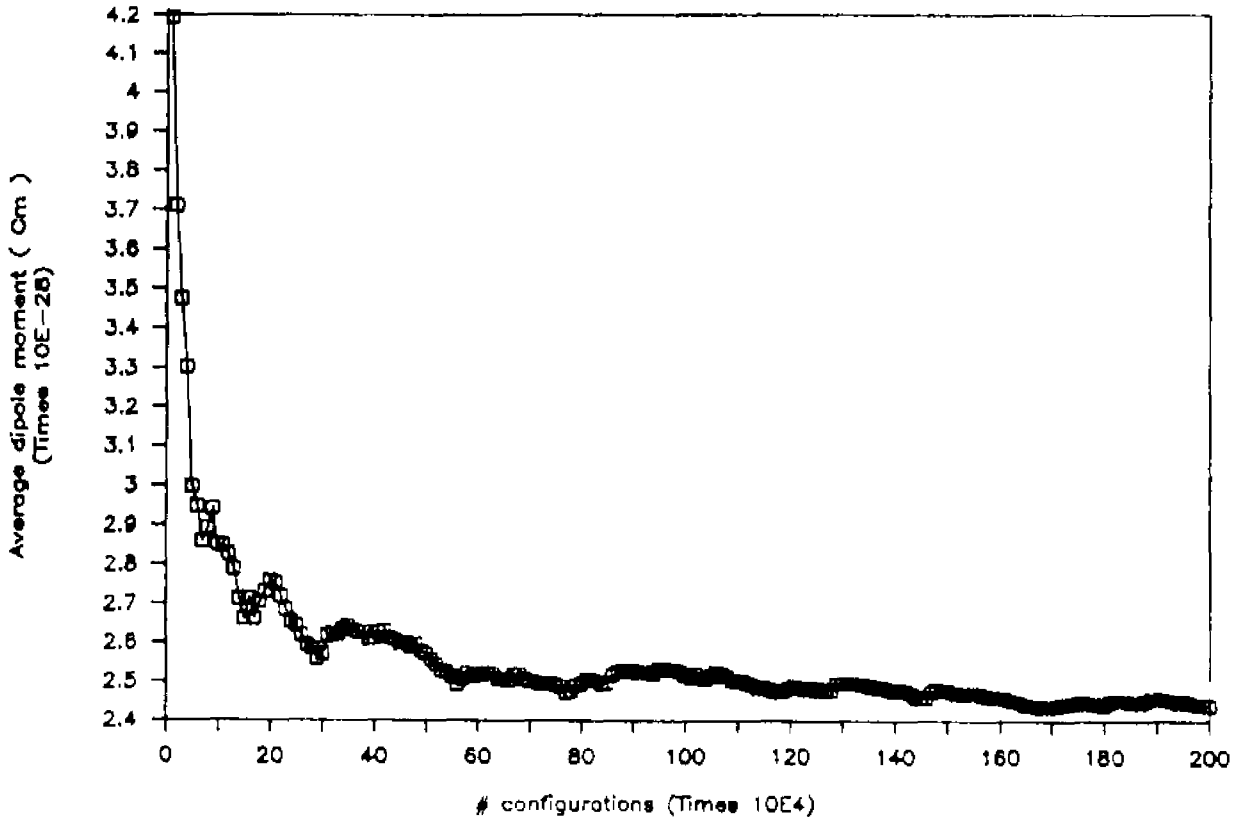

FIG. 2-3 Average dipole moment against number of configurations for 4 pair of ions

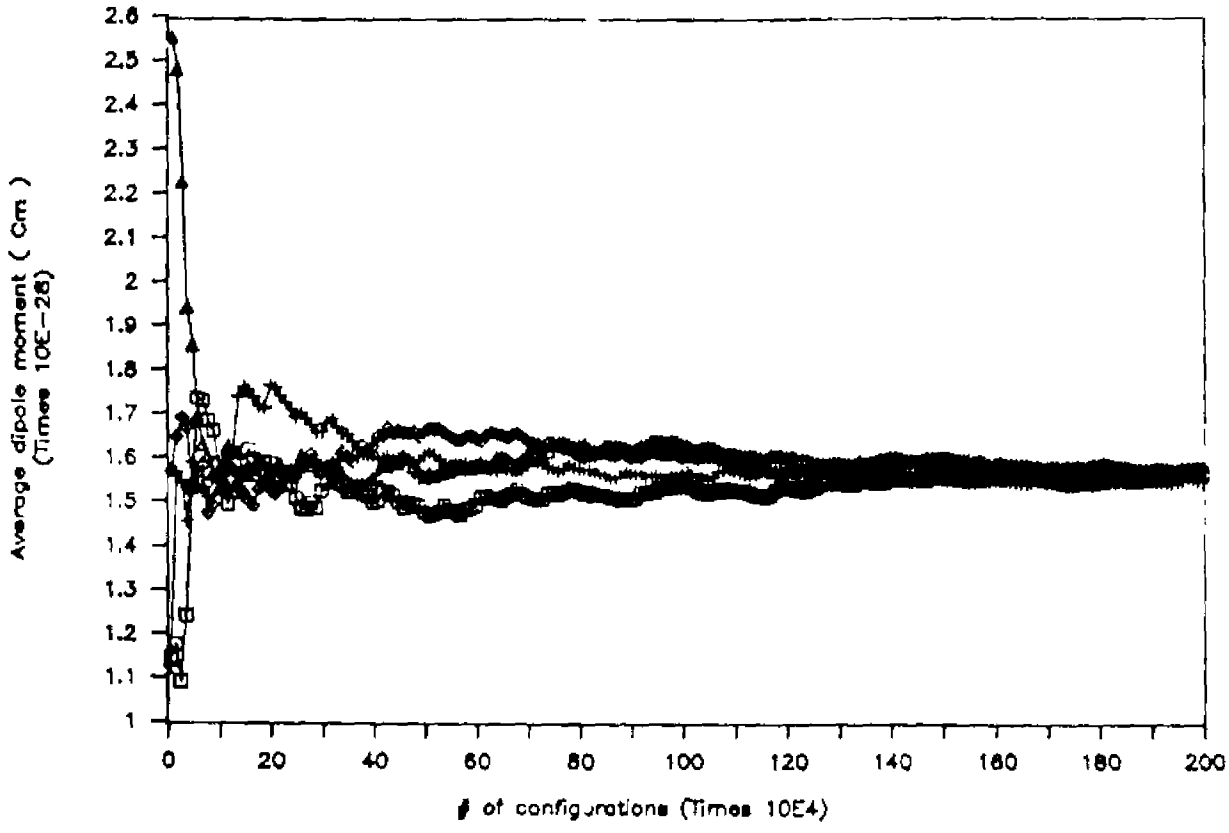

FIG. 2-4 Average dipole moment against number of configurations for 1 pair of ions with 4 different initial configurations

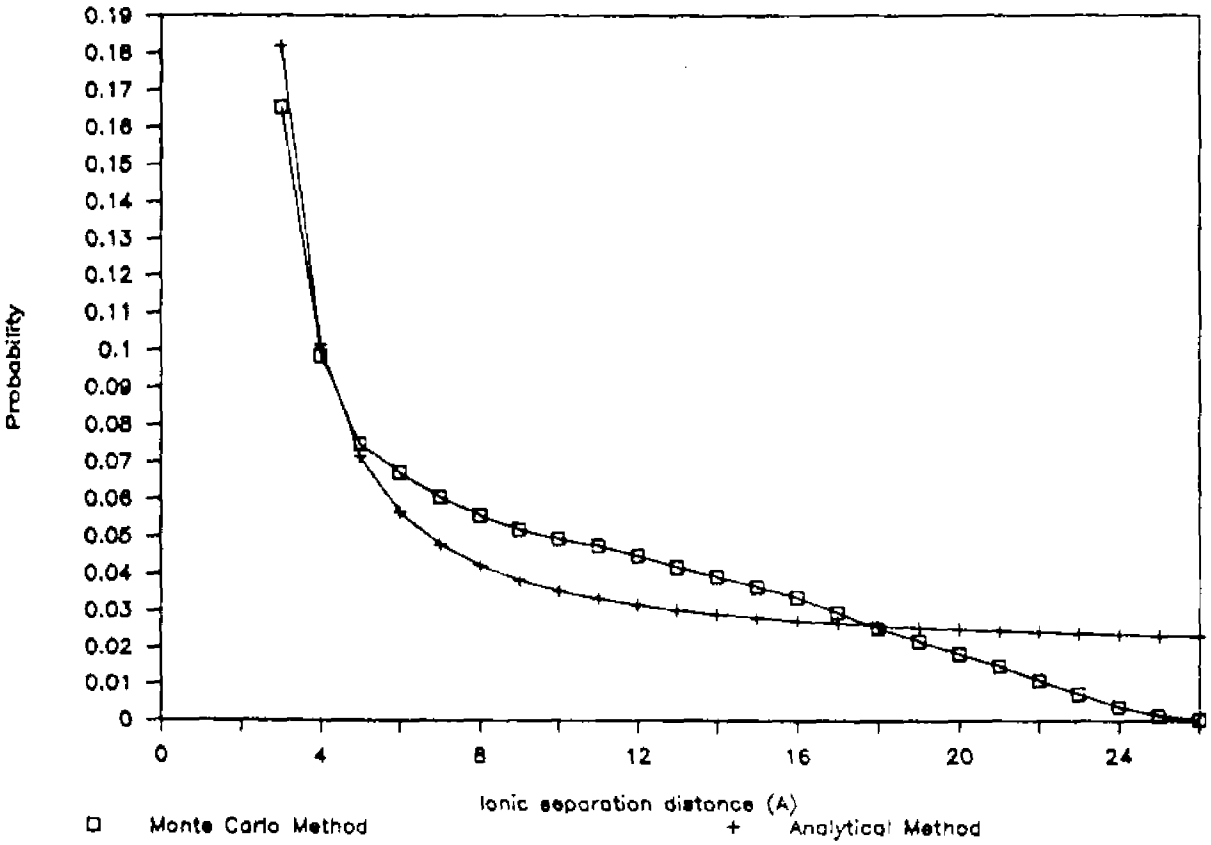

FIG. 2-5 Probability distribution function for 1 pair of ions

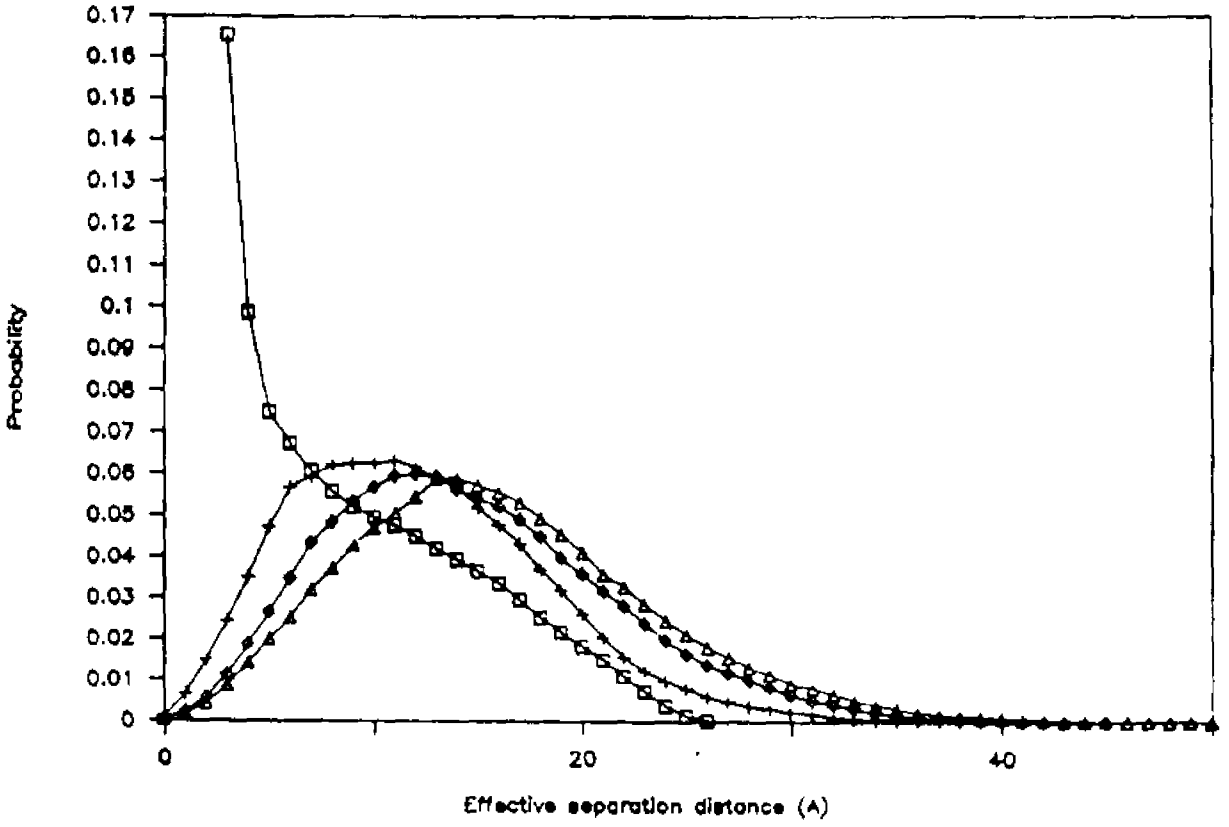

FIG. 2-6 Probability distribution function for various pairs of ions

□ 1 pair
\+ 2 pair
◇ 4 pair
△ 8 pair

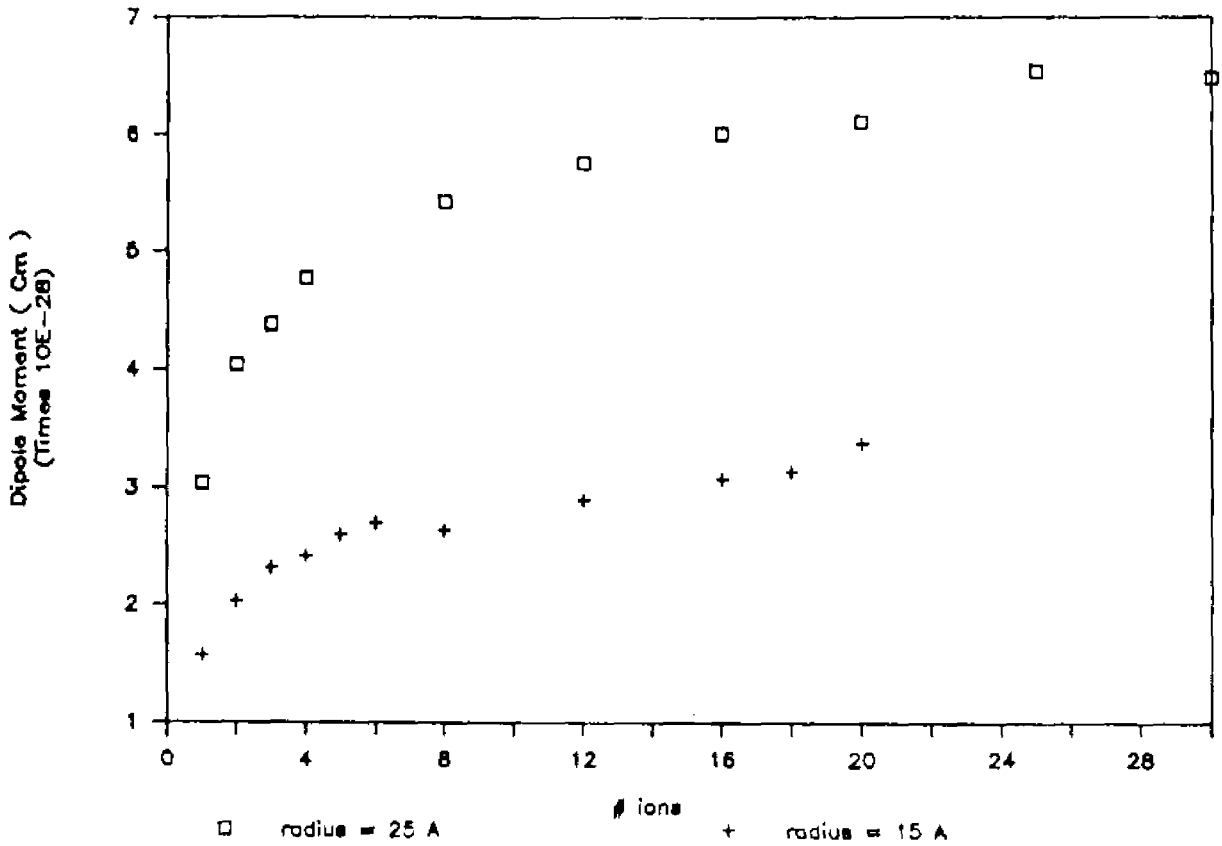

FIG. 2-7 Dipole moment against number of ions

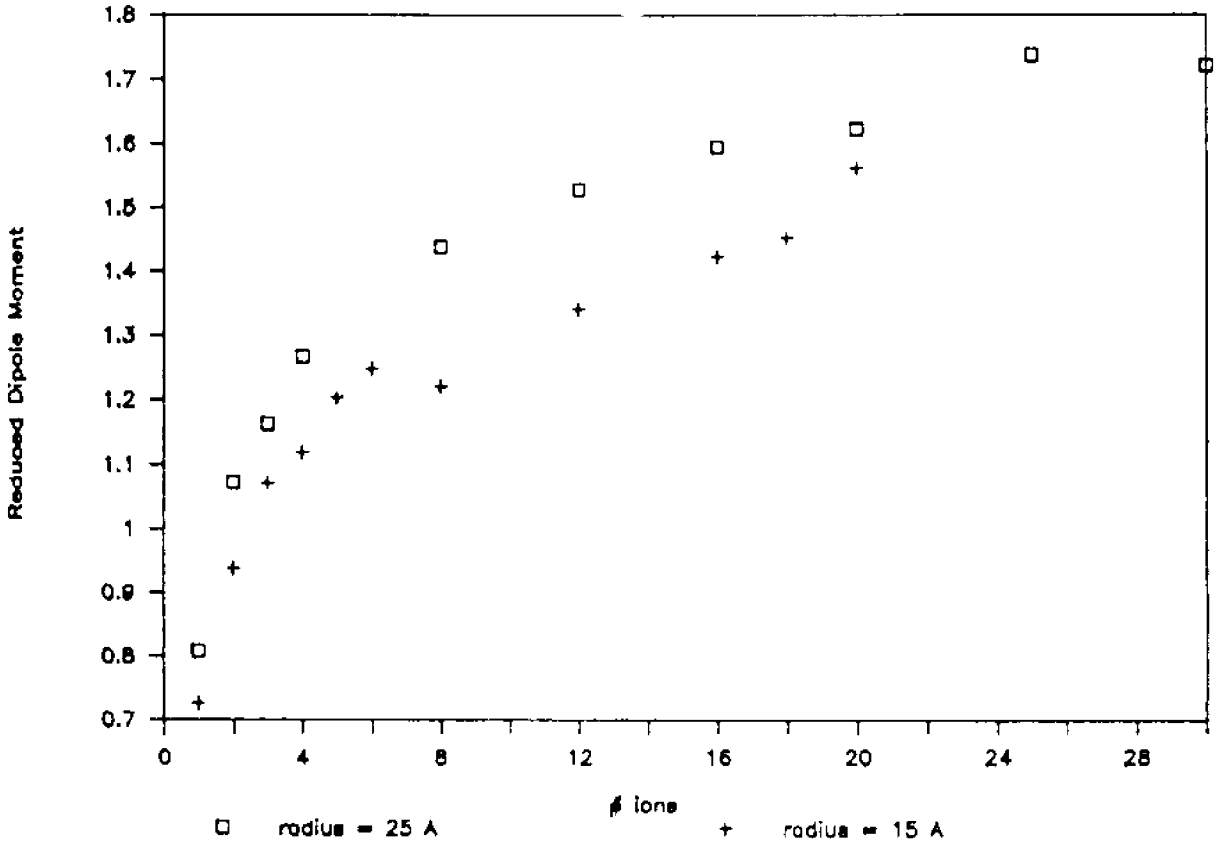

FIG. 2-8 Reduced dipole moment against number of ions

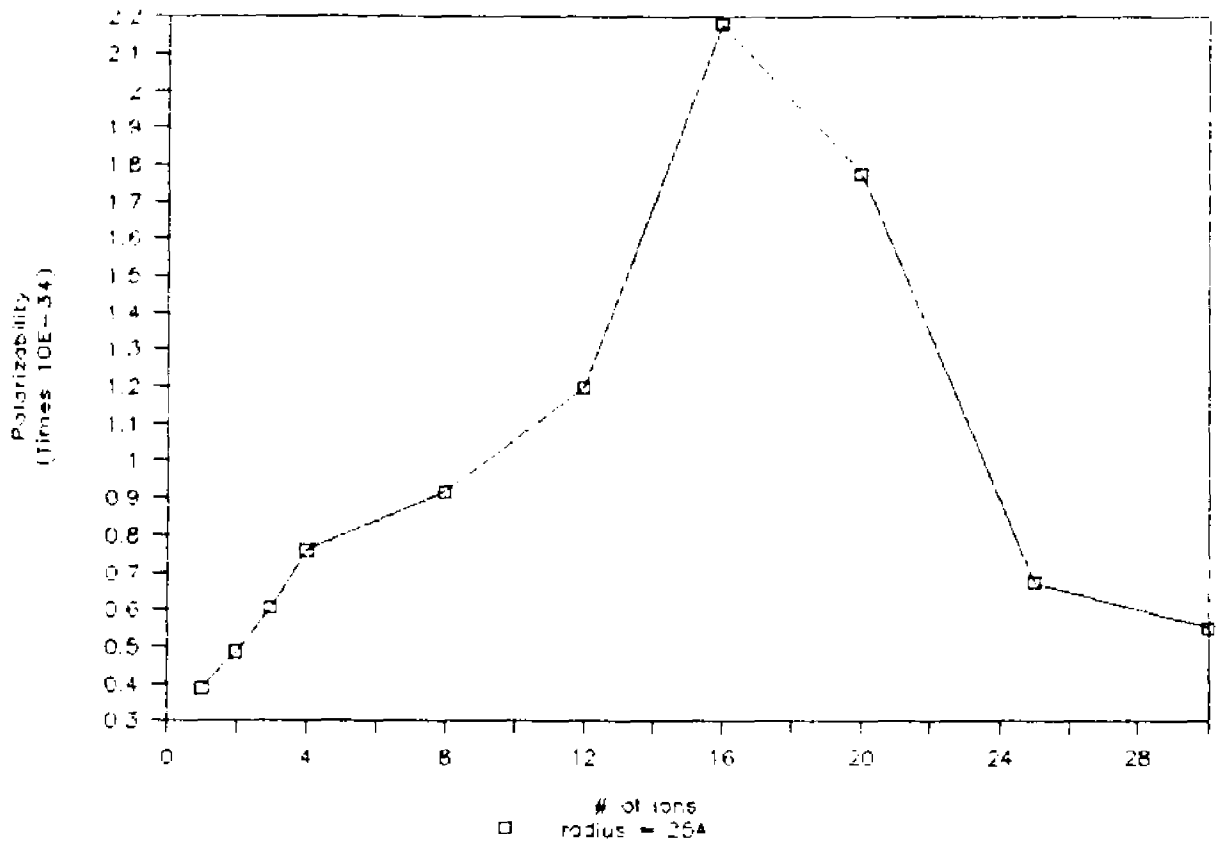

FIG. 2-9 Polarizability against number of ions

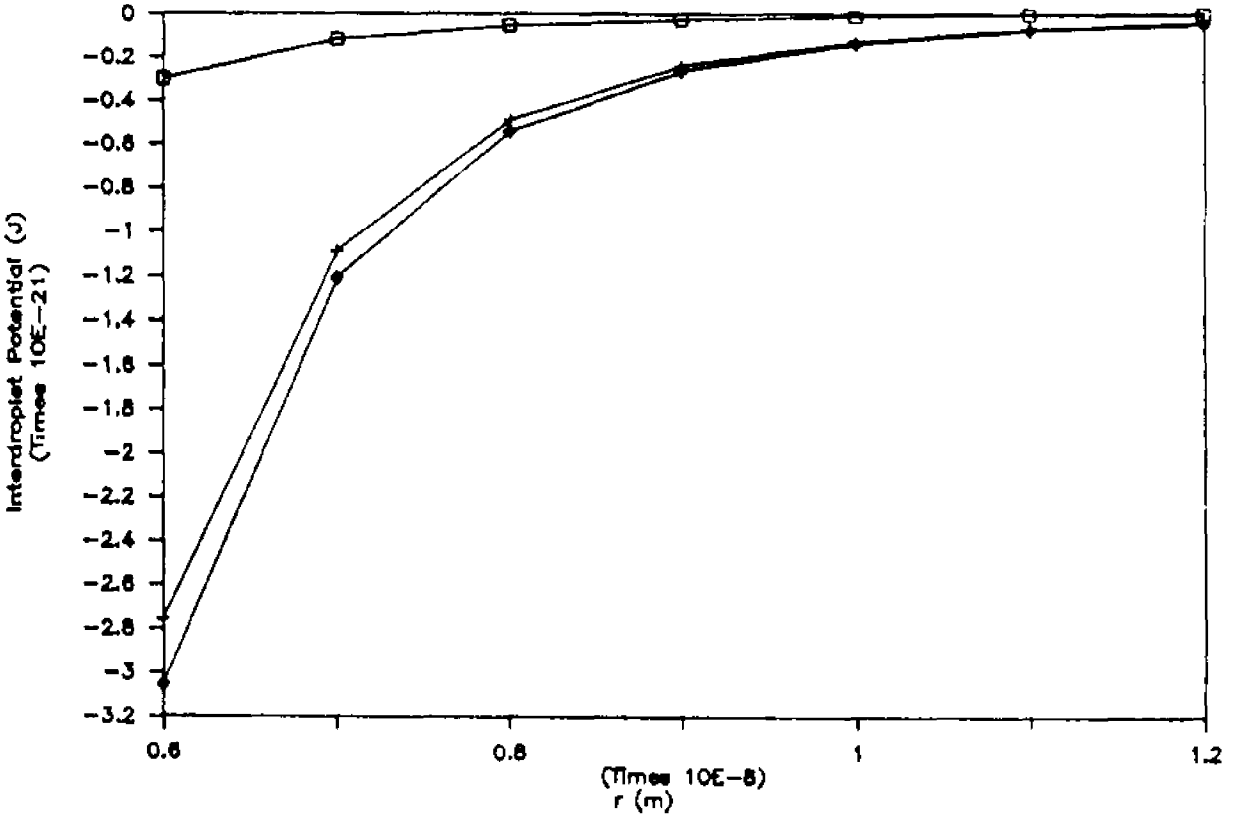

FIG. 2-10 Attractive potential against distance of separation for 1 pair of ions

□ dipole - dipole potential

\+ dipole - induced dipole potential

◇ total attractive potential

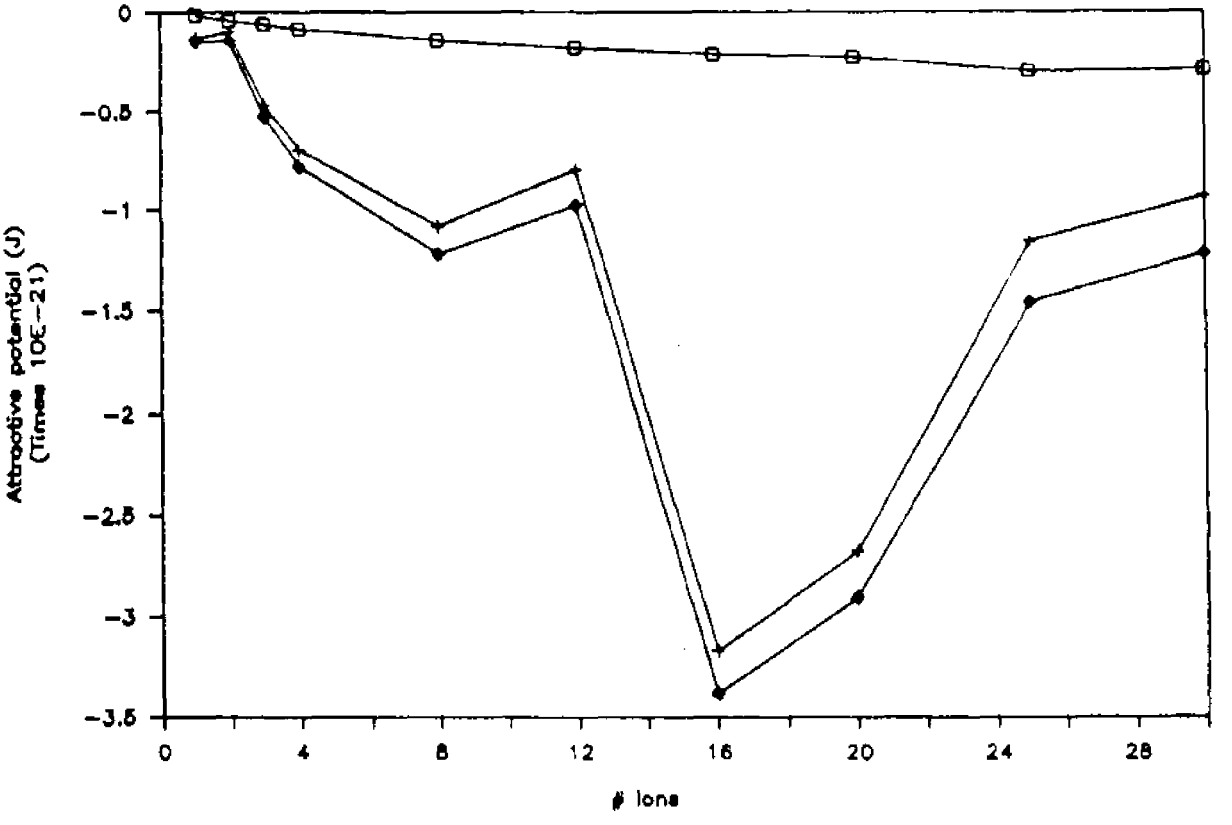

FIG. 2-11 Attractive potential against number of ions at a separation distance of 100 A

□ dipole - dipole potential

\+ dipole - induced dipole potential

◇ total attractive potential

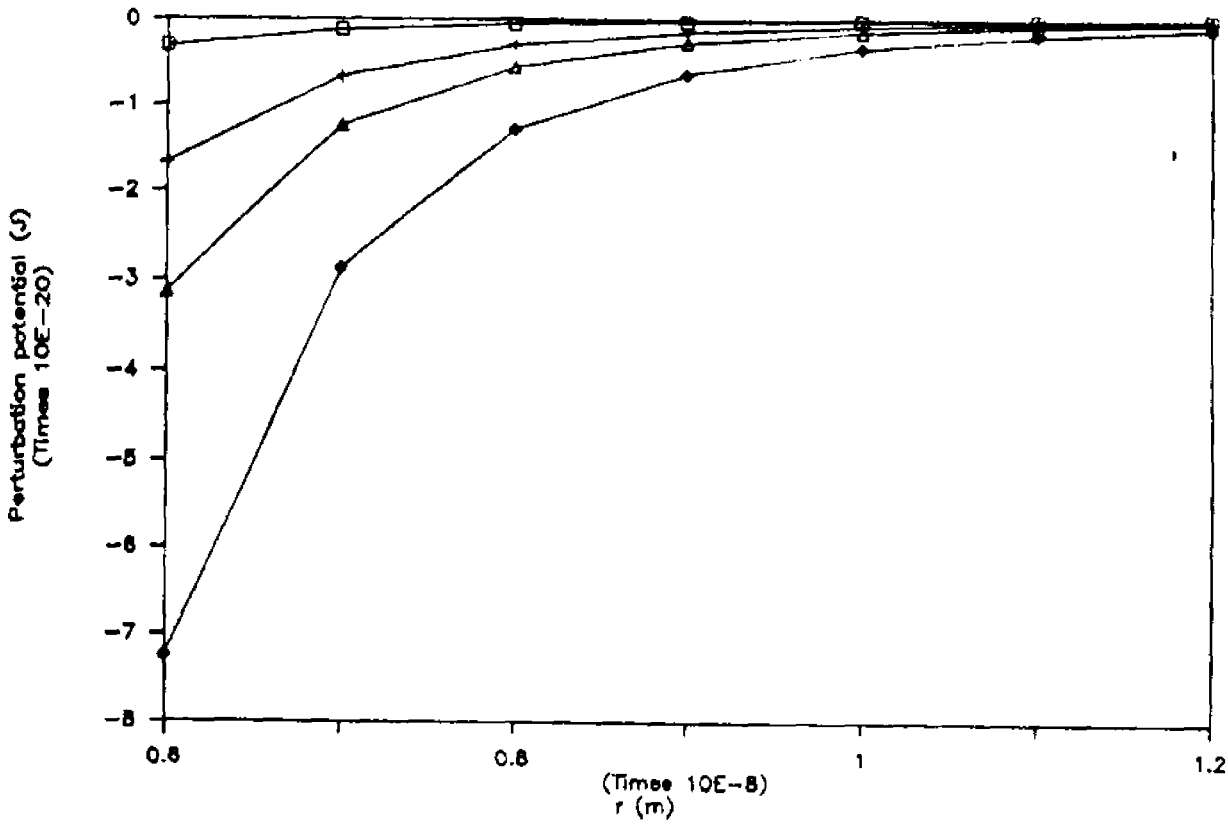

FIG. 2-12 Perturbation potential against distance of separation for various pair of ions

□ 1 pair
\+ 4 pair
◇ 16 pair
△ 25 pair

CHAPTER 3

Simulations of Water-in-Oil Microemulsions II : AOT/Water/Oil System

ABSTRACT

In an extension of a previous investigation, Monte Carlo simulations are performed on a model AOT/water/oil microemulsion droplet. Both the dipole moment and the polarizability were confirmed to exist at the aqueous core of the droplet. Possibly because of electrostatic stabilization, the value of polarizability is found to decrease with increasing salt concentration. Similar to their counterparts in system with non-ionic surfactants, the dipole - induced dipole interactions are dominant over both dipole - dipole interactions and the droplets' molecular van der Waals interactions. Thus, the overall attractions between droplets are found to decrease with increasing salt concentration, a result in agreement with experimental findings.

I. INTRODUCTION

Water-in-oil (W/O) microemulsions are collections of small, stable, and monodisperse "water" droplets dispersed in an oil continuous phase[1]. Because of their small size and thermodynamic stability, such microemulsion systems have been proposed for uses in a wide range of novel technologies[2-8], including the commercially important enhanced oil recovery processes[9]. To obtain a detailed and accurate understanding of the various observed macroscopic phase behavior in water-in-oil microemulsions, interactions between droplets have been studied extensively in the literature[10-23]. However, due to the empirical nature of most of these studies, a sufficiently accurate and verifiable model of interparticle interactions in microemulsions is still unavailable despite an abundance of excellent experimental data.

In a previous paper[24], we developed a new theory of interdroplet interactions in water-in-oil microemulsions. Based on the hypothesis that a sizable dipole moment could arise from the non-symmetrical arrangement of ions in the water core of a microemulsion droplet, the source of interdroplet interactions could then be the sum of dipole - dipole and the dipole - induced dipole attractions. The results from a series of Monte Carlo simulations indeed confirmed the accuracy of this prediction. A "configurational dipole moment" was found to exist in the water core of a W/O microemulsion. Also, the interdroplet attractions calculated

based on such a dipole moment were in fairly good agreement with experimental data. Even more significant is the fact that the results predicted qualitatively the existence of the "electrolyte-moderated interactions" , a phenomenon that have been observed experimentally[11-12] but could not be explained by any previous theories.

Since the system studied in that paper[24] was a microemulsion system with a non-ionic surfactant, it is unclear by how much the magnitude of the configurational dipole moment and the polarizability will be affected by using a microemulsion system with ionic surfactants. Clearly, in addition to ions contributed by electrolyte, some of the counter-ions from the polar head groups of ionic surfactants would also dissociate into the water core. There are two objectives in the present work. The first is to determine the magnitude of the configurational dipole moment as a function of electrolyte concentration and degrees of dissociation of the counter-ions. The second objective is to determine the polarizability of the droplet by monitoring the changes in the dipole moment when the droplet is subject to an applied electric field. Taking the same approach as in the previous paper, equilibrium ionic distribution in the water core of W/O microemulsion droplets are generated by the Metropolis Monte Carlo method[25-27], a widely used stochastic technique that allows accurate calculation of equilibrium properties. The present paper is in essence an extension of our previous

investigations.

In the present study, a sodium bis(2-ethylhexyl) sulfosuccinate (AOT) water-in-oil microemulsion will be used as our model system. There are couple of advantages for choosing this anionic surfactant. First, because of its structure, AOT can form a thermodynamically stable microemulsion without the addition of short chain alcohols as cosurfactants. This will enable our theoretical model to have a better representation of the physical system. In addition, the AOT water in oil microemulsion is one of the most thoroughly studied systems in the colloid literature. It has been investigated extensively using fluorescence probes[10], laser light scattering[11-14], NMR[15], small-angle neutron scattering (SANS)[16], small angle X-ray scattering[17], phase diagram determinations[18], dielectric response measurements[19-20], ultrasonics[21], and electrical conductivity measurements[22-23]. Results obtained from our investigation can easily be compared to this wealth of data to check for the validity of the model.

II. MODEL AND COMPUTER SIMULATIONS

The Metropolis Monte Carlo method is an importance sampling technique that utilizes the theory of the Markov chain. Its underlying theories have been thoroughly discussed in our previous paper[24] and elsewhere in the literature[25-27].

In this work, the simulations were performed in an NVT ensemble (number of particles, volume, and temperature constant). The water core of the microemulsion droplet was modeled by a spherical simulation cell with a radius of 25 A and bounded by hard structureless wall. The surrounding surfactant interface and the non-polar (oil) region are treated as a continuum. Inside the water core, in addition to the equal number of positive and negative ions contributed by the electrolytes, there are excess positive ions dissociated from the polar head groups of the surfactants. The electroneutrality of the system was maintained by same amount of immobile negative ions at the interface of the droplet. Interactions among these ions were evaluated explicitly according to the restrictive primitive model. That is, the potentials were assumed to be purely coulombic and pairwise additive. Each ion was modeled as a hard sphere of radius 1.5A with the appropriate charge located at the center of the ionic sphere. The solvent, water in this case, was represented as a continuous medium of uniform dielectric constant ε_{H2O}. The interionic potential of mean force (PMF), $U_{ij}(r)$, between ions i and j having respective charges of q_i and q_j can therefore be expressed as

$$U_{ij}(r) = \infty \qquad \text{for } r < \sigma_{hs}$$

$$= \frac{q_i q_j}{4\pi\varepsilon_0\varepsilon_{mc} r} \qquad \text{for } r > \sigma_{hs} \qquad \ldots(1)$$

Hence, the total potential energy of the system is given as

$$U_N = \sum_{i>j}^{n} \frac{q_i q_j}{4\pi\varepsilon_0\varepsilon_{mc}|r_i - r_j|} \qquad \ldots(2)$$

Due to the small size of the system and the close resemblance of the model to an actual W/O microemulsion droplet, the customary periodic boundary condition was not imposed. Instead, a non-standard boundary condition[27] was applied where the entry and exit of ions from the water core is prohibited. Such a procedure allows the equilibrium properties to be obtained by averging over the entire system rather than just a small fraction of the system as is usually the case. The properties reported in this paper are obtained by averging four runs, each with two million configurations. During each of those runs, the first one million configurations are discarded to reduce the initial configuration effect.

III. RESULTS AND DISCUSSIONS

A. Dipole Moment

One of the main objective of this work is to determine the magnitude of the configurational dipole moment. For an assembly of charges located in a certain limited region, the dipole moment, p, is defined as

$$\mathbf{p} = \sum_i q_i \mathbf{d}_i \qquad \ldots(3)$$

where $\mathbf{d}_i$ is the displacement of charge i from the reference point. In the present system, the center of the water core is conveniently chosen as this point. Since ionic distribution (i.e. the probability of finding the ions at a certain distance apart) inside a microemulsion droplet can be readily

obtained from the Monte Carlo simulations, we can utilize equation (3) to calculate the dipole moment distribution by multiplying the ionic distribution with respective charges q_i. The average dipole moment could then be evaluated by finding the mean of the dipole distribution.

Figure 1 shows the average configurational dipole moment plotted against the number of counter ions (positive ions in the present system) dissociated from the surfactant head groups. The average dipole moment increases with increasing degree of dissociation. This rate of increase, however, is not linear. The dipole moment increases sharply at low ion concentration but is nearly constant in the presence of a large number of counter-ions. This feature can be easily explained by basic principles of statistical mechanics and electrostatics. When the number of ions is large, the formation of a sizable dipole moment is unlikely as it correspond to a state where ions of the same sign being held close to each other while opposite sign ions are all far apart. Both the law of probability and the formidable magnitude of Coulombic attraction and repulsion dictate that the chance for such a state to occur is vanishingly small. Thus, increasing the number of ions at high ionic concentration should not dramatically increase the dipole moment.

Another behavior observed in the same figure is that

increasing the amount of salt from 0% to 3% does not have any noticeable effect of the magnitude of dipole moment generated. Since these concentrations of salt correspond to only a few pairs of extra ions, it is not surprising to see that their effects on dipole moment are negligible.

B. Polarizability and Induced Dipole Moment

The electric field from a dipole can cause a polarizing force on ions in nearby droplets. Consequently, besides dipole - dipole interactions, dipole - induced dipole type attraction also has to be taken into account. To calculate the magnitude of this dipole - induced dipole interaction, the polarizability of a W/O microemulsion droplet first has to be determined. From electromagnetic theory, the polarizability α of a particle is defined according to the strength of the induced dipole moment p_{ind} acquired in an applied electric field E:

$$\alpha = p_{ind} / E \qquad \ldots(4)$$

This parameter α , however, can be conveniently evaluated from Monte Carlo calculation by using the following equation rather than the expression in equation (2) as the total potential energy of the system

$$U_N = \sum_{i>j} \frac{q_i q_j}{4\pi\varepsilon_0\varepsilon_{mic}|R - r_j|} + \sum_i \frac{p_{ext} q_i}{4\pi\varepsilon_0\varepsilon_{eff} l_i^3} \qquad \ldots(5)$$

where p_{ext} is the external dipole moment, l_i is the distance of external dipole from ion i, and ε_{eff} is the effective

dielectric constant of the interacting medium, which is expressed as

$$\varepsilon_{eff} = (\varepsilon_{H2O}^{1/3} X_{H2O} + \varepsilon_{oil}^{1/3} X_{oil})^3 \quad ...(5a)$$

and X_{H2O} and X_{oil} are the volume fraction of water and oil respectively. The actual procedures for this simulations have been discussed in detail in ref. 24.

The polarizability is plotted as a function of the number of counter ions dissociated. When there are no salt in the system, we found that the rate of increase of the polarizability is very significant at low ionic concentration (the water core has 8 dissociated counter ions or less). Beyond that, the polarizability remains about constant with increasing ionic concentration. In contrast, for salted system, the magnitude of the polarizability varies inversely with the concentration of salt. An even more interesting feature is that the polarizability will reach a maximum value at certain number of ions. Above this number, any additional ions will result in a decrease of the droplet's polarizability, with the biggest reduction coming in the system with the highest concentration of salt. While this result may be unexpected, it is reasonable given the physical situation. The presence of an external field will polarize the ions, causing oppositely charged ions to move apart from each other and creating an induced dipole moment, explaining the initial increase in induced dipole moment and thus the polarizability. However, as the number of counter-ions in the

aqueous core get larger, a critical stage will eventually be reached where the ionic separation distance is close enough for the short range coulombic interaction to dominate over any external polarizing force. Since increasing salt concentration implies an increase of negative ions in the water core where there is an excess of positive ions, the level of local ordering is significantly enhanced due to this electrostatic stabilization. As a consequence, the magnitude of induced dipole moment and thus the polarizability will decrease with increasing concentration of salt.

C. Interdroplet Potential

From the Monte Carlo results, we have established that there is indeed the existence of a dipole moment and polarizability in a model AOT/water/oil microemulsion droplet. To determine the magnitude of interactions in microemulsion, however, we have to convert these parameters into an interdroplet potential function. In this paper, basic statistical mechanics theories are utilized to formulate this interdroplet potential function. Applying perturbation theory[28-29], the attractive interaction forces are treated as a perturbation to a repulsive hard sphere potential. That is, the total interaction energy U(r) is separated into two parts, a reference part, $U_{hs}(r)$, and a perturbation part, $U_a(r)$

$$U(r) = U_{hs}(r) + U_a(r) \qquad \ldots(6)$$

where the hard sphere potential of mean force $U_{hs}(r)$ is given

by

$$U_{hs}(r) = \infty \quad \text{for } r < \sigma_{hs}$$
$$= 0 \quad \text{for } r > \sigma_{hs} \qquad \ldots(7)$$

and the attractive perturbation part is solely the superposition of the dipole - dipole and the dipole - induced dipole attraction. From electromagnetic theory, the dipole - dipole interaction energy for two droplets with identical dipole moment p_1 is[24]

$$U_1(r) = \frac{p_1^2 p_1^2}{3(4\pi\varepsilon_0\varepsilon_{oil})^2 kT r^6} \qquad \ldots(8)$$

and the dipole - induced dipole interaction for two droplets with dipole moment p_1 and polarizability α is[24]

$$U_2(r) = \frac{2 p_1^2 \alpha}{(4\pi\varepsilon_0\varepsilon_{oil})^2 r^6} \qquad \ldots(9)$$

where k = Boltzmann constant, T = temperature

ε_{oil} = dielectric constant of the non-polar medium

r = separation distance between two droplets

Hence, the attractive perturbation is the sum of equation (8) and (9), and is given as

$$U_a(r) = \frac{p^2}{(4\pi\varepsilon_0\varepsilon_{oil})^2 r^6}\left(\frac{p^2}{3kT} + 2\alpha\right) \qquad \ldots(10)$$

Figure 3 is a plot of this perturbative (attractive) potential against the number of counter ions dissociated from surfactant molecules. At very low ionic concentration (when the number of counter ions is 6 or less), we found that the magnitude of the attractive potential increases with

increasing salt concentration. Apparently, when the number of ions are very small, the addition of extra ions leads to the formation of both a larger dipole moment and a greater polarizability. Hence, adding salt will increase attraction between droplets. This, however, is not the case at higher ionic concentration. The magnitude of the attractive potential is found to be inversely proportional to the salt concentration. As discussed in the previous section, addition of salt at high ionic concentration lead to an increase of local ordering, thus significantly reducing the polarizability of a droplet. Since the dipole - induced dipole interaction is about an order of magnitude larger than the dipole - dipole attraction, it is therefore not surprising to see that the plot of attractive potential would have the same characteristics as observed in the plot of polarizability.

When we plot the attractive potential against dipole - dipole separation distance for unsalted system in figure 4a, we found that the magnitude of the attractive potential rapidly decays with increasing separation distances between dipoles. This result is expected as both the dipole - dipole and the dipole - induced dipole terms have the $1/r^6$ dependence. Moreover, we also observed that the magnitude of the attractive potential $U_a(r)$ is directly proportional to the number of dissociated counter ions. However, when we repeated the same plot in figure 4b for a system with 3% salt, a relationship between $U_a(r)$ and number of dissociated counter

ions different from that in figure 4a appears. Unlike the case of unsalted system, the magnitude of attractive potential $U_a(r)$ initially increases with increasing counter ions, reaches a maximum, then declines with the further addition of ions. This difference is due to the same phenomenon observed in the plot of polarizability.

Finally, a most telling picture of the salt effect on interdroplet potential is depicted in figures 5a and 5b. The system in figure 5a correspond to a droplet with 8 counter ions in the water core. We immediately notice that the magnitude of the attractive potential decreases with increasing salt concentration. This dependence of the attractive potential on salt concentration is even more enhanced when the number of counter ions increased from 8 to 16 in fig. 5b. In short, when more than 5% of the counter ions dissociate from the surfactant interface into the aqueous core, we would expect the increase of electrolyte concentration to lead directly to a decrease of attraction between droplets, a result in good qualitative agreement with experimental data.

IV. CONCLUSIONS

Monte Carlo simulations were performed to verify the existence of a dipole moment and polarizability in a W/O microemulsion droplet due to the non-symmetrical arrangement

of ions in the aqueous core. Their existence were indeed confirmed by our simulation results. While the dipole moment generally increases with increasing degree of surfactant dissociation and does not depend on the addition of salt, the same cannot be said about the polarizability. Under the condition when there is more than several percent of the counter ions dissociated from the surfactants, it is observed that the polarizability decreases with increasing salt concentration.

Finally, in the proposed interdroplet potential function, the dipole - induced dipole attraction is about an order of magnitude larger than the corresponding dipole - dipole interactions. Consequently, the attraction between droplets is found to decrease with increasing salt concentration, a result in qualitative agreement with experimental data.

BIBLIOGRAPHY

1. deGennes, P.G., and Taupin, C., J. Phys. Chem., 86, 2294 (1982).

2. Tang, H.I., Johnson, P.L., and Gulari, E., in "Measurement of Suspended Particles by Quasi-Elastic Light Scattering," B.E. Dahneke, ed., Wiley, New York, 1983.

3. Beckman, E.J., and Smith, R.D., J. Phys. Chem., 94, 345 (1990).

4. Petit, C., and Pileni, M.P., J. Phys. Chem., 92, 2282 (1988).

5. Petit, C., Lixon, P., and Pileni, M.P., J. Phys. Chem., 94, 1598 (1990).

6. Fubini, B., Gasco, M.R., and Gallarate, M., Int. J. Pharm., 42, 19 (1988).

7. Xenakis, A., and Tondre, C., J. Colloid Interface Sci., 117, 442 (1987).

8. Tondre, C., and Derouiche, A., J. Phys. Chem., 94, 1624 (1990).

9. Leong, Y.S., and Candau, F., J. Phys. Chem., 86, 2269 (1982).

10. Lang, J, Jada, A., and Malliaris, A., J. Phys. Chem., 92, 1946 (1988).

11. Bedwell, B., and Gulari, E., J. Colloid Interface Sci., 102, 88 (1984).

12. Hou, M.J., Kim, M., and Shah, D.O., J. Colloid Interface Sci., 123, 398 (1988).

13. Leung, R., and Shah, D.O., J. Colloid Interface Sci., 120, 320 (1987).

14. Leung, R., and Shah, D.O., J. Colloid Interface Sci., 120, 330 (1987).

15. Wong, M., Thomas, J.K., and Nowak, T., J. Am. Chem. Soc., 99, 4730 (1977).

16. Ober, R., and Taupin, C., J. Phys. Chem., 84, 2418 (1980).

17. Pileni, M.P., Zemb, T., and Petit, C., Chem. Phys. Lett.,

118, 414 (1985).

18. Kuneida, H., and Shinoda, K., J. Colloid Interface Sci., 33, 215 (1970).

19. Peyrelasse, J., and Boned, C., J. Phys. Chem., 89, 370 (1985).

20. Gestblom, B., and Sjoblom, J., Langmuir, 4, 360 (1988).

21. D'Arrigo, A., Paparelli, A., D'Aprano, A., Donato, I.D., Goffredi, M., and Turco Liveri, V., J. Phys. Chem., 93, 8367 (1989).

22. Eicke, H.F., Borkovec, M., and Das-Gupta, B., J. Phys. Chem., 93, 314 (1989).

23. Hall, D.G., J. Phys. Chem., 94, 429 (1990).

24. Chan, Y.Y., and McKeigue, K., (Chapter 2 of this thesis, to be published).

25. Metropolis, N., Rosenbluth, A.W., Rosenbluth, M.N., Teller, A.H., and Teller, E., J. Chem. Phys., 21, 1087 (1953).

26. Binder, K., ed., "Application of the Monte Carlo Method," Springer-Verlag, New York, 1983.

27. Heermann, D.W., "Computer Simulation Methods in Theoretical Physics," Springer-Verlag, New York, 1986.

28. Barker, J.A., and Henderson, D., J. Chem. Phys., 47, 2856 (1967).

29. Barker, J.A., and Henderson, D., J. Chem. Phys., 47, 4714 (1967).

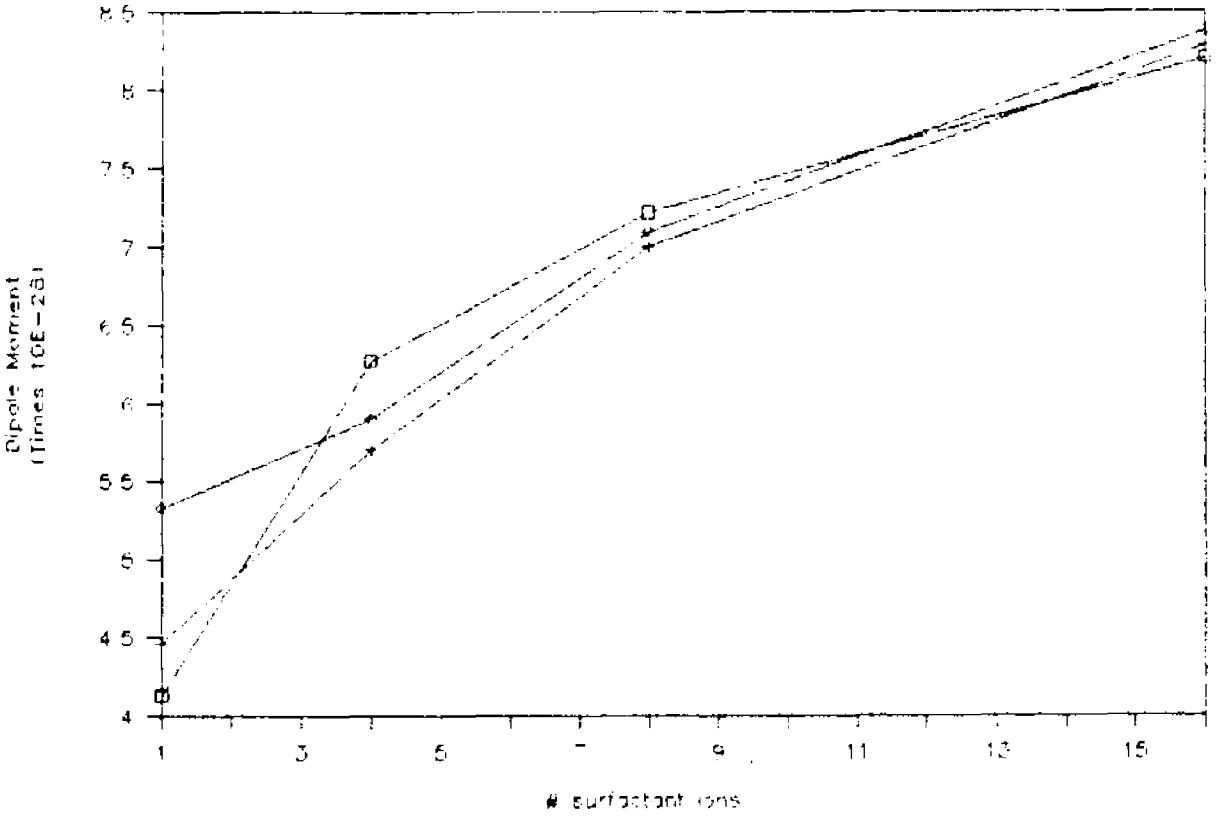

FIG. 3-1 Dipole moment vs. number of ions

- ▢ 0% NaCl
- + 1% NaCl
- ◇ 3% NaCl

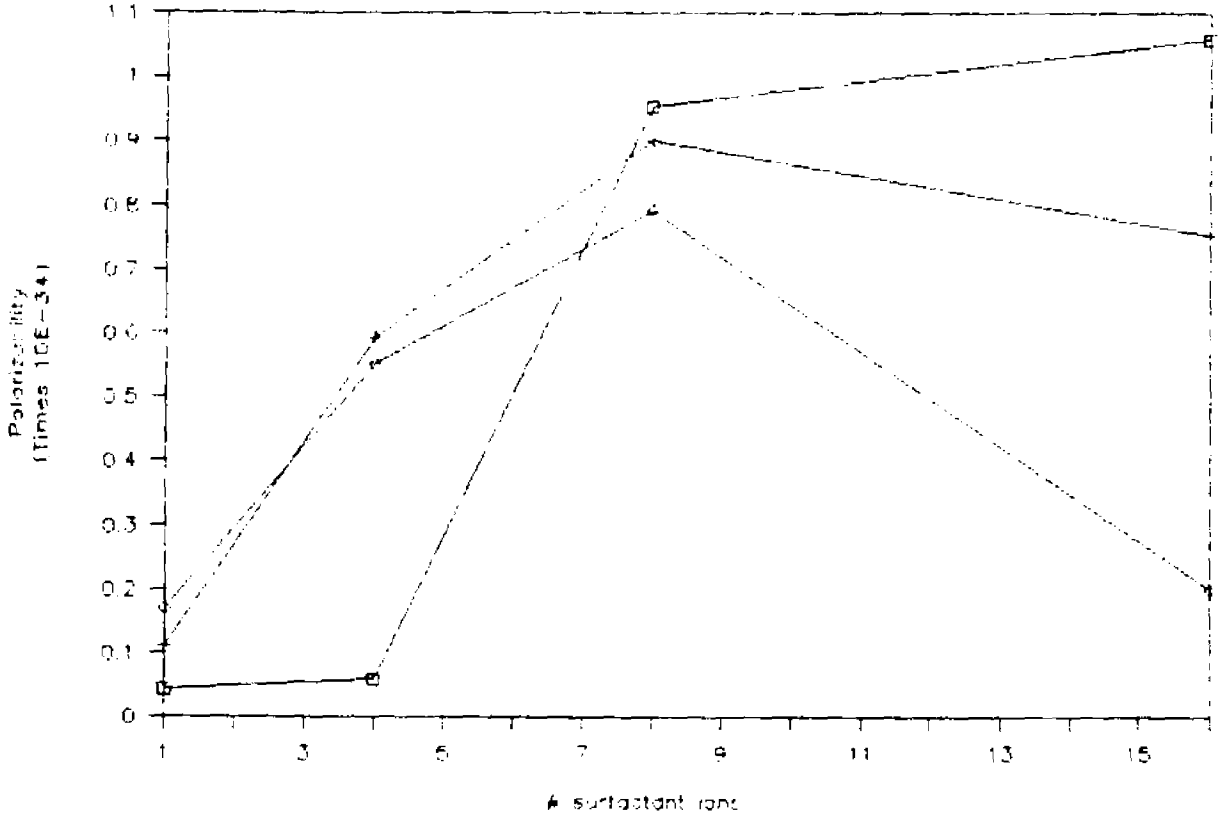

FIG. 3-2 Polarizability vs. number of ions

□ 0% NaCl

\+ 1% NaCl

◇ 3% NaCl

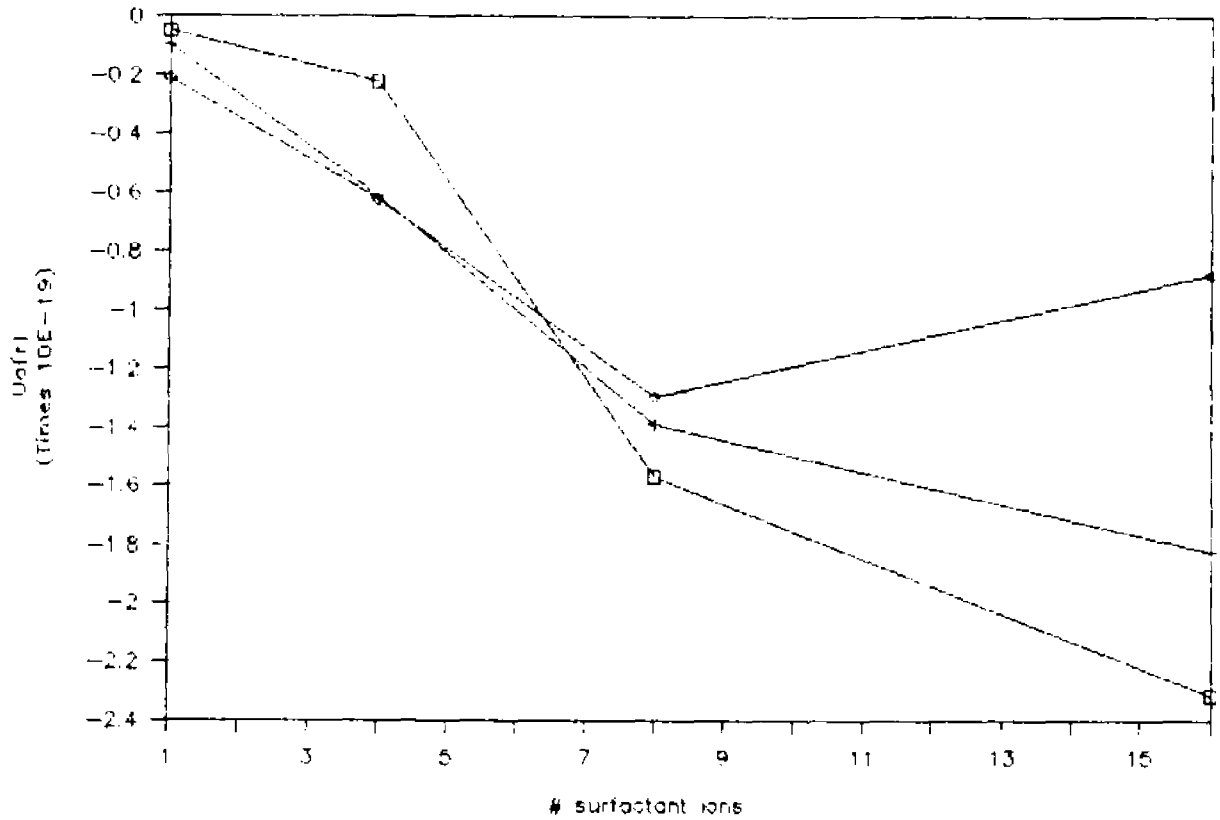

FIG. 3-3 Attractive potential vs. number of ions at a separation distance of 50 A

□ no salt

\+ 1 pair of ions (salt)

◇ 3 pair of ions (salt)

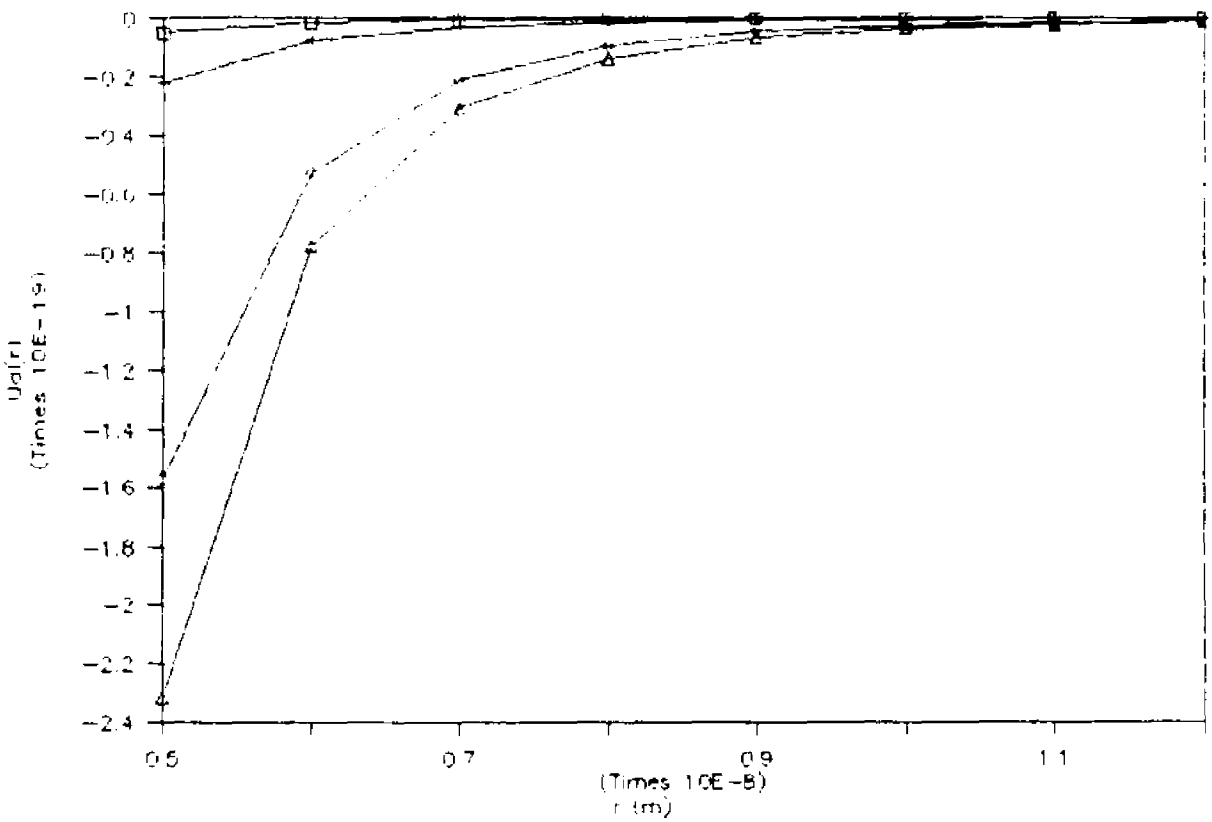

FIG. 3-4a Attractive potential vs. separation distance for system with no added salt

- □ 1 ion
- \+ 4 ions
- ◇ 8 ions
- △ 16 ions

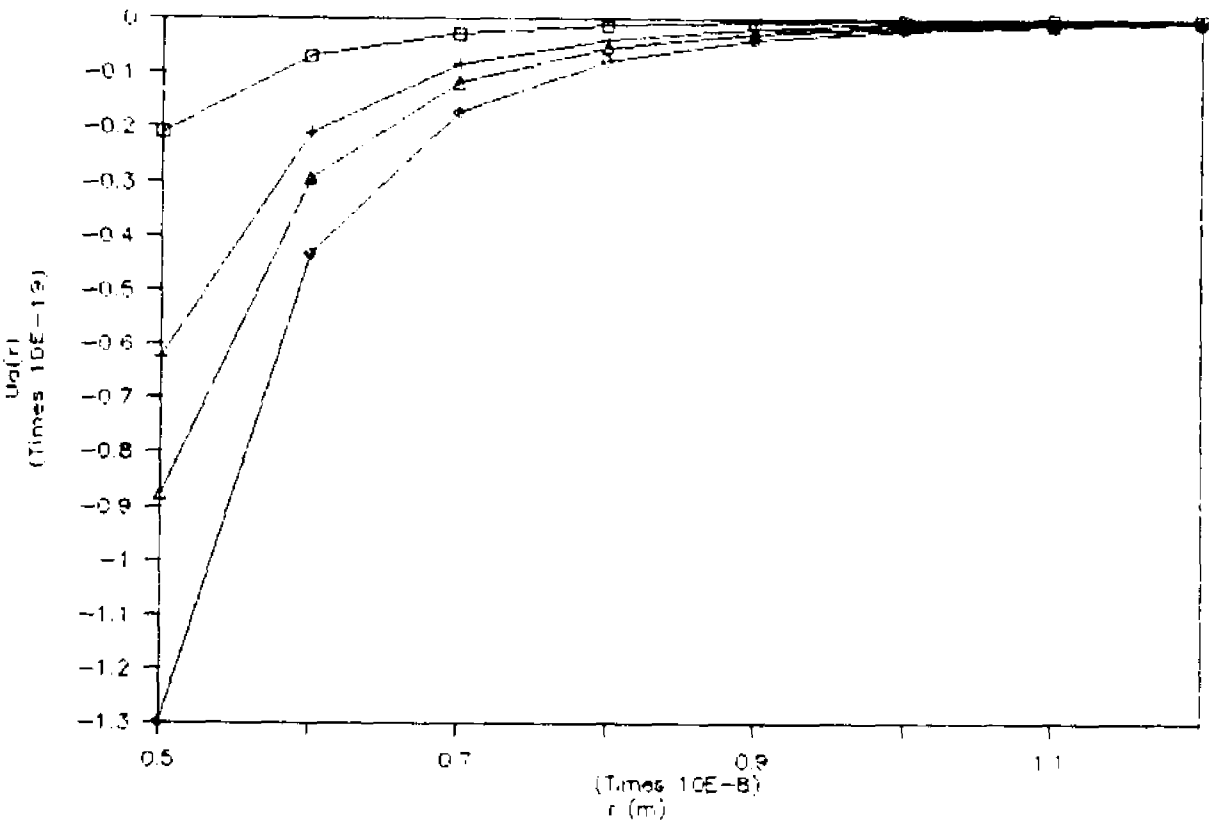

FIG. 3-4b Attractive potential vs. separation distance for system with 3% salt

- □ 1 ion
- \+ 4 ions
- ◇ 8 ions
- △ 16 ions

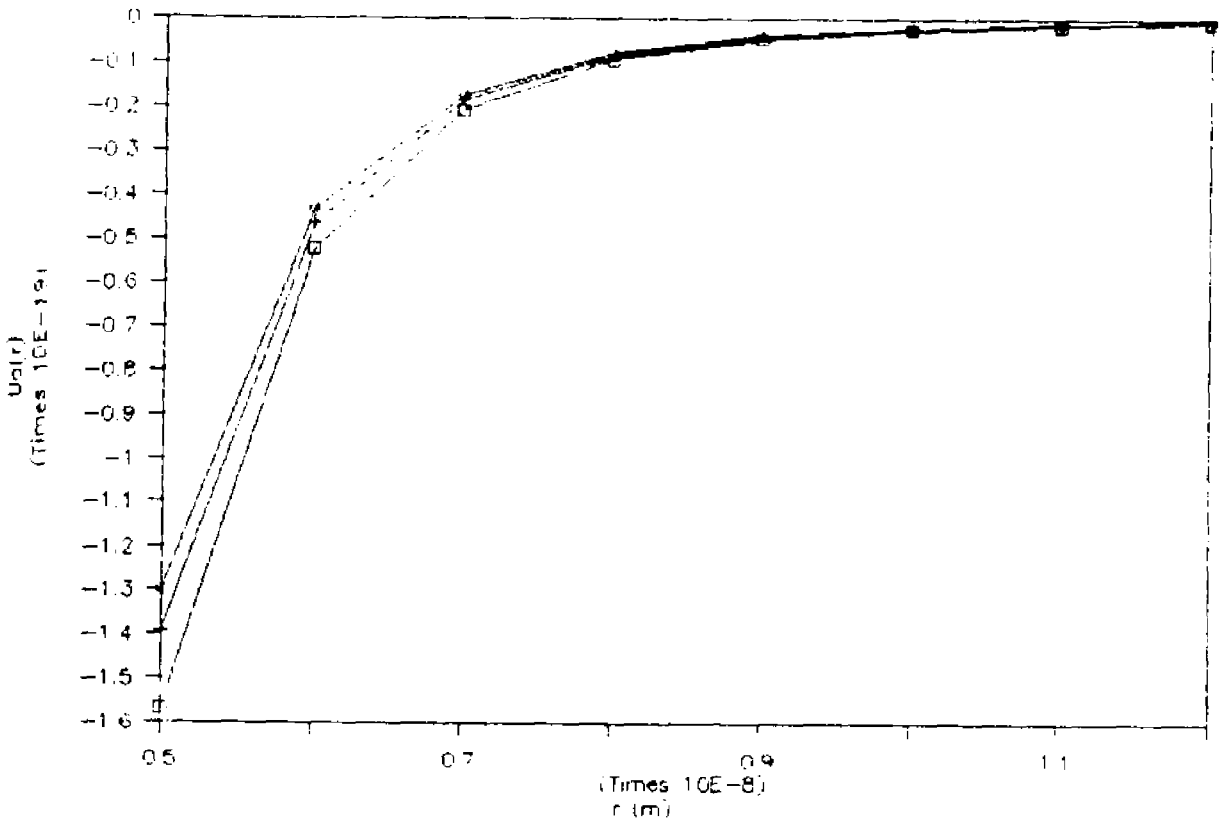

FIG. 3-5a Attractive potential vs. separation distance for system with 8 dissociated ions

□ 0% salt

\+ 1% salt

◇ 3% salt

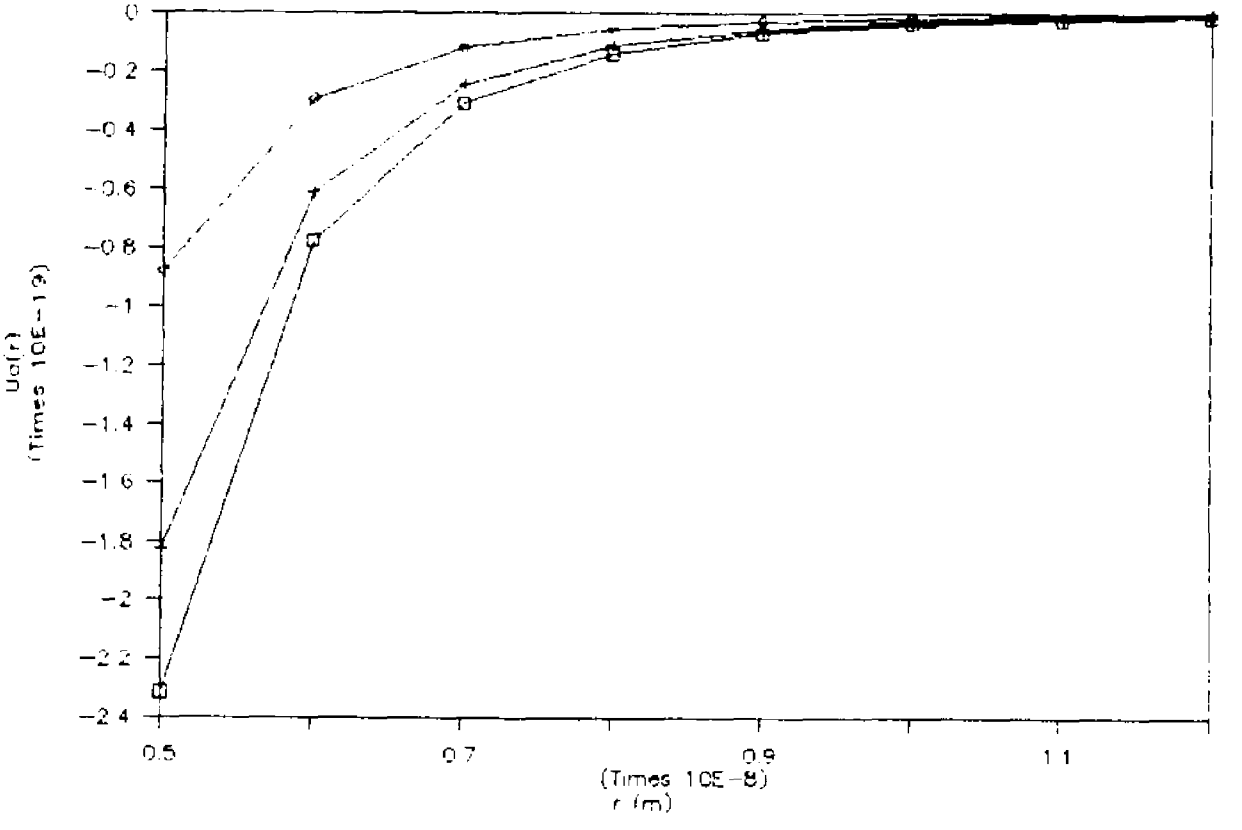

FIG. 3-5b Attractive potential vs. separation distance for system with 16 dissociated ions

□ 0% salt

+ 1% salt

◇ 3% salt

CHAPTER 4

Dipole Attraction Forces in AOT/Water/Oil Microemulsions

ABSTRACT

Statistical fluctuations in the arrangement of ions within the aqueous core of a water-in-oil microemulsion can cause a significant overall dipole moment in the droplet. This phenomenon is shown to lead to dipole-dipole and dipole-induced dipole interactions between droplets which can be as much as two orders of magnitude stronger than the van der Waals attractions between droplets. Equilibrium properties of the microemulsion which take these interactions into account are obtained using a perturbation approach in which the microemulsion droplets interact through a hard-sphere potential perturbed by the attractive dipole interactions. The osmotic compressibilities and Hamaker constants calculated using this approach are found to be in good agreement with experimental light scattering studies, explaining the origin of the electrolyte-moderated interactions observed in such systems.

I. INTRODUCTION

Microemulsions are thermodynamically stable, isotropic, transparent dispersions of oil and water[1,2], consisting of at least three components: water, oil, and surfactant. To obtain a thermodynamically stable system, often a fourth component - a cosurfactant - is needed. Depending on the amount of oil and water in the system, microemulsions can display a wide variety of structures, ranging from dispersions of monodisperse spherical droplets[1] to polydisperse bicontinuous structure[3]. Among the microstructures, the so called water-in-oil (W/O[4]) microemulsions will be the subject of investigation in the present work. This system has been studied extensively as it hold great promise in a wide range of emerging technologies, especially in enhanced oil recovery[5] and microemulsion polymerization[6-8].

The central issue of major concern in the study of W/O microemulsions is the interaction between droplets[9-18], in particular the development of an accurate interdroplet potential function. This information, if available, will lead to quantitative results for various thermodynamic, transport, and structural properties observed in microemulsions. Unfortunately, in the above studies, interdroplet potentials are usually obtained by fitting a suitable functional form such as square will potential[9,12] or Yukawa potential[13-14] to experimental viscosity data or osmotic compressibility data

from laser light scattering. Few attempts[15,17-18] have been made to model the interactions based on theoretical considerations alone. Thus, while there are many excellent experimental results available, no one has yet been able to convert these data into an accurate or verifiable picture of microemulsions interactions.

Among the theoretical models that have been proposed, deRozieres and coworkers[15] suggested that the origin of the interaction is an induced dipole - induced dipole type attraction resulting from the mobility of counterions in the aqueous core. Using a different approach, Eicke et. al.[17] and Hall[18] proposed that the migration of fluctuating charged droplets is responsible for the interaction. However, none of these models is able to account for the electrolyte moderated interactions phenomena[11-12] observed in water-in-oil microemulsions, viz., the attraction between droplets decrease with increasing electrolyte concentration.

In a previous paper[19], we have reported the development of a new theoretical model on interdroplet interactions. It is to our knowledge the first theoretical model that have successfully explained the peculiar electrolyte moderated interaction behavior. The primary objective of the present work is to generate osmotic compressibility data and Hamaker constant from the new model and compare them with existing data in the literature. In particular, the data will be

compared to a model microemulsions of Aerosol-OT/water/heptane. Any close agreement with experimental data will further validate the new model. This will enable us to reveal a more accurate and reliable picture of interactions between droplets in a Winsor II microemulsions.

Because of their structures, some surfactants can form thermodynamically stable water-in-oil (W/O) microemulsions without the addition of short chain alcohol as cosurfactant. A typical example is the sodium bis(2-ethylhexyl) sulfosuccinate (AOT). Over a fairly wide concentration range, the AOT/water/oil microemulsions can effectively be described as a stable collection of "water" microdroplets with hard sphere behavior suspended in an oil continuous phase. Microemulsions without the cosurfactant is a more suitable candidate in studying interaction between droplets as the presence of any alcohol partitioning between the interface and the continuum is likely to complicate the analysis of results. Since AOT/water/oil system satisfies this requirement, it has been investigated extensively[11-14,16-18,20-22] in the literature. This abundance of experimental data makes it the ideal system to be used in the present study.

In the following section, we will first recall the theories behind the current study. Section III is the results and discussions of osmotic pressure, osmotic compressibility, and Hamaker constant calculated from the new model. In the

final section, conclusions from the results will be drawn.

II. THEORETICAL BACKGROUND

In a preceding paper[19], we have presented a new theoretical model for interactions between droplets in a Winsor II microemulsions. Prior to any discussion of the current work, it seems appropriate to give a brief summary of the model and the resulting interdroplet potential. Figure 1 is a schematic description of the microemulsion droplets being studied. The AOT surfactants form a monolayer interface that partition between the spherical aqueous core and the oil continuum. In this model, ions from electrolytes and counterions dissociated from the surfactants are all present at the water core. Their non-symmetrical spatial arrangement give rise to a dipole moment. By assuming the interactions between water cores essentially account for all the attraction observed, the interdroplet interactions is concluded to be the sum of a dipole - dipole and a dipole - induced dipole type attraction.

Treating the interacting microemulsion droplets as macroscopic analogues of simple atomic and molecular fluids, the perturbation theory[23-25] is applied to the interdroplet potential. In this approach, the interaction force is treated as a perturbation on the hard sphere potential. That is, the pair potential of mean force U(r) is separated into two part,

a reference hard sphere and a perturbation part :

$$U(r) = U_{hs}(r) + U_a(r) \qquad \ldots (1)$$

where the potential of mean force for the hard sphere is :

$$U_{hs}(r) = \infty \qquad r < \sigma_{HS}$$
$$= 0 \qquad r > \sigma_{HS} \qquad \ldots (2)$$

As discussed in the previous paper[19], the perturbation in our model is considered to be the result of dipole - dipole and dipole - induced dipole attraction. The perturbation potential of mean force is therefore defined as :

$$U_a(r) = -\frac{\beta_{11}}{r^6} \qquad \ldots (3a)$$

where $$\beta_{11} = \frac{p_1^2}{(4\pi\varepsilon_0\varepsilon)^2}\left(\frac{p_1^2}{3kT} + 2\alpha\right) \qquad \ldots (3b)$$

and p_1 = dipole moment of the particle

α = polarizability of the particle

ε = dielectric constant of the oil continuum

k = Boltzmann constant

T = temperature

One of the thermodynamic equilibrium properties directly accessible from a knowledge of pair interaction potential is

the osmotic compressibility. This is also a quantity that can conveniently be obtained from experimental laser light scattering studies. As a consequence, the simplest method to interpret the interdroplet interactions from experimental data is through the development of the osmotic pressure according to the virial series[24].

$$\Pi = \left(\frac{\phi kT}{V_{hs}}\right)\left(1 + \frac{B}{2}\phi + \frac{C}{3}\phi^2 \cdots\right) \quad \ldots (4)$$

$$v_{hs} = \frac{\pi \sigma_{hs}^3}{6} \quad \ldots (5)$$

where B and C are virial coefficients.

In the limit of very small volume fraction, the osmotic pressure can be approximated by

$$\Pi \sim \left(\frac{\phi kT}{V_{hs}}\right)\left(1 + \frac{B}{2}\phi\right) \quad \ldots (6)$$

Using perturbation theory, the osmotic pressure can also be separated into two parts, one contributed by hard sphere while the other by perturbation[9]

$$\Pi = \Pi_{hs} + \Pi_a \quad \ldots (7)$$

Based on the solution for the Percus-Yevick equation, the osmotic pressure of hard sphere can be accurately described by the equation of state proposed by Carnahan and Starling[26]

$$\Pi_{hs} = \frac{kT\phi}{V_{hs}} \frac{1+\phi+\phi^2-\phi^3}{(1-\phi)^3} \qquad \ldots (8)$$

The attractive perturbation of osmotic pressure can be written as[9]

$$\Pi_a = 2\pi \left(\frac{\phi}{V_{hs}}\right)^2 \int_c^{\infty} U_a(r)\, g_{hs}(r)\, r^2 dr \qquad \ldots (9)$$

Again, by using the fact that the AOT/water/oil microemulsions correspond to a dilute dispersions, we can simplify the radial distribution function by the following approximation[9]

$$\begin{aligned} g_{hs}(r) &= 0 \qquad & r < \sigma_{HS} \\ &= 1 \qquad & r > \sigma_{HS} \end{aligned} \qquad \ldots (10)$$

Substitute this into equation (9), we can obtain

$$\Pi_a = \left(\frac{kT}{V_{hs}} \frac{A}{2}\right) \phi^2 \qquad \ldots (11)$$

where

$$A = \frac{4\pi}{kT V_{hs}} \int_{\sigma_{HS}}^{\infty} U_a(r) r^2 dr \qquad \ldots (12)$$

The parameter that can be obtained directly from light scattering data is osmotic compressibility $\frac{\partial \Pi}{\partial \phi}$. Hence, it is beneficial to derive its relationship with osmotic pressure. Using the same approach as osmotic pressure, $\frac{\partial \Pi}{\partial \phi}$ can be

expressed as:

$$\frac{\partial \Pi}{\partial \phi} = \frac{\partial \Pi_{hs}}{\partial \phi} + \frac{\partial \Pi_a}{\partial \phi} \qquad \ldots (13)$$

Differentiating equation (8) gives the hard sphere contribution to osmotic compressibility. i.e.

$$\frac{\partial \Pi_{hs}}{\partial \phi} = \frac{kT}{V_{hs}} \frac{(1 + 4\phi + 4\phi^2 - 4\phi^3 + \phi^4)}{(1-\phi)^4} \qquad \ldots (14)$$

Similarly, the osmotic compressibility caused by perturbation is

$$\frac{\partial \Pi_a}{\partial \phi} = \frac{kT}{V_{hs}} A\phi \qquad \ldots (15)$$

with A having been defined in equation (12).

III. RESULTS AND DISCUSSIONS

A. Osmotic pressure

To assess the validity of the new interdroplet interactions theory, several equilibrium properties of a water-in-oil microemulsion are evaluated and compared with experimental data in the literature. One is osmotic pressure, a parameter conveniently computed by integrating the functional form of $U_a(r)$ in equation (3a) to get

$$A = \frac{-2\pi^2\beta_{11}}{9kTV_{hs}^2} \qquad \ldots (16)$$

Subsequent substitution of this equation into equation (11) immediately gives us the perturbation part of the osmotic pressure

$$\Pi_a = -\frac{\pi^2\beta_{11}}{9V_{hs}^3}\phi^2 \qquad \ldots (17)$$

The value of β_{11} is based on the results of Monte Carlo simulations discussed in a previous paper[19].

The total osmotic pressure of the system is therefore

$$\Pi = \Pi_{hs} + \Pi_a$$

$$= \frac{kT\phi}{V_{hs}}\left\{\frac{1+\phi+\phi^2-\phi^3}{(1-\phi)^3} - \frac{\pi^2\beta_{11}\phi}{9kTV_{hs}^2}\right\} \qquad \ldots (18)$$

Figure 2 is a plot of the osmotic pressure as a function of particle solute concentration in the absence of NaCl. The experimental values used in this plot are based on a microemulsion with a water/AOT ratio of 8.4 and a hard sphere radius of 28 A[11].

It can be observed that the new theory gives a very good agreement with experimental data at dilute concentration (< 0.2 gm/cm^3). In this region, the errors are in fact less than 5%. Only at higher particle concentration was larger discrepancy developed between the new theory and experiment.

This, however, is not unexpected as the implicit assumption of pairwise additive potential will no longer be valid in the concentrated region.

Figure 3 is a plot of osmotic pressure against particle concentration for systems with varying NaCl concentration. The theoretical calculations show that the attraction among microemulsion droplets is inhibited upon increasing the concentration of NaCl. As the amount of salt is increased, the droplets increasingly resemble a suspension of hard spheres. This prediction in fact agrees with the experimental observations of anomalous electrolyte moderated interactions. Moreover, at dilute particle concentration, the values calculated from the theory have excellent quantitative agreement with experimental data. All these results suggest that the new theory is able to explain successfully the interactions among water-in-oil microemulsion droplets.

B. Osmotic compressibility

Another equilibrium property that will be examined in this paper is osmotic compressibility $\frac{\partial \Pi}{\partial \phi}$, a parameter obtained directly from light scattering studies. Substituting equation (16) into equation (15) gives us the perturbative part of the compressibility

$$\frac{\partial \Pi_a}{\partial \phi} = \frac{-2\pi^2 \beta_{11}}{9 V_s^3} \phi \qquad \ldots (19)$$

and the total osmotic compressibility is

$$\frac{\partial \Pi}{\partial \phi} = \frac{\partial \Pi_{hs}}{\partial \phi} + \frac{\partial \Pi_{e}}{\partial \phi}$$

$$= \frac{1}{V_{hs}} \left\{ \frac{kT(1+4\phi+4\phi^2-4\phi^3+\phi^4)}{(1-\phi)^4} - \frac{2\pi^2 \beta_{11} \phi}{9 V_{hs}^2} \right\} \quad \ldots (20)$$

In figure 4, osmotic compressibility data computed from the new theory is plotted against particle concentration for systems with various amounts of NaCl. Similar to the previous figure, the unsalted system displays the strongest interdroplet attraction. This attraction is decreased by increasing the electrolyte concentration. Another interesting feature of this figure is the curvature in the osmotic compressibility near zero concentration. For the unsalted system, the data increases at low concentration, while the corresponding salted systems tend to approach the intercept with a slope closer to zero. The addition of electrolyte moderates the curvatures observed in the unsalted system. Again, the new theory is able to predict a characteristic that had been reported experimentally but one which no previous theories could successfully account for. Similar to osmotic pressure, the theoretical and experimental values for osmotic compressibility show good agreement at dilute concentrations. The most significant aspect of the results, though, is the ability of the new model to predict all the qualitative features of the interdroplet interactions in a water-in-oil microemulsion that have been observed experimentally.

C. Ionic dissociation

One parameter that is crucial in determining the magnitude of dipole moment and polarizabilities of a microemulsion droplet is the number of ions present in its aqueous core. While the number corresponding to the NaCl added could easily be calculated, the number of counterions dissociated from the surfactant head groups is usually unknown. However, this quantity can be obtained from a fit to the experimental data. The best fit corresponds to the case of 16 counterions, or 37% of the surfactant head groups dissociated. This is in reasonable agreement with the only experimental data on AOT dissociation in microemulsions. In a study of a larger diameter AOT w/o microemulsion by Wong et. al.[27] using proton and sodium-23 NMR, it was estimated that about 28% of the sodium ions from the AOT surfactants were dissociated into the aqueous core of a microemulsion droplet.

D. Hamaker constant

Another parameter that can be determined from a knowledge of interdroplet potential is the Hamaker constant. This also can be conveniently obtained from light scattering studies and is available in the literature. By convention, the Hamaker constant is defined as

$$A_{12} = \pi^2 \rho_1 \rho_2 \beta_{12} \qquad \ldots (21a)$$

In this study, we have assumed the microemulsions to be monodisperse spherical droplets. Hence, the Hamaker constant can be rewritten as

$$A_{11} = \pi^2 \rho_1^2 \beta_{11} \qquad \ldots (21b)$$

where ρ_1 = number of molecules per unit volume of the interacting bodies.

β_{11} = van der Waals energy constant defined in equation (3b)

Treating each droplet as a single macroscopic body that possess a dipole moment, ρ_1 can be defined as

$$\rho_1 = 1 / V_{hs} \qquad \ldots (22)$$

The Hamaker constants calculated from this approach are given in Table I. Although the theoretical results are larger than the experimental values, the agreement with the literature data[9,11] to within an order of magnitude is actually quite good for a Hamaker constant. One possible explanation for the discrepancy is the error introduced by approximating the radial distribution function. A more realistic value of g(r) should lower the calculated Hamaker constant. Another important feature of the result is that the dipole interactions is able to account for the attraction between droplets. Without this ionic dipole moment, the

Hamaker constant calculated by considering the contribution of water molecules alone is only about $5*10^{-14}$ erg[9], some two orders smaller than experimental data. As discussed by Calje et. al[9], this value is too small to account for the interdroplet interaction.

Again, the new theoretical model is able to predict the qualitative trend associated with Hamaker constant in a w/o microemulsion. Namely, the Hamaker constant is reduced by increasing the salt concentration.

IV. CONCLUSIONS

As illustrated by the osmotic pressure, osmotic compressibility, and Hamaker constant calculations, the new theoretical model is able to predict the essential qualitative (and partially quantitative) features of interdroplet interactions in a water-in-oil microemulsion. In particular, it correctly predicts the existence of electrolyte moderated interactions. One conclusion that is confirmed by the current work is that the interaction between droplets in a W/O microemulsions is the result of a dipole - dipole and a dipole - induced dipole attractions.

Another important result obtained in this study is the dissociation constant of the counterions from the AOT surfactants. By fitting the experimental data in literature

to the new model, it is estimated that about 37% of the AOT surfactant headgroups is dissociated into the aqueous core. This also is in good agreement with data in the literature.

BIBLIOGRAPHY

1. deGennes, P.G., and Taupin, C., J. Phys. Chem., 86, 2294 (1982).

2. Prince, L.M., "Microemulsions : Theory and Practice," Academic Press, New York, 1977.

3. Scriven, L.E., Nature, 263, 2984 (1976).

4. Winsor, P.A., Trans. Faraday Soc., 44, 376 (1948).

5. Shah, D.O., ed., "Surface Phenomena in Enhanced Oil Recovery," Plenum, New York, 1982.

6. Candau, F., Leong, Y.S., Pouget, G., and Candau, S., J. Colloid Interface Sci., 101, 167 (1984).

7. Candau, F., Zekhnini, Z., and Durand, J.-P., J. Colloid Interface Sci., 114, 398 (1986).

8. Beckman, E.J., and Smith, R.D., J. Phys. Chem., 94, 345 (1990).

9. Calje, A.A., Agterof, W.G.M., and Vrij, A., in "Micellization, Solubilization and Microemulsions," K.L. Mittal, ed., Plenum, New York, 1977.

10. Cazabat, A.M., and Langevin, D., J. Chem. Phys., 74, 3148 (1981).

11. Bedwell, B., and Gulari, E., J. Colloid Interface Sci., 102, 88 (1984).

12. Hou, M.J., Kim, M., and Shah, D.O., J. Colloid Interface Sci., 123, 398 (1988).

13. Hayter, J.B., and Penfold, J., Mol. Phys., 42, 109 (1981).

14. Hayter, J.B., and Penfold, J., J. Chem. Soc. Faraday Trans. I, 77, 1851 (1981).

15. deRozieres, J., Middleton, M.A., and Schechter, R.S., J. Colloid Interface Sci., 124, 407 (1988).

16. Lang, J., Jada, A., and Malliaris, A., J. Phys. Chem., 92, 1946 (1988).

17. Eicke, H.F., Borkovec, M., and Das-Gupta, B., J. Phys. Chem., 93, 314 (1989).

18. Hall, D.G., J. Phys. Chem., 94, 429 (1990).

19. Chan, Y.Y., and McKeigue, K. (Chapter 2 of this thesis, to be published).

20. Peyrelasse, J., and Boned, C., J. Phys. Chem., 89, 370 (1985).

21. D'Arrigo, A., Paparelli, A., D'Aprano, A., Donato, I.D., Goffredi, M., and Turco Liveri, V., J. Phys. Chem., 93, 8367 (1989).

22. Waaler, D., Strand, K.A., Stromme, G., and Sikkeland, T., J. Chem. Phys., 91, 3360 (1989).

23. Barker, J.A., and Henderson, D., J. Chem. Phys., 47, 2856 (1967).

24. Barker, J.A., and Henderson, D., J. Chem. Phys., 47, 4714 (1967).

25. McQuarrie, D.A., "Statistical Mechanics," Harper & Row, New York, 1976.

26. Carnahan, N.F., and Starling, K.E., J. Chem. Phys., 51, 635 (1969).

27. Wong, M., Thomas, J.K., and Nowak, T., J. Amer. Chem. Soc., 99, 4730 (1977).

TABLE 4-1

Experimental and Estimated Hamaker Constants

%NaCl	A_{11} (Experimental) ($*10^{11}$ erg)	A_{11} (Theory) ($*10^{11}$ erg)
0	0.84	3.63
1	0.37	2.48
2		1.46
3	0.20	

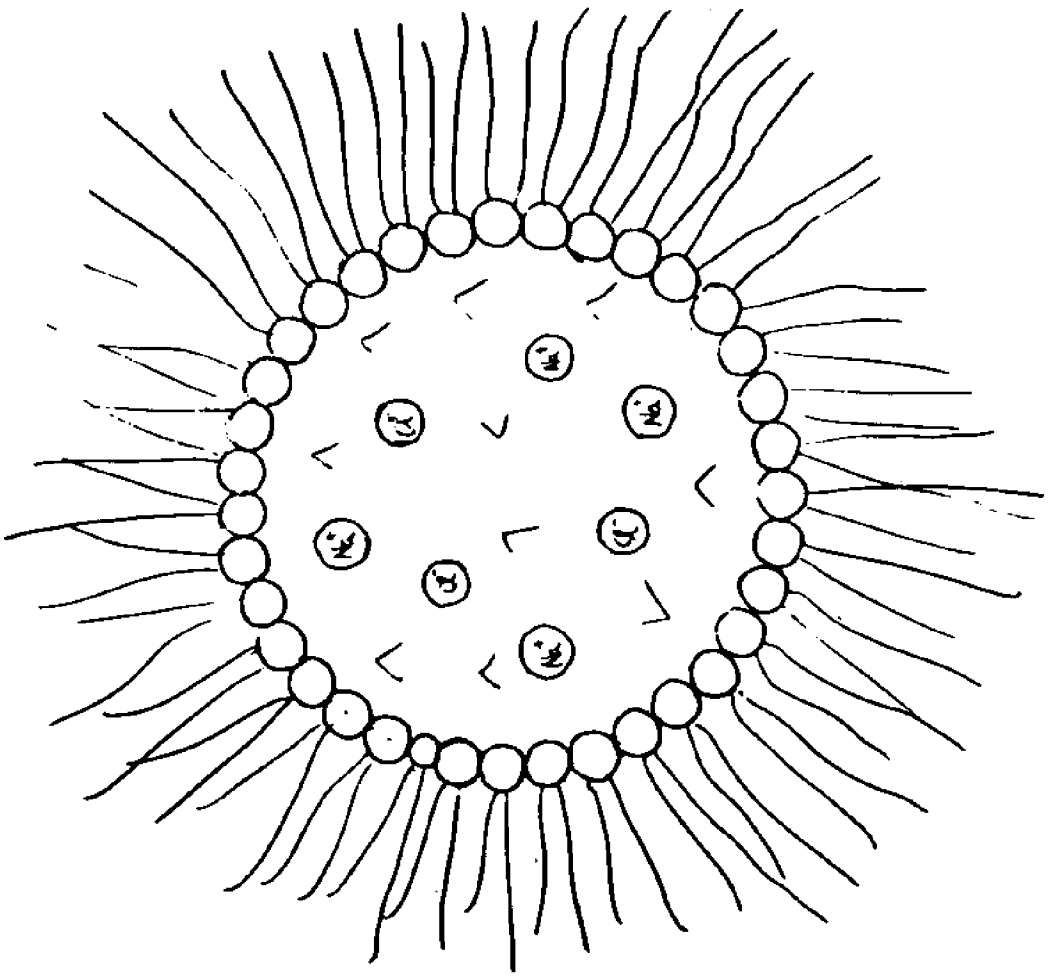

FIG. 4-1 Schematic description of a water-in-oil microemulsion droplet

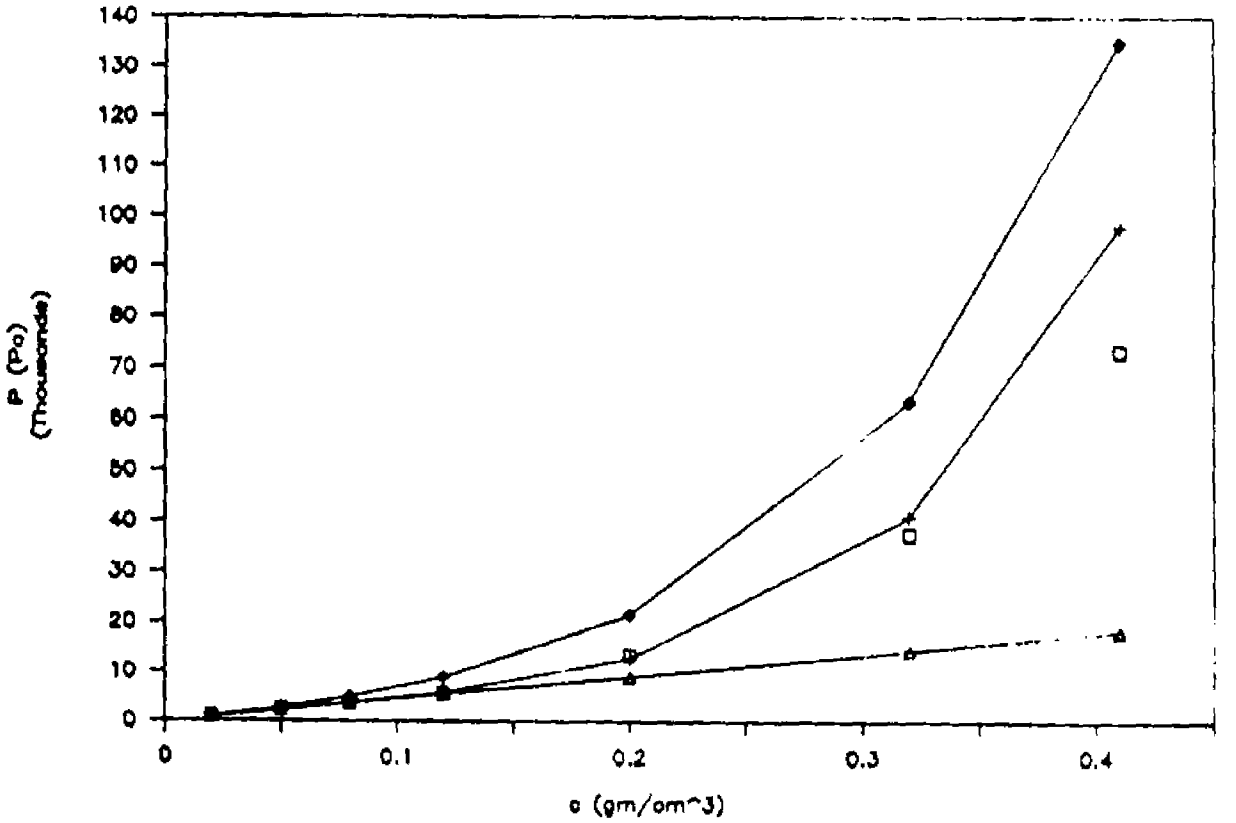

FIG. 4-2 Osmotic pressure vs. particle concentration with no NaCl added

- ▢ system with 0% NaCl (expt.)
- \+ system with 0% NaCl (theory)
- ◇ hard sphere system
- △ ideal system

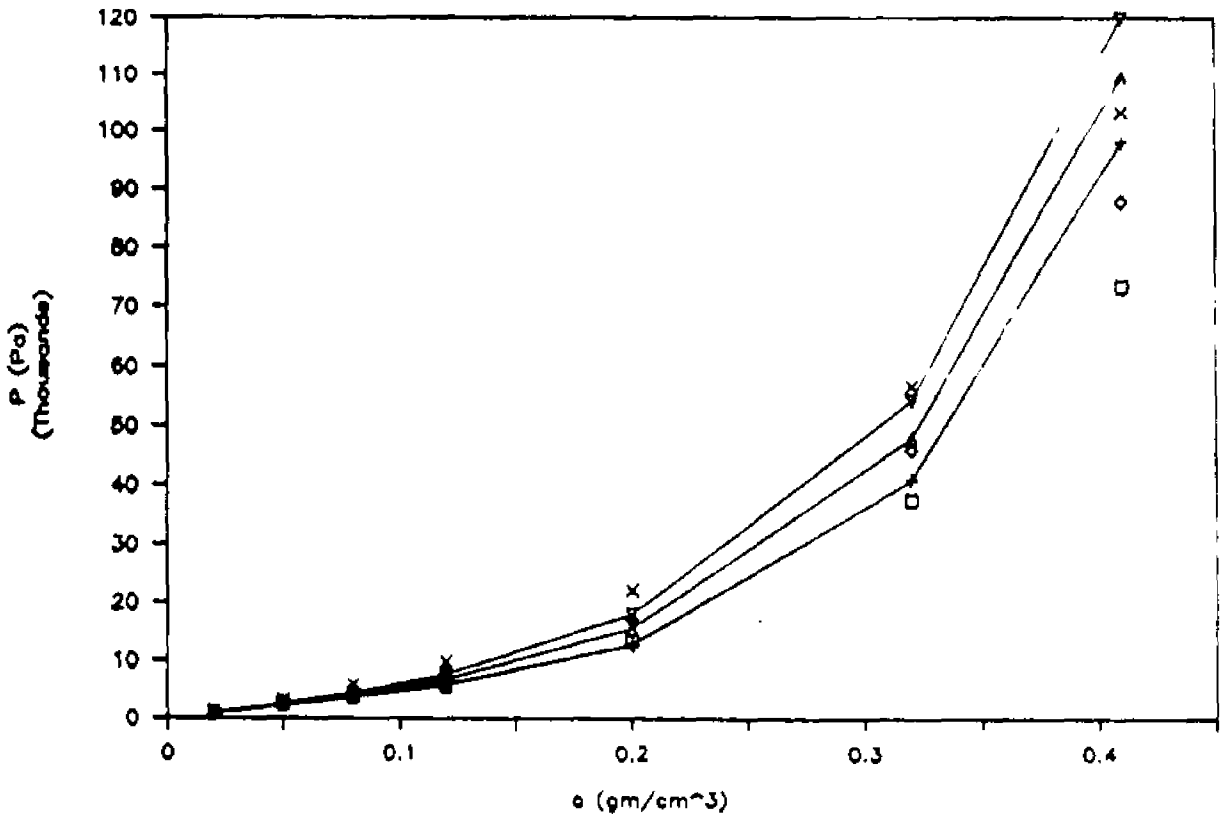

FIG. 4-3 Osmotic pressure vs. particle concentration for various NaCl concentrations

□ 0% NaCl (expt.)
\+ 0% NaCl (theory)
◇ 1% NaCl (expt.)
△ 1% NaCl (theory)
× 3% NaCl (expt.)
▽ 2% NaCl (theory)

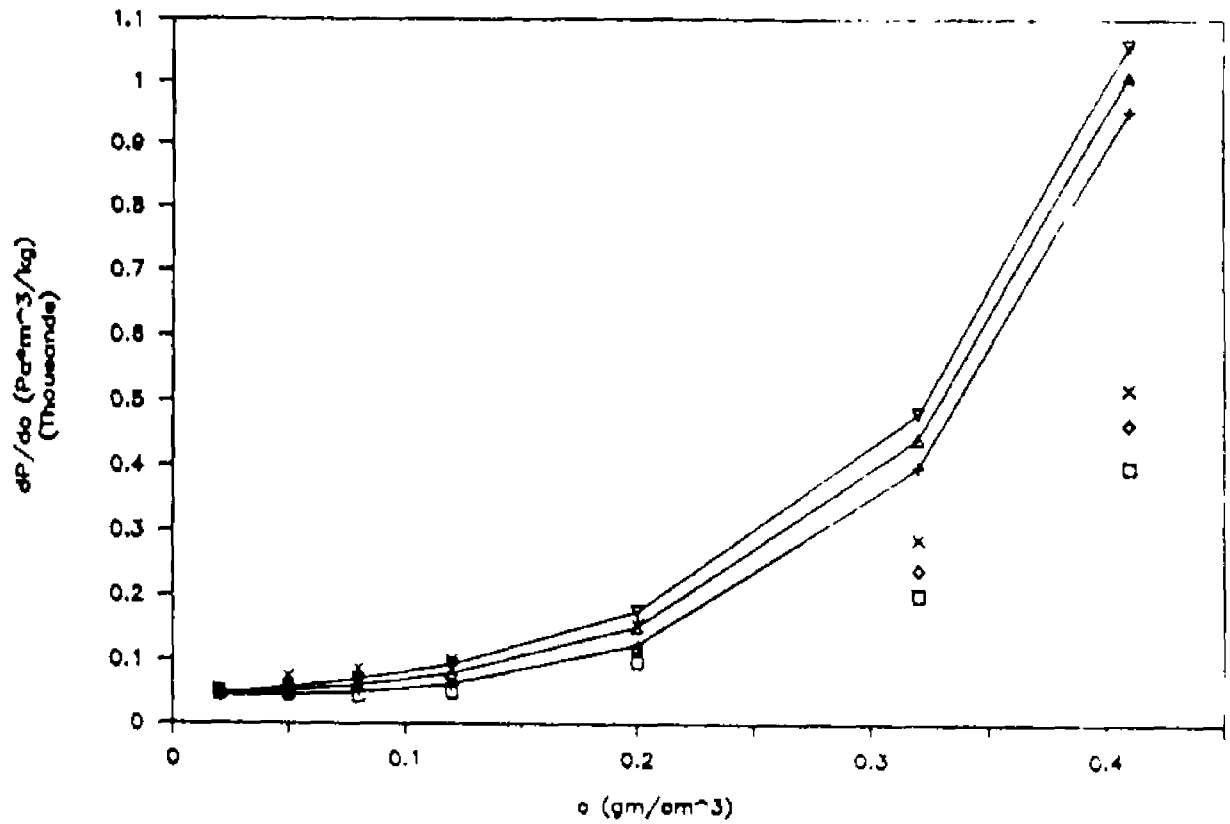

FIG. 4-4 Osmotic compressibility vs. particle concentration for various concentrations of NaCl

□ 0% NaCl (expt.)
+ 0% NaCl (theory)
× 1% NaCl (expt.)
△ 1% NaCl (theory)
◇ 3% NaCl (expt.)
▽ 2% NaCl (theory)

CHAPTER 5

Effect of Interdroplet Mass Transfer on Microemulsion Polymerization

ABSTRACT

To study the effect of interdroplet mass tranfer on the product size distribution in microemulsion polymerization processes, a coupled mass transfer and polymerization problem is formulated. Solutions to this problem are obtained via stochastic dynamics simulations. The results indicate that the ratio of interdroplet mass transfer rate, R_t, to the rate of reaction, R_p, is crucial in determining the final product size distribution. Monodisperse polymer particles are not formed unless this ratio is very small ($R_t/R_p < 0.001$). When the value of this ratio is large, polymerization in microemulsions possesses characteristics that resemble emulsion polymerization.

I. INTRODUCTION

Water-in-oil (W/O) microemulsions are small monodisperse, transparent, and thermodynamically stable "water" droplets dispersed in an oil continuum. Their typical sizes range from 10A - 100A[1]. Because of their unique properties, some innovative and technologically important applications for microemulsions have been proposed in recent years. Among them, the production of fine colloidal polymer particles[2-8] has received a lot of attention as the stable water-soluble polymers so produced have many potential applications, including enhanced oil recovery[5]. In such polymerization processes, water soluble monomers are solubilized at the core of a water-in-oil (W/O) microemulsion droplet and polymerization is then initiated by ultra-violet light. Provided there is no appreciable amount of material exchanged between the droplets, or between the droplet and the continuum during the course of the reaction, the microemulsion should offer an ideal reaction environment for control of the polymer particle size distribution.

While there have been a number of attempts[2-8] to produce such particles, the results in general have not lived up to expectations. In a study by Tang et al.[2], the latex particles produced by the photo-induced microemulsion polymerization process had a bimodal product distribution, with final particle size an order of magnitude larger than the initial

microemulsion droplets. In other similar studies, Candau et al.[3] and Beckman et al.[8] showed that the polymer particles formed are some 5 to 20 times larger than the initial microemulsion droplets. These results are indicative of a significant exchange of material between droplets, which consequently led to the formation of larger than expected polymer particles. In short, even though polymer particles with some interesting properties have been produced, the objective of achieving a narrow product size distribution was unsuccessful because of this rapid exchange of materials between droplets. Instead of acting as a system of small batch reactors, it appears that the microemulsions were acting more in the capacity of a dispersing agent that increased the number of nucleation sites.

Exchange of mass between microemulsion droplets has been shown by various researchers[9-13] to be a very fast phenomenon, on the order of microseconds. To achieve the desired products and product size distributions, the instantaneous interdroplet mass transfer rate must be significantly slowed. Unfortunately, few people have recognized the importance of this aspect of microemulsions research. Early studies of microemulsion polymerization were mainly focused on the product size and product size distribution, whereas there were no attempt to investigate either the interdroplet mass transfer phenomenon or its impact on the final products in microemulsion polymerization.

In a previous paper[14], we have started an effort to study mass transfer process in microemulsion by examining the nature of interdroplet interactons in water-in-oil micromeulsions. From a series of Monte Carlo simulations, it was demonstrated that attractions between microemulsion droplets is a result of dipole - dipole and dipole - induced dipole interactions. Utilizing the interdroplet potential function obtained from that study, a new interdroplet mass transfer model based on fundamental principles of colloid stability theory will be formulated in this paper. An assessment of the interdroplet mass transfer effects on product size and product size distribution in microemulsion polymerization will then be analyzed.

II. THEORETICAL BACKGROUND

A. Mass Transfer Model

The main feature of this mass transfer model is that the interdroplet mass transfer occurs primarily through coalescence/redispersion of microemulsion droplets, a conclusion that is agreed upon by many researchers[10-12]. This is actually a rather reasonable assumption for W/O microemulsions as water droplets do not contain any material that is appreciably soluble in the oil continuum.

To model the mass transfer process, colloid stability

theories can be applied to analyze the present problem. In this approach, it is assumed that because of interparticle attraction, the collision of two droplets result in their being trapped within one another's influence and acting as a single particle unit. The interdroplet mass transfer rate is therefore equal to the rate of coalescence process, which can be calculated by the method first proposed by Smoluchowski[15]. Assuming the interdroplet potential U(r) to be pairwise additive and the concentration of singlets, N^1, is constant, the rate at which the singlets disappear equals the rate at which a spherical droplet diffuse toward a stationary target droplet. From Fick's law, the number of droplets crossing a spherical surface of radius r and area A around the reference droplet per unit time, JA, is given by

$$JA = -(4\pi r^2)\left(D\frac{dN}{dr} + \frac{ND}{kT}\frac{dU(r)}{dr}\right) \quad \ldots (1)$$

where D is the diffusion coefficient of the droplet and N is the number of droplets per unit volume.

By removing the restriction that the reference droplet be stationary, the rate of change of JA is given by

$$\frac{-(JA)'}{8\pi r^2 D} = \frac{dN}{dr} + \frac{N}{kT}\frac{dU(r)}{dr} \quad \ldots (2)$$

Applying the following boundary conditions

at $r = \infty$, $N = N_1$ and $U(r) = 0$ ... (3a)

$r = \sigma_{HS}$, $N = 0$ ... (3b)

gives the solution to this differential equation

$$N_1 = \frac{-(JA)'}{8\pi D} \int_{2R}^{\infty} \exp\left(\frac{U(r)}{kT}\right) r^{-2} dr \qquad \ldots (4)$$

The rate of mass transfer between droplets is therefore

$$R_t = -(JA)'N_1 = (8\pi D N_1^2) / \int_{\sigma_{HS}}^{\infty} \exp(U(r)/kT) r^{-2} dr \qquad \ldots (5)$$

To demonstrate the practical applications of this method, estimates of the interdroplet mass transfer rate for a W/O microemulsion system are presented in Table 5-1. The potential functions required in the calculations are based on the results in one of our previous paper[18]. Other parameters used includes droplet radius of $2.5*10^{-7}$ cm, diffusion coefficient of $2.44*10^{-7}$ cm^2/sec, and a volume fraction of 0.05. Mass transfer rate for hard sphere particles are also computed as reference.

This approach, however, will not be valid for concentrated systems where the potential is no longer pairwise additive. A complex many body treatment must be employed to analyze such a system.

B. Mass Transfer Effect

Molecular Weight Distributions (M.W.D.) can be calculated by considering the primary reactions in detail. In a photo-induced microemulsion polymerization process, the monomers have to be activated by light quanta for reaction to occur.

$$M \xrightarrow{h\nu} M^* \qquad \ldots (6)$$

Unlike bulk polymerization, there are the following restrictions:

1). polymerization take place at the water core of the W/O microemulsion droplets, which act in the capacity as batch reactors;

2). termination of polymerization occurs when either there is no monomers left in the droplet or polymer chains couple through mass transfer between two initiated droplets.

Using these assumptions, a mass balance in a single microemulsion droplet can be performed as follows.

The rate of monomer loss through polymerization is given by

$$R_p = -k_p M P_x^* \quad \text{for initiated droplet}$$
$$R_p = 0 \quad \text{for uninitiated droplet} \qquad \ldots (7)$$

The rate of monomer loss through mass transfer is

$$f_1(R_t) = - k_1(M_1,M_2) R_t \qquad \ldots (8)$$

where k_1 is a random function of variable M_1, M_2, the number of monomers in the two colliding droplets.

The rate of monomer gain through mass transfer is

$$f_2(R_t) = k_2(M_1,M_2)\ R_t \qquad \ldots (9)$$

where k_2 is also a random function of variables M_1, M_2.

Combining equations (8) and (9) gives the total change of rate of monomers due to interdroplet mass transfer

$$f_1(R_t) + f_2(R_t) = k'(M_1,M_2)\ R_t \qquad \ldots (10)$$

where k' is a new random function of M_1 and M_2.

The mass balance for monomers in a single droplet is therefore given by

$$dM / dt = R_p + k'(M_1,M_2)\ R_t \qquad \ldots (11)$$

Defining $\int$, a new dimensionless variable to express the ratio of interdroplet mass transfer rate to the rate of intradroplet polymerization

$$\int = R_t/R_p \qquad \ldots (12)$$

Equation (11) therefore becomes

$$(1/R_p)\ (dM/dt) = 1 + k'(M_1,M_2) \qquad \ldots (13)$$

The rate of coupling in the system is

$$f_3(R_t,N_1^*) = k_3(P_1^*,P_2^*)(N_1^*/N_1)^2 R_t \qquad \ldots (14)$$

where N_1^* is number of initiated droplets

k_3 is a random function of variables P_1^* and P_2^*, degree of polymerization in the 2 colliding droplets respectively

and N_1^* can be calculated by the equation

$$dN_1^*/dt = f(I_{h\nu}) \qquad \ldots (15)$$

To calculate the product size distribution, we have to solve equations (13) to (15) simultaneously in many similar droplets. By its random nature, the problem suggest that a deterministic analytical approach is not feasible. Accordingly, stochastic dynamics simulation is employed to tackle this coupled mass transfer and reaction kinetics problem.

Stochastic dynamics[16] is a hybrid of the deterministic molecular dynamics method and the stochastic monte carlo technique. Unlike the molecular dynamics method, where all degrees of freedom were explicitly taken into account, some degrees of freedom in stochastic dynamics are represented only through their stochastic influence on the others. In this problem, while the polymerization process in a microemulsion droplet is deterministic with a constant rate, the detailed coalescence and mass transfer between deoplets is neglected and only taken into account by the stochastic elements.

At the beginning of the simulations, 2000 microemulsion droplets each with equal units of monomers in the water core were present. The evolution of the system was then followed over time, with degree of polymerization and monomer numbers in each droplet being recorded at each time step. Ater the passing of 4000 iterations when the polymerization was completed, the product size distribution of the system was then calculated. To simplify the formulation of the physical

model and the subsequent computer simulations, the following assumptions have been employed :

i). The microemulsions were treated as dilute systems. That is, there were only two body collisions and coalescence, many-body iteractions were neglected.

ii). The rate of polymerization, R_p, was assumed to be a constant and was arbitrarily set to 1 per unit time. This simplification is justified by the fact that the final product size distribution is solely a function of the ratio of the mass transfer rate to the reaction rate, thus, the actual magnitude of R_p is irrelevant except in relation to R_t.

iii). Whenever coalescence occurred, monomers were evenly divided between the 2 colliding droplets.

iv). Termination of the reaction happened when either there was no monomers left in a droplet or coupling occurred between 2 polymer chains from different initiated droplets.

To facilitate the calculation of product size distribution, the following parameters are defined

X = normalized degree of polymerization = P_X/P_o ... (16)

where P_o is theoretical degree of polymerization achieved in each droplet if there is no mass transfer between droplets.

P_X is actual degree of polymerization

The dimensionless number average molecular weight is defined as

$$M_n = \sum_i N_i X_i \; / \; \sum_i N_i \qquad \ldots (17)$$

whereas the dimensionless weight average molecular weight is

$$M_w = \sum_i N_i X_i^2 \; / \; \sum_i N_i X_i \qquad \ldots (18)$$

and the polydispersity of the system can be measured by the ratio of M_w to M_n, which is

$$\text{polydispersity index} = M_w/M_n \qquad \ldots (19)$$

III. RESULTS AND DISCUSSIONS

Figures 1 to 5 are the product size distribution of polymerization for various values of the ratio R_t/R_p. The mole fraction and weight fraction distributions corresponding to a system with an interdroplet mass transfer rate equal to the rate of polymerization ($R_t/R_p = 1$) are shown in figures 1a and 1b respectively. For such system, the particles have a very board size distribution, as indicated by the value of the polydispersity index of $_3$.16. In fact, some of the polymer particles produced are 3 orders of magnitude larger than the normalized unit degree of polymerization (the theoretical particle size produced when there is no mass transfer between droplets). This clearly indicates that significant amount of material has exchanged between droplets during the course of polymerization. As a consequence, many polymer chains linked and formed much larger particles.

In successive figures (figures 2 to 5), the product size distribution from simulations with various values of the ratio R_t/R_p are plotted. It is evident from these figures that the width of the distribution varies directly with the ratio R_t/R_p. By reducing the ratio R_t/R_p, the width of the distribution becomes narrower, i.e., more monodisperse. In addition, a larger fraction of the product particles have the unit degree of polymerization (i.e. X=1), as expected. Physically, when ratio R_t/R_p is lowered, fewer droplets will exchange mass with their neighbors. As a result, more droplets will have their reactions completed before any mass transfer with other droplets can occur, thus having X equal to 1. Though the polydispersity can be reduced by lowering the mass transfer rate, the polymer particles do not become monodisperse until R_t/R_p has a ratio of less than 0.0005.

The relationship between polydispersity and R_t/R_p is better illustrated in figure 6. Here, the calculated polydispersity ratio M_w/M_n is plotted against the ratio R_t/R_p. When the value of R_t/R_p is less than 0.1, we observe that the polydispersity ratio has a very steep positive slope. Thus, any slight increase of the mass transfer rate compared to the reaction rate will lead to a very dramatic increase in the polydispersity of the product. Beyond 0.1, however, there is a much weaker dependence of the polydispersity index on the value of R_t/R_p, suggesting that there exist two regimes of different characteristics for microemulsion polymerization

processes. To pursue this point further, the dimensionless number-averaged molecular weight M_n and the weight-averaged molecular weight M_w are plotted against the R_t/R_p ratio in figures 7 and 8 respectively. In these figures, when R_t/R_p has a value less than 0.1, both molecular weights remain about constant. For R_t/R_p greater than 0.1, however, there is a steep increase of the molecular weight with increasing R_t/R_p ratio. Clearly, this evidence further supports the existence of two different processes with distinct characteristics. One possible explanation for this behavior is that the rapid interdroplet mass transfer had turned some of the microemulsion droplets to be the reservoir of monomer reactants for the other droplets where reaction is taking place. Thus, the microemulsion polymerization process had been transformed into a process that resembles emulsion or solution polymerization. It is therefore not surprising to see the resulting polymers having molecular weight similar to the one obtained in emulsion polymerization processes.

The advantages of microemulsion polymerization is its potential of producing very small and rather monodisperse polymer particles. However, our present theory clearly demonstrates that this objective can not be achieved unless we are able to manipulate the ratio R_t/R_p to become a very small number. The first logical approach would be to lower the rate of interdroplet mass transfer to such an extent that it is negligible when compared to the rate of polymerization. Based

on experiments performed by Bedwell[17], this condition might be achieved by adding electrolytes to the microemulsions. Alternatively, one can choose a polymer system that have an extremely rapid rate of polymerization.

IV. CONCLUSIONS

In this paper, we have demonstrated the importance of the interdroplet mass transfer rate in controlling the final products and product size distribution in a microemulsion process. Comparing the rate of interdroplet mass transfer to the rate of polymerization, we found that nearly monodisperse particles were not produced until the R_t/R_p ratio was less than 0.001. In any practical design of such process or any other microemulsion-based fine colloidal production process, efforts should be spent to ensure the ratio of R_t/R_p be as small as possible. In fact, the result suggest that when the ratio of R_t/R_p is larger than 0.1, the microemulsion polymerization would be transformed into emulsion polymerization process.

BIBLIOGRAPHY

1. deGennes, P.G., and Taupin, C., J. Phys. Chem., 86, 2294 (1982).

2. Tang, H.I., Johnson, P.L., and Gulari, E., in "Measurement of Suspended Particles by Quasi-Elastic Light Scattering," B.E. Dahneke, ed., Wiley, New York, 1983.

3. Candau, F., Leong, Y.S., Pouget, G., and Candau, S., J. Colloid Interface Sci., 101, 167 (1984).

4. Lianos, P., J. Phys. Chem., 86, 1935 (1982).

5. Leong, Y.S., and Candau, F., J. Phys. Chem., 86, 2269 (1982).

6. Candau, F., Zekhnini, Z., and Durand, J.-P., J. Colloid Interface Sci., 114, 398 (1986).

7. Schauber, C., and Riess, G., Polym. Mater. Sci. Eng., 57, 945 (1987).

8. Beckman, E.J., and Smith, R.D., J. Phys. Chem., 94, 345 (1990).

9. Eicke, H.F., Shepard, J.C., and Steinman, A.J., J. Colloid Interface Sci., 56, 168 (1975).

10. Lang, J., Jada, A., and Malliaris, A., J. Phys. Chem., 92, 1946 (1988).

11. Fletcher, P.D.I., Howe, A.M., and Robinson, B.H., J. Chem. Soc. Faraday Trans. I, 83, 185 (1987).

12. Howe, A.M., McDonald, J.A., and Robinson, B.H., J. Chem. Soc. Faraday Trans. I, 83, 1007 (1987).

13. Jada, A., Lang, J., Zana, R., Makhloufi, R., Hirsch, E., and Candau, S.J., J. Phys. Chem., 94, 387 (1990).

14. Chan, Y.Y., and McKeigue, K. (Chapter 2 of this thesis, to be published).

15. Heimenz, P.C., "Principles of Colloid and Surface Chemistry," Marcel Dekker, New York, 1986.

16. Heermann, D.W., "Computer Simulation Mehtods in Theoretical Physics," Springer-Verlag, New York, 1986.

17. Bedwell, B., and Gulari, E., J. Colloid Interface Sci., 102, 88 (1984).

18. Chan, Y.Y., and McKeigue, K. (Chapter 3 of this thesis, to be published).

TABLE 5-1

Estimated Interdroplet Mass Transfer Rates

% NaCl	Mass transfer rate ($\#^2/cm^3$)
0	$3.9 * 10^{23}$
1	$3.7 * 10^{23}$
3	$3.3 * 10^{23}$
hard sphere	$2.0 * 10^{23}$

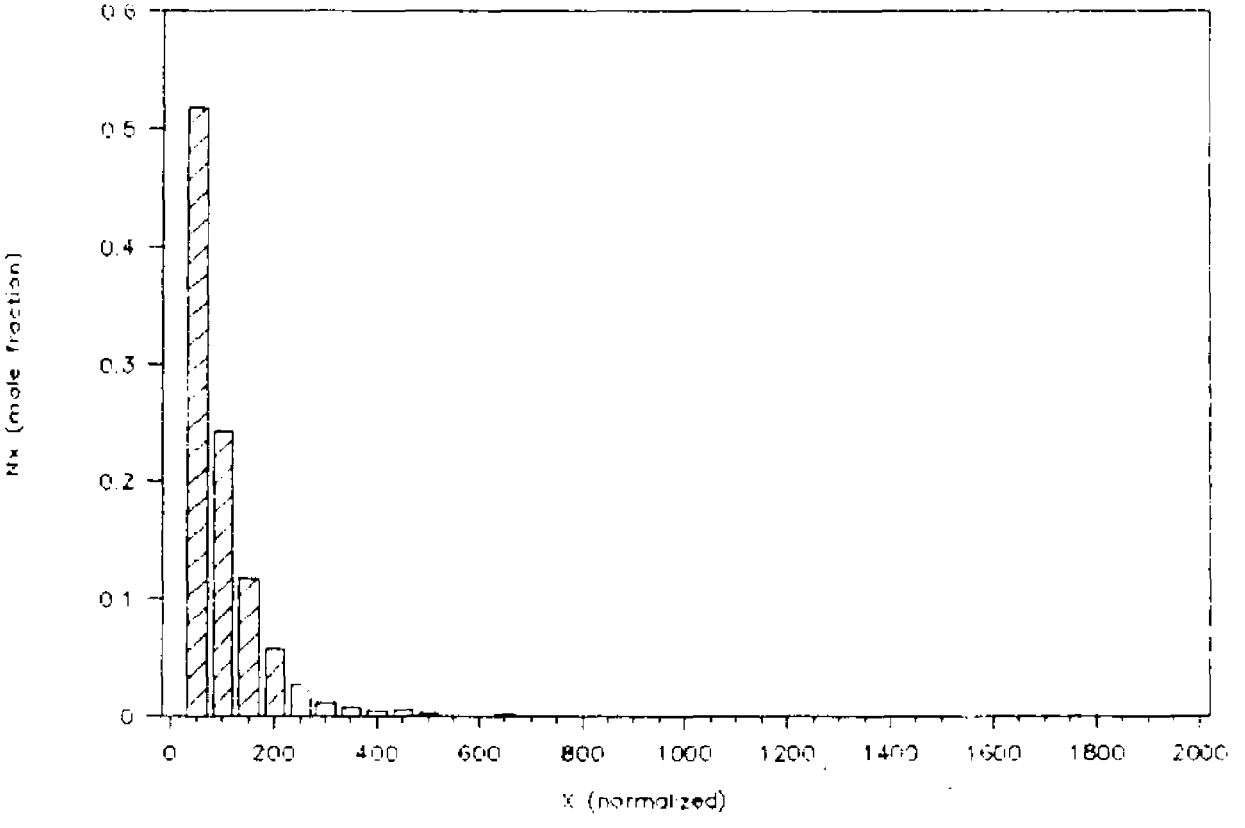

FIG. 5-1a Mole fraction distribution with Rt/Rp=1

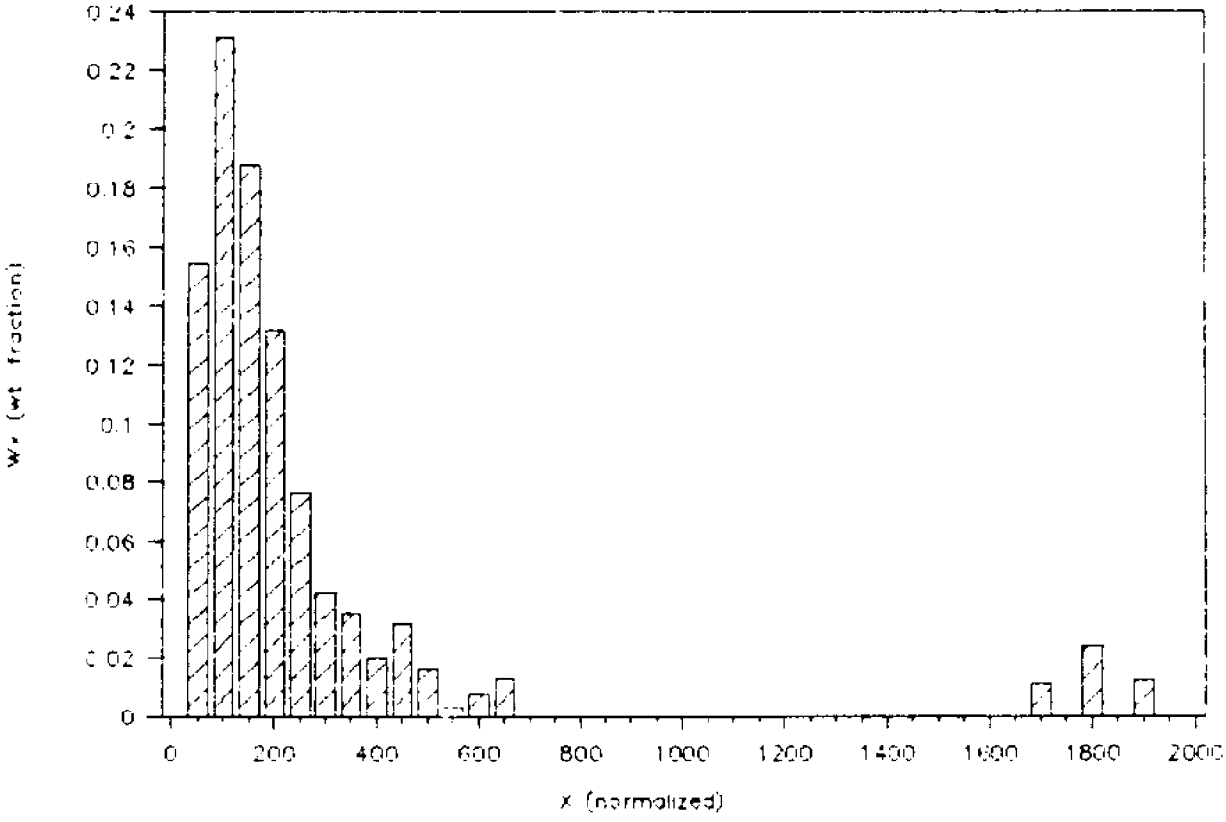

FIG. 5-1b Weight fraction distribution with Rt/Rp=1

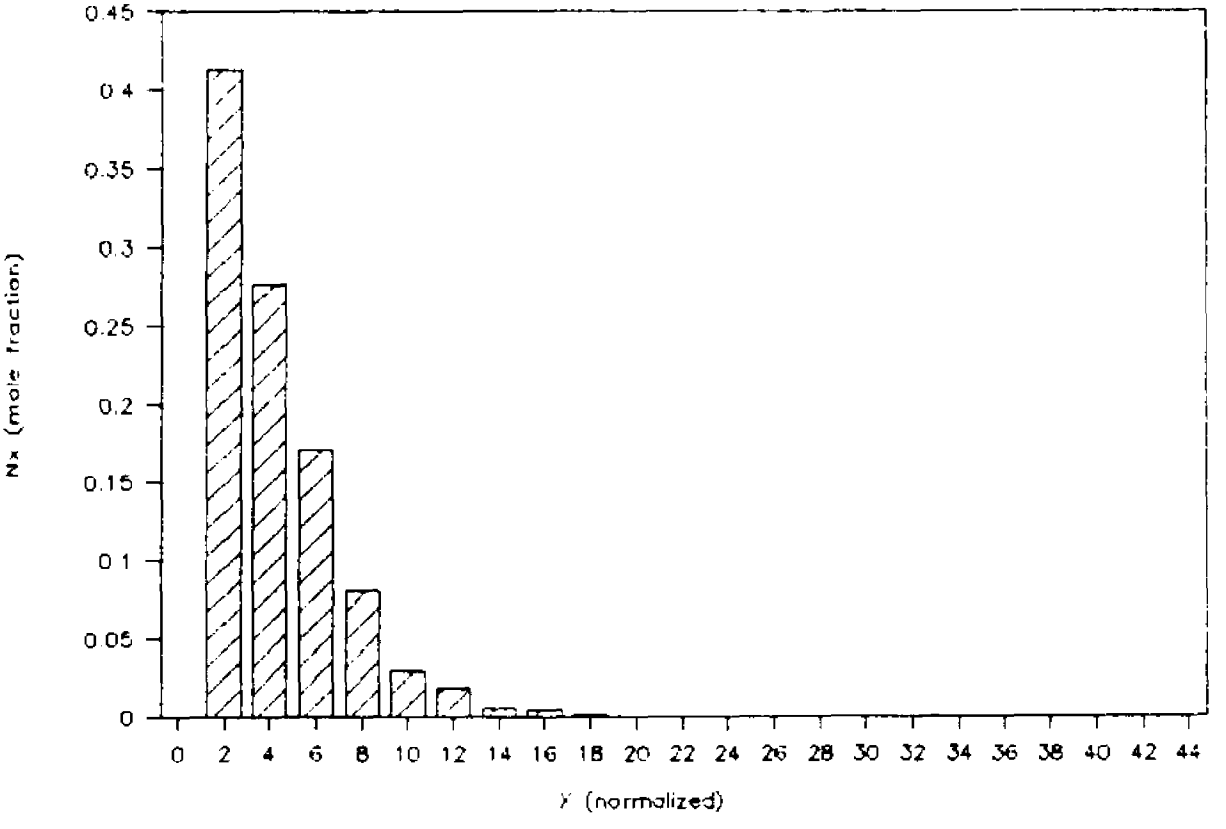

FIG. 5-2a Mole fraction distribution with Rt/Rp=0.1

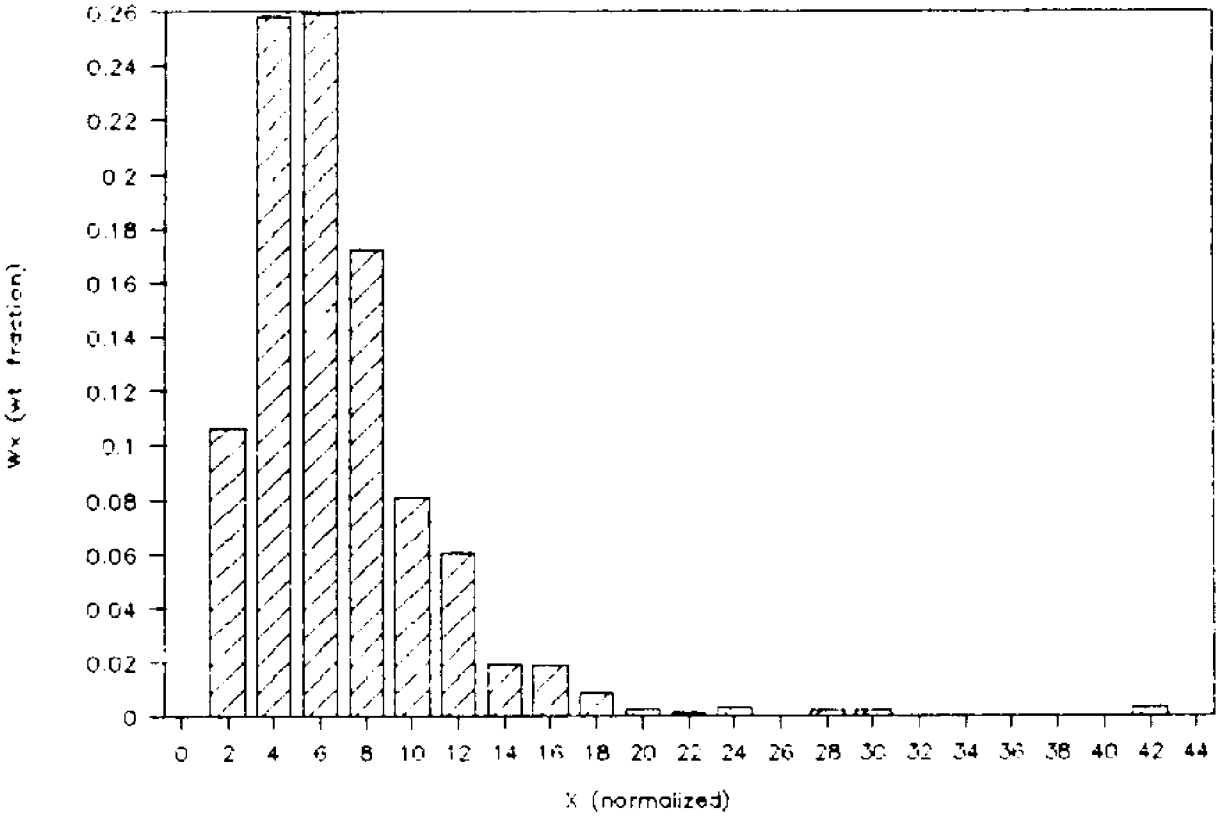

FIG. 5-2b Weight fraction distribution with Rt/Rp=0.1

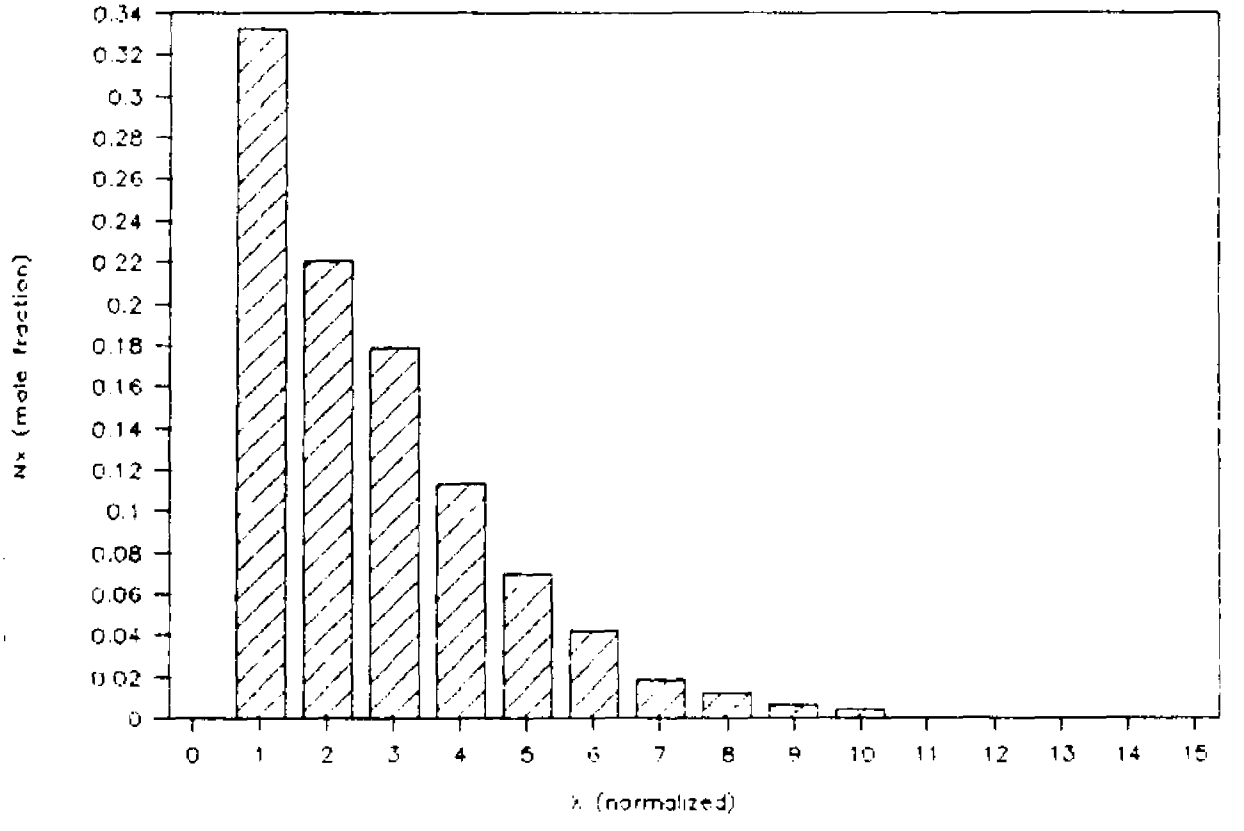

FIG. 5-3a Mole fraction distribution with Rt/Rp=0.05

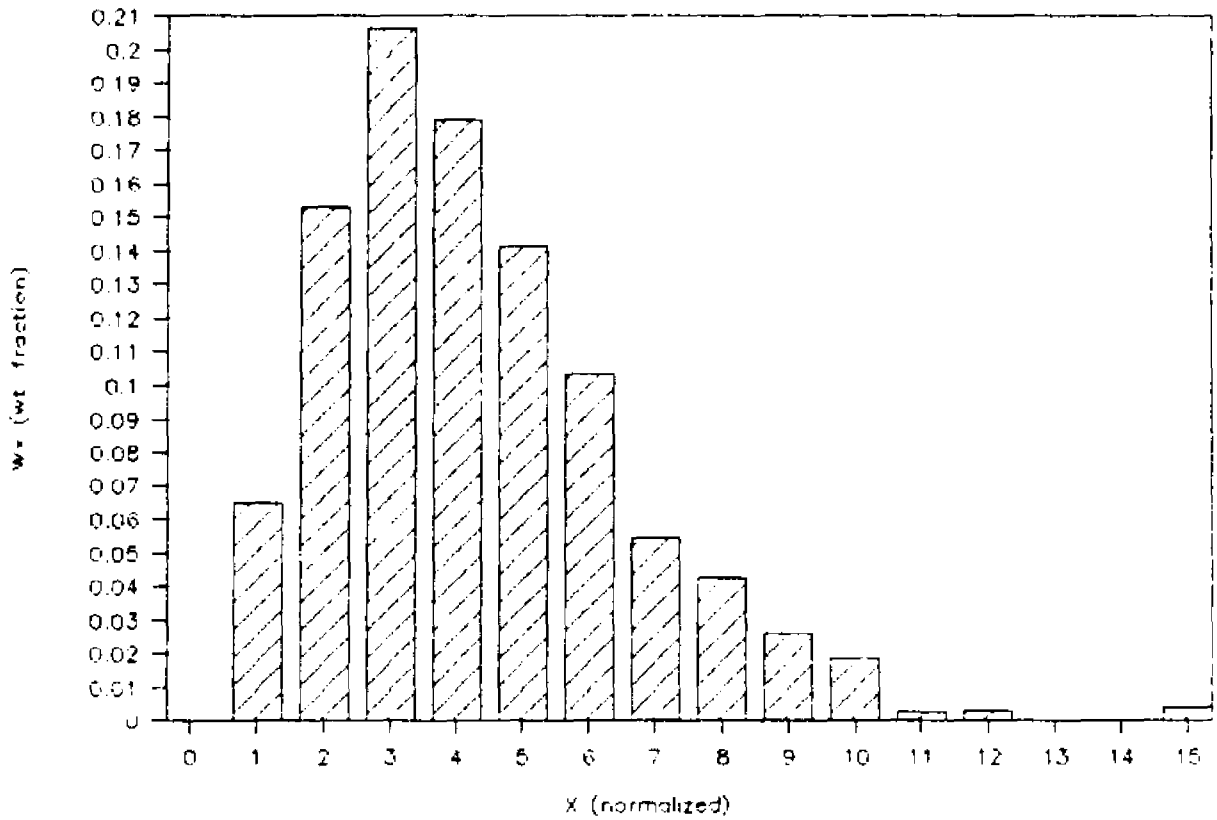

FIG. 5-3b Weight fraction distribution with Rt/Rp=0.05

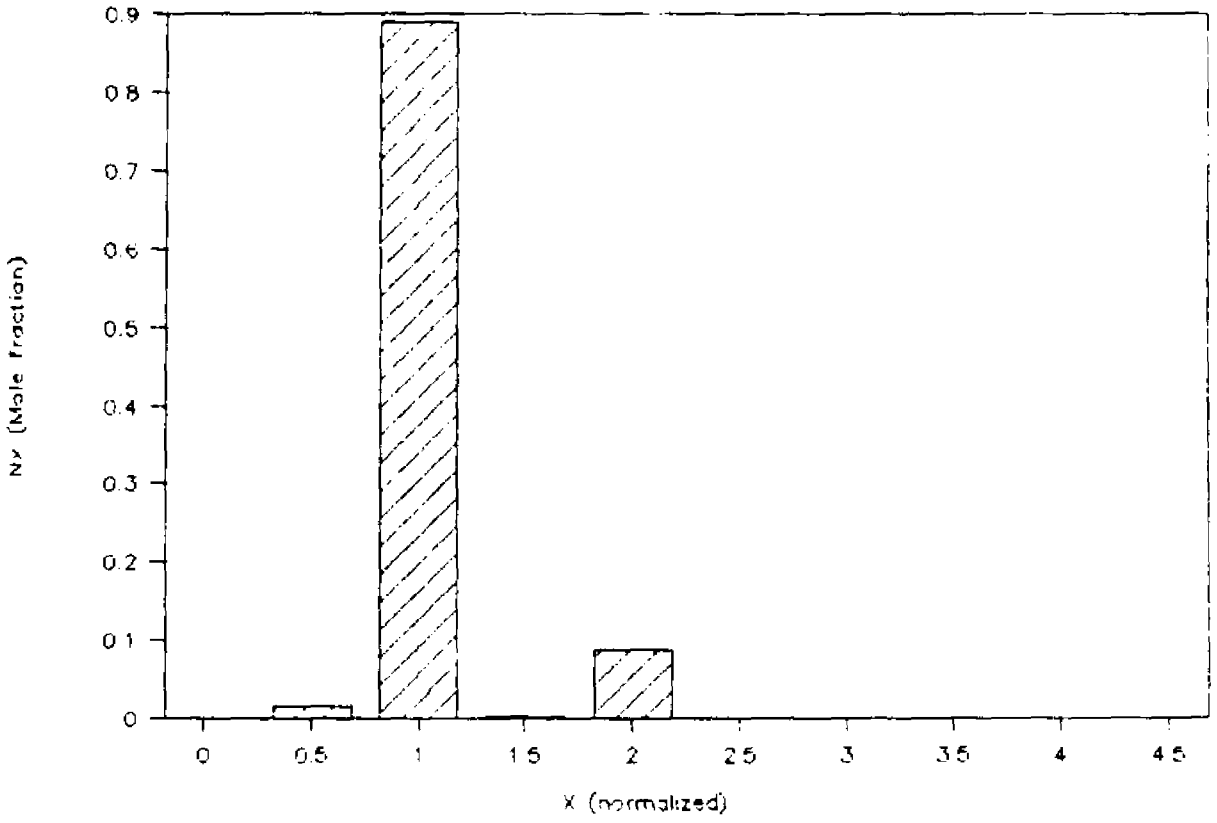

FIG. 5-4a Mole fraction distribution with Rt/Rp=0.001

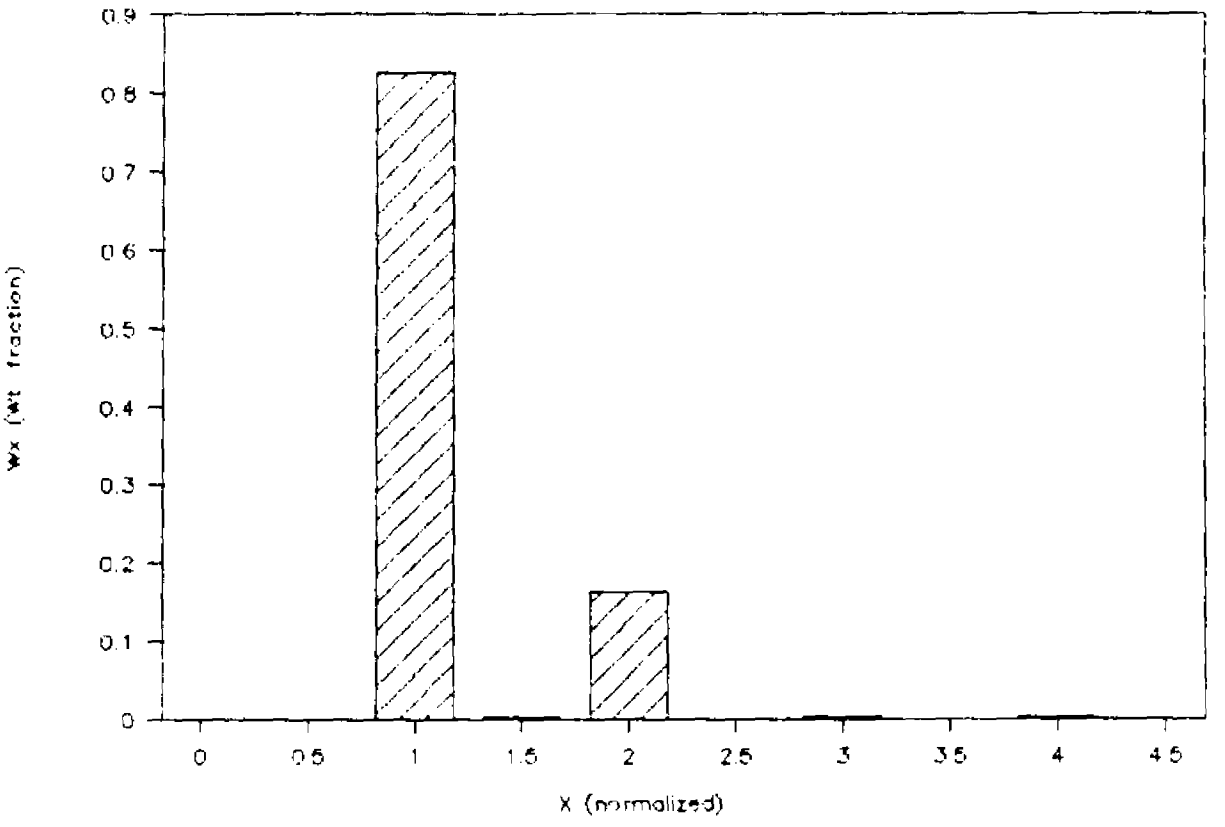

FIG. 5-4b Weight fraction distribution with Rt/Rp=0.001

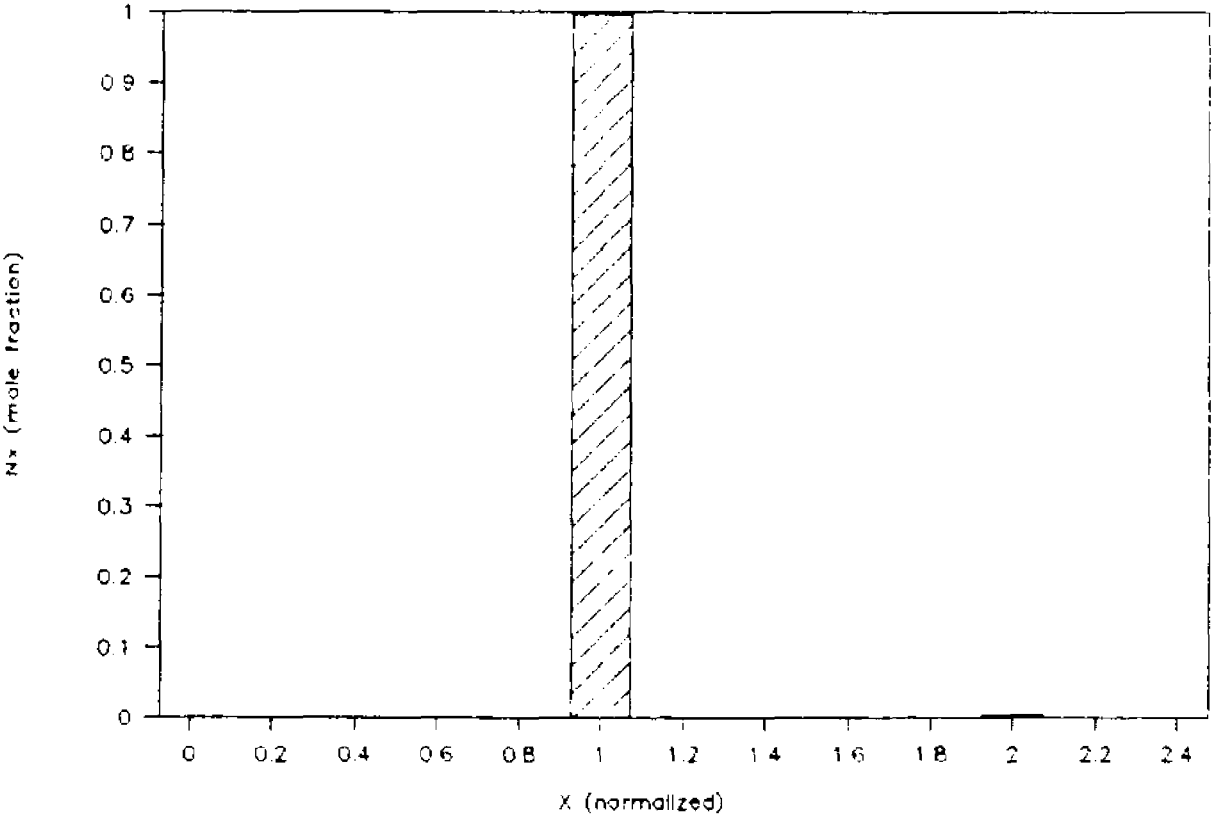

FIG. 5-5a Mole fraction distribution with Rt/Rp=0.0001

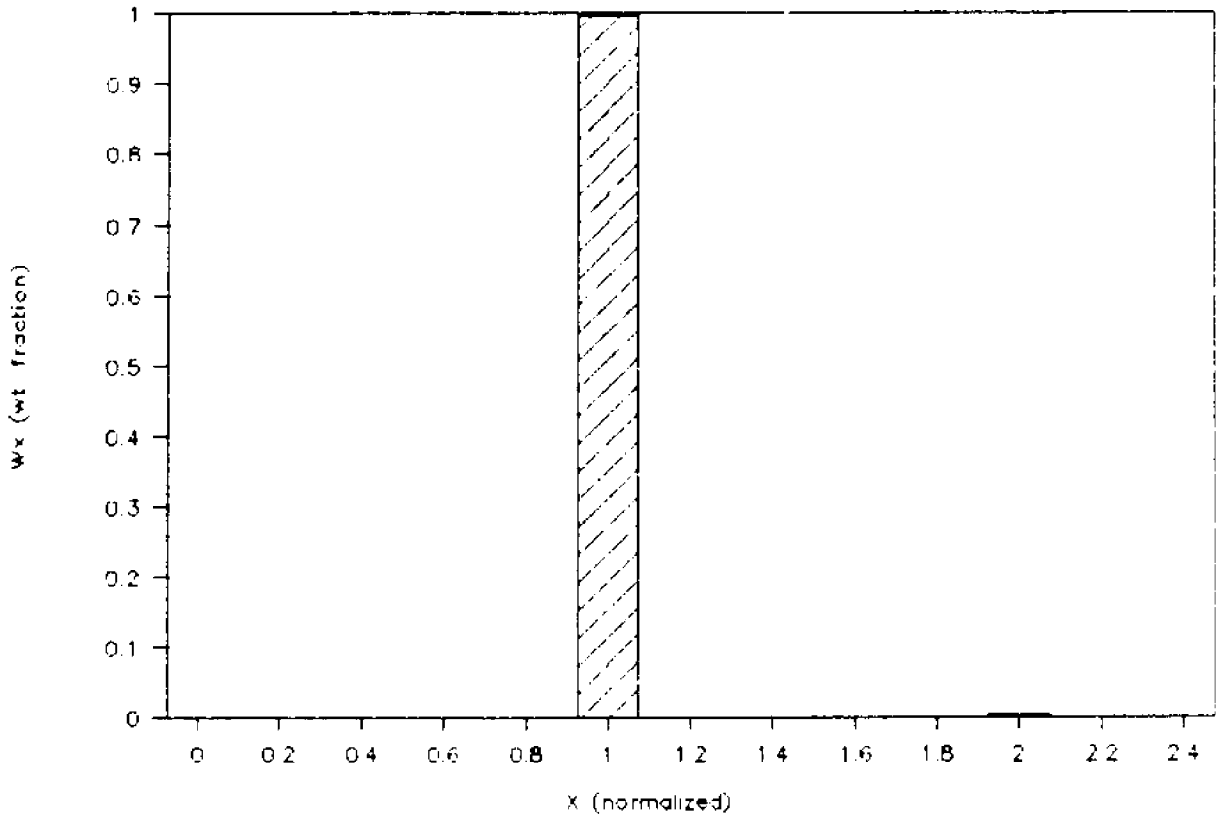

FIG. 5-5b Weight fraction distribution with Rt/Rp=0.0001

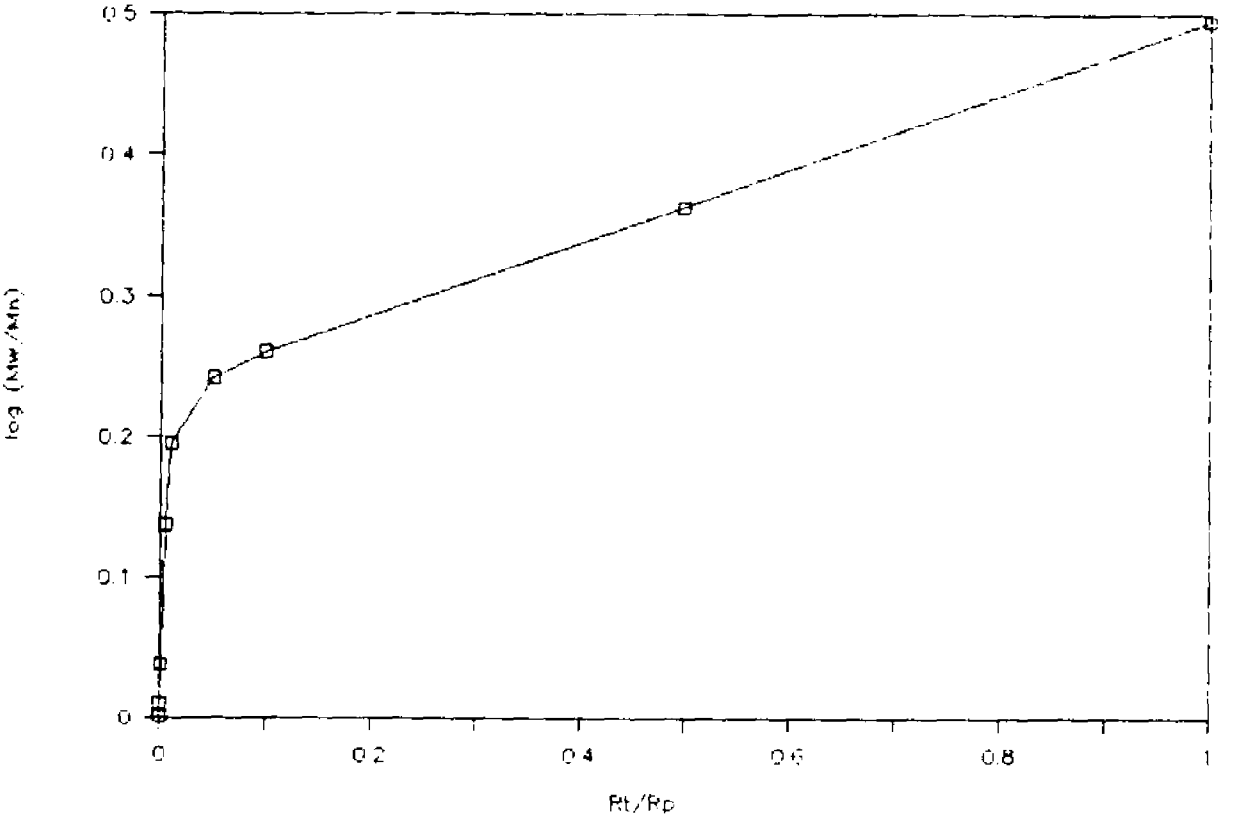

FIG. 5-6 Plot of polydispersity ratio vs. Rt/Rp

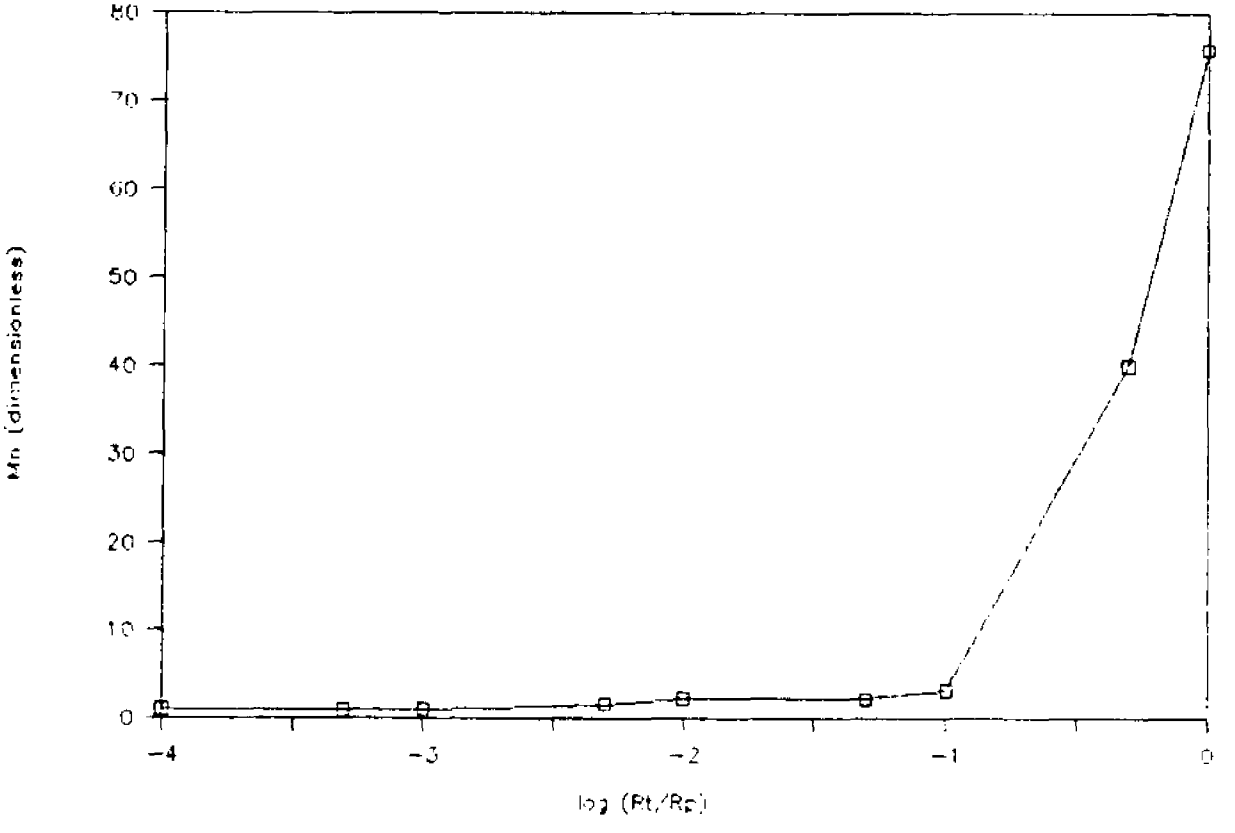

FIG. 5-7 Plot of number-averaged molecular weight vs. Rt/Rp

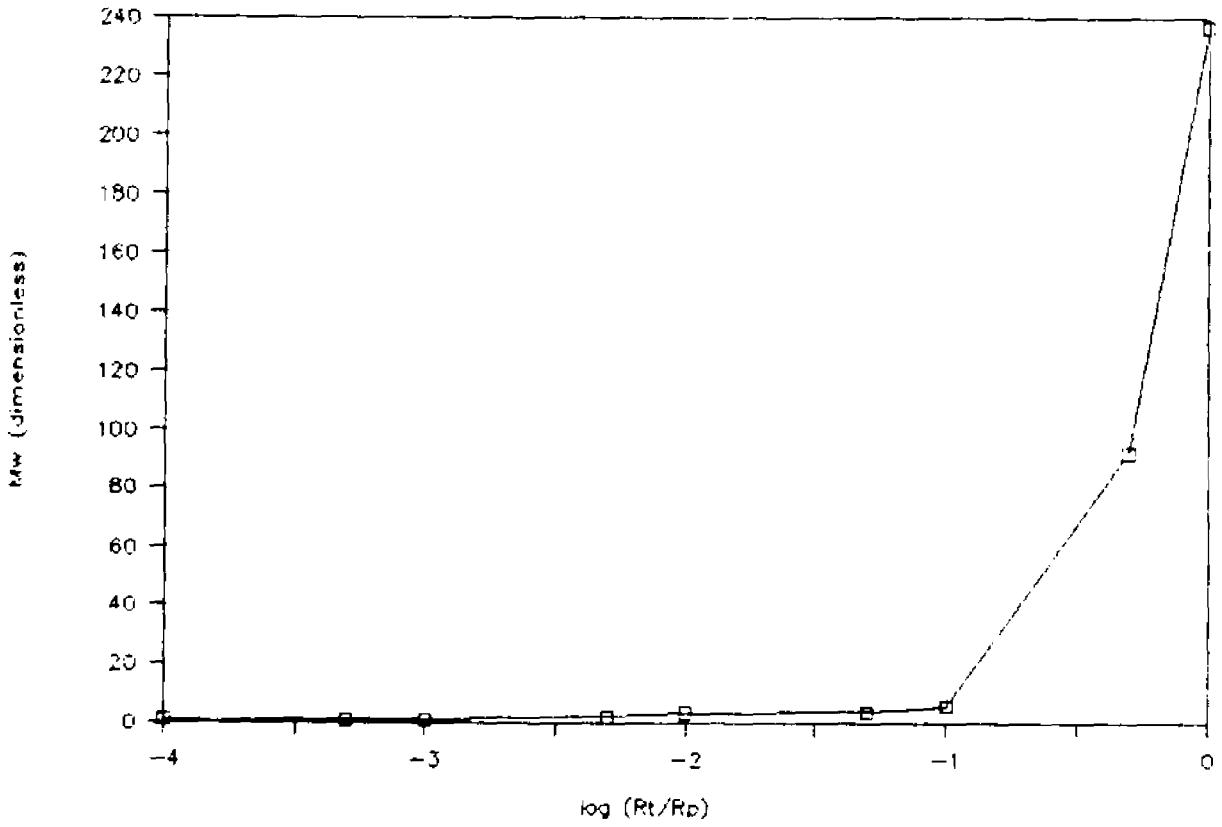

FIG. 5-8 Plot of weight-averaged molecular weight vs. Rt/Rp

CHAPTER VI

CONCLUSIONS AND RECOMMENDATIONS

We have shown that attractions between W/O microemulsion droplets are the result of dipole - dipole and dipole - induced dipole interaction forces. The study of such interdroplet interactions is essential in understanding the interdroplet mass transfer phenomenon, which critically governs the success of many novel microemulsions based technologies.

In Chapter II, from a series of Monte Carlo simulations, we demonstrated the existence of a configurational dipole moment and polarizability in a W/O microemulsion system consisting of water, oil, and a non-ionic surfactant. A new theory for the interactions between microemulsion droplets was developed based on the dipole - dipole and the dipole - induced dipole attractions.

In Chapter III, Monte Carlo technique was again employed to evaluate the magnitude of the dipole moment and the polarizability in a W/O microemulsion system containing an anionic surfactant. We showed that the salt added to the microemulsions has a profound effect on the attractions between droplets. The results was also compared to a W/O microemulsion system with non-ionic surfactants.

In Chapter IV, the interaction potential calculated from our new theory was transformed into experimentally accessible parameters such as Hamaker constants and osmotic compressibility. Comparison with the literature data was made to verify the accuracy of the theory.

In Chapter V, the relationship between the interdroplet potential function and the interdroplet mass transfer phenomenon was established. We also explored in detail the effect of interdroplet mass transfer on the particle size distribution in a microemulsion polymerization process.

The results in this dissertation suggested that addition of salt to a W/O microemulsion system would decrease the interdroplet mass transfer rate and thus offer a better control of the product size distribution in microemulsion polymerization process. To establish the extent to which this theoretical prediction is correct and to pinpoint any potential problems in actual applications, experimental studies of the salt effects on microemulsion polymerization are currently being carried out in a collaborating laboratory.

The investigation of the intra-droplet production of other fine colloidal particles such as metallic crystallites and cadmium sulfide is a logical extension of the present study. This dissertation has laid the groundwork for examining the control of particle size and particle size

distribution in these processes.

In addition to microparticle production, mass transfer phenomena is also critical in determining the success of other novel microemulsions based technologies. Following the same approach as in the calculation of Hamaker constant, it is conceivable to modify the droplet - droplet potential to a droplet - planar potential function by taking the geometrical shapes of the various systems into consideration. This would enable the mass transfer parameters to be evaluated and applied in technologies including but not limited to liquid membrane separation process and controlled drug delivery technique.

BIBLIOGRAPH

1. Heimenz, P.C., "Principles of Colloid and Surface Chemistry," Marcel Dekker, New York, 1986.

2. Shaw, D.J., "Introduction to Colloid and Surface Chemistry, " Butterworths, London, 1980.

3. Hoar, T.P., and Schulman, J.H., Nature, **152**, 102 (1943).

4. Eicke, H.F., J. Colloid Interface Sci.. **68**, 440 (1979).

5. Cebula, D.J., Myers, D.Y., and Ottewill, R.H., Collid & Polymer Science, **260**, 96 (1982).

6. Prince, L.M., "Microemulsions : Theory and Practice," Academic Press, New York, 1977.

7. Mitchell, D.J., and Ninham, B.W., J. Phys. Chem., **87**, 2996 (1983).

8. deGennes, P.G., and Taupin, C., J.Phys. Chem., **86**, 2294 (1982).

9. Talmon, Y., and Prager, S., J. Chem. Phys., **69**, 2984 (1978).

10. Scriven, L.E., Nature, **263**, 2984 (1976).

11. Winsor, P.A., Trans. Faraday Soc., **44**, 376 (1984).

12. Widom, B., J. Chem. Phys., **81**, 1030 (1984).

13. Shah, D.O., ed., "Surface Phenomena in Enhanced Oil Recovery," Plenum, New York, 1982.

14. Taber, J.J., Pure & Appl. Chem., **52**, 1323 (1980).

15. Fendler, J.H., and Fendler, E.J., "Catalysis in Micellar and Macromolecular Systems," Academic Press, New York, 1975.

16. LePesant, J.P., and Tantot, G., (Hotchkins-Brandt Sogeme H.B.S.), Eur. Patent Appl. EP 36,790 (1981).

17. Robbins, M.L., and Brownawell, D.W., (Esso Res. and Eng. Co.), U.S. Patent 3,641,181 (1972).

18. Mackay, R.A., Adv. Colloid Interface Sci., **15**, 131 (1981).

19. Jones, C.E., and Mackay, R.A., J. Phys. Chem., **82**, 63 (1978).

20. Jones, C.E., and Mackay, R.A., J. Phys. Chem., **83**, 803 (1979).

21. Kiwi, J., and Graetzel, M., J. Phys. Chem., **84**, 1503 (1980).

22. Atik, S.S., and Thomas, J.K., J. Am. Chem. Soc., **103**, 3543 (1981).

23. Atik, S.S., and Thomas, J.K., J. Am. Chem. Soc., **103**, 4367 (1981).

24. Tang, H.I., Johnson, P.L., and Gulari, E., in "Measurement of Suspended Particles by Quasi-Elastic Light Scattering," B.E. Dahneke, ed., Wiley, New York, (1983).

25. Candau, F., Leong, Y.S., Pouget, G., and Candau, S., J. Colloid Interface Sci., **101**, 167 (1984).

26. Lianos, P., J.Phys. Chem., **86**, 1935 (1982).

27. Leong, Y.S., and Candau, F., J. Phys. Chem. **86**, 2269 (1982).

28. Boutonnet, M., Kizling, J., Stenius, P., and Marie, G., Colloids and Surfaces, **5**, 209 (1982).

29. Candau, F., Zekhnini, Z., and Durand, J.-P., J. Colloid Interface Sci., **114**, 398 (1986).

30. Schauber, C., and Riess, G., Polym. Mater. Sci. Eng., **57**, 945 (1987).

31. Beckman, E.J., and Smith, R.D., J. Phys. Chem., **94**, 345 (1990).

32. Petit, C., and Pileni, M.P., J. Phys. Chem., **92**, 2282 (1988).

33. Lianos, P., and Thomas, J.K., Chem. Phys. Lett., **125**, 299 (1986).

34. Lianos, P., and Thomas, J.K., J. Colloid Interface Sci., **117**, 505 (1987).

35. Dannhauser, T., O'neal, M., Johansson, K., Witten, D., and McLennon, G., J. Phys. Chem., 90 6074 (1986).

36. Steigewald, M.L., Alirisatos, A.P., Gibson, J.M., Harris, T.D., Korten, R., Muller, A.J., Thoyer, A.M., Duncan, T.M., Douglas, D.C., and Brus, L.E., J. Am. Chem. Soc., 110, 3046 (1988).

37. Petit, C., Lixon, P., and Pileni, M.P., J. Phys. Chem., 94, 1598 (1990).

38. Petit, C., Brochette, P., and Pileni, M.P., J. Phys. Chem., 90, 6517 (1986).

39. Tanquary, A.C., and Lacey, R.e., eds., "Controlled Release of Biologically Active Agents," Plenum, New York, 1974.

40. Ziegenmeyer, J., and Fuehrer, C., Acta Pharm. Technol., 26, 273 (1980).

41. Fubini, B., Gasco, M.R., and Gallarate, M., Int. J. Pharm., 42, 19 (1988).

42. Halbert, G.W., Stuart, J.F.B., and Florence, A.T., Int. J. Pharm., 21, 219 (1984).

43. Tondre, C., and Xenakis, A., Colloid & Polymer Sci., 260, 232 (1982).

44. Tondre, C., and Xenakis, A., Faraday Discuss. Chem. Soc., 77, 115 (1984).

45. Xenakis, A., and Tondre, C., J. Phys. Chem., 87, 4737 (1983).

46. Xenakis, A., and Tondre, C., J. Colloid Interface Sci., 117, 442 (1987).

47. Kim, H.S., and Tondre, C., Sep. Sci. Technol., 24, 485 (1989).

48. Tondre, C., and Derouiche, A., J. Phys. Chem., 94, 1624 (1990).

49. Derouiche, A., and Tondre, C., J. Chem. Soc., Faraday Trans. I, 85, 3301 (1989).

50. Eicke, H.F., Shepard, J.C., and Steinman, A.J., J. Colloid Interface Sci., 56, 168 (1975).

51. Robinson, B., in "Surfactants in Solution," K.L. Mittal, ed., Plenum, New York, 1984.

52. Lang, J., Jada, A., and Malliaris, A., J. Phys. Chem., 92, 1946 (1988).

53. Fletcher, P.D.I., Howe, A.M., and Robinson, B.H., J. Chem. Soc. Faraday Trans. I, 83, 185 (1987).

54. Howe, A.M., McDonald, J.A., and Robinson, B.H., J. Chem. Soc. Faraday Trans. I, 83, 1007 (1987).

55. Jada, A., Lang, J., Zana, R., Makhloufi, R., Hirsch, E., and Candau, S.J., J. Phys. Chem., 94, 387 (1990).

56. Bedwell, B., and Gulari, E., J. Colloid Interface Sci., 102, 88 (1984).

57. Hou, M.J., Kim, M., and Shah, D.O., J. Colloid Interface Sci., 123, 398 (1988).

58. Cazabat, A.M., Chatenay, D., Langevin, D., and Pouchelon, A., J. Physique Lett., 41, 441 (1980).

59. Agterof, W.G.M., van Zomeren, J.A.J., and Vrij, A., Chem. Phys. Lett., 43, 363 (1976).

60. Calje, A.A., Agterof, W.G.M., and Vrij, A., in "Micellization, Solubilization and Microemulsions," K.L. Mittal, ed., Plenum, New York, 1977.

61. Cazabat, A.M., Langevin, D., and Pouchelon, A., J. Colloid Interface Sci., 73, 1 (1980).

62. Cazabat, A.M., and Langevin, D., J. Chem. Phys., 74, 3148 (1981).

63. Gulari, E., Bedwell, B., and Alkhafaji, S., J. Colloid Interface Sci., 77, 202 (1980).

64. Hou, M.J., and Shah, D.O., Langmuir, 3, 1086 (1987).

65. Leung, R., and Shah, D.O., J. Colloid Interface Sci., 120, 320 (1987).

66. Leung, R., and Shah, D.O., J. Colloid Interface Sci., 120, 330 (1987).

67. Cebula, D.J., Ottewill, R.H., Ralston, G., and Pusey, P.N., J. Chem. Soc. Faraday Trans. I, 77, 2585 (1981).

68. Dvolaitzky, M., Guyot, M., Lagues, M., Lepesant, J.P., Ober, R., Sauterey, C., and Taupin, C., J. Chem. Phys., 69, 3279 (1987).

69. Ober, R., and Taupin, C., J. Phys. Chem., 84, 2418 (1980).

70. Atik, S., and Thomas, J.K., J. Phys. Chem., 85, 3921 (1981).

71. Jada, A., Lang, J., and Zana, R., J. Phys. Chem., 94, 381 (1990).

72. de Rozieres, J., Middleton, M.A., and Schechter, R.S., J. Colloid Interface Sci., 124, 407 (1988).

73. Hayter, J.B., and Penfold, J., Mol. Phys., 42, 109 (1981).

74. Hayter, J.B., and Penfold, J., J. Chem. Soc. Faraday Trans. I, 77, 1851 (1981).

75. Feynman, R.P., Leighton, R.B., and Sands, M., "The Feynman Lectures on Physics," Addison-Wesley, Reading, Mass., 1964.

76. Metropolis, N., Rosenbluth, A.W., Rosenbluth, M.N., Teller, A.H., and Teller, E., J. Chem. Phys., 21, 1087 (1953).

77. Binder, K., ed., "Applications of the Monte Carlo Method," Springer-Verlag, New York, 1983.

78. Heermann, D.W., "computer Simulation Methods in Theoretical Physics," Springer-Verlag, New York, 1986.

79. Barker, J.A., and Henderson, D., J. Chem. Phys., 47, 2856 (1967).

80. Barker, J.A., and Henderson, D., J. Chem. Phys., 47, 4714 (1967).

81. Martin, C.A., and Magid, L.J., J. Phys. Chem., 85, 3938 (1981).

82. Wong, M., Thomas, J.K., and Nowak, T., J. Am. Chem. Soc., 99, 4730 (1977).

83. Kotlarchyk, M., Chen, S.H., and Huang, J.S., J. Phys. Chem., 86, 3273 (1982).

84. Kotlarchyk, M., Chen, S.H., Huang, J.S., and Kim, M.W., Phys. Rev. A, 29, 2054 (1984).

85. Kotlarchyk, M., Huang, J.S., and Chen, S.H., J. Phys. Chem., 89, 4382 (1985).

86. Robinson, B.H., Toprakcioglu, C., Dore, J.C., and Chieux, P., J. Chem. Soc. Faraday Trans. I, 80, 13 (1984).

87. Toprakcioglu, C. Dore, J.C., Robinson, B.H., and Howe, A., J. Chem. Soc. Faraday Trans. I, 80, 413 (1984).

88. Cabos, C., and Marignan, J., J. Phys. Lett., 46, L-267 (1985).

89. Pileni, M.P., Zemb, T., and Petit, C., Chem. Phys. Lett., 118, 414 (1985).

90. Assih, T., Larche, F., and Delord, P., J. Colloid Interface Sci., 89, 35 (1982).

91. Kuneida, H., and Shinoda, K., J. Colloid Interface Sci., 33, 215 (1970).

92. Peyrelasse, J., and Boned, C., J. Phys. Chem., 89, 370 (1985).

93. Henze, R., and Schreiber, U., Colloid & Polymer Sci., 263, 164 (1985).

94. Gestblom, B., and Sjoblom, J., Langmuir, 4, 360 (1988).

95. Ganz, A.M., and Boeger, B.E., J. Colloid Interface Sci., 109, 504 (1986).

96. D'Arrigo, A., Paparelli, A., D'Aprano, A., Donato, I.D., Goffredi, M., and Turco Liveri, V., J. Phys. Chem., 93, 8367 (1989).

97. Eicke, H.F., Borkovec, M., and Das-Gupta, B., J. Phys. Chem., 93, 314 (1989).

98. Hall, D.G., J. Phys. Chem., 94, 429 (1990).

99. Waaler, D., Strand, K.A., Stromme, G., and Sikkeland, T., J. Chem. Phys., 91, 3360 (1989).

100. Barker, J.A., and Henderson, D., Mol. Phys., 21, 187 (1971)

101. Israelachvili, J.N., "Intermolecular and Surface Forces," Academic Press, London, 1985.

102. McQuarrie, D.A., "Statistical Mechanics," Harper & Row, New York, 1976.

103. Pettitt, B.M., and Rossky, P.J., J. Chem. Phys., 84, 5836 (1986).

104. Kusalick, P.G., and Patey, G.N., J. Chem. Phys., 88, 7715 (1988).

105. Rashin, A.A., J. Phys. Chem., 93, 4664 (1989).